

12-1-2015

The effects of ketorolac and its enantiomers on breast cancer proliferation and metastasis

Amanda Peretti

Follow this and additional works at: https://digitalrepository.unm.edu/biom_etds



Part of the [Medicine and Health Sciences Commons](#)

Recommended Citation

Peretti, Amanda. "The effects of ketorolac and its enantiomers on breast cancer proliferation and metastasis." (2015).
https://digitalrepository.unm.edu/biom_etds/100

This Thesis is brought to you for free and open access by the Electronic Theses and Dissertations at UNM Digital Repository. It has been accepted for inclusion in Biomedical Sciences ETDs by an authorized administrator of UNM Digital Repository. For more information, please contact disc@unm.edu.

Amanda Sheree Peretti

Candidate

Biomedical Sciences

Department

This thesis is approved, and it is acceptable in quality and form for publication:

Approved by the Thesis Committee:

Dr. Laurie Hudson, Chairperson

Dr. Helen Hathaway

Dr. Eric Prossnitz

Dr. Angela Wandinger-Ness

**THE EFFECTS OF KETOROLAC AND ITS ENANTIOMERS ON BREAST
CANCER PROLIFERATION AND METASTASIS**

by

AMANDA S. PERETTI

**B.S. BIOLOGY
NEW MEXICO INSTITUTE OF MINING AND TECHNOLOGY, 2008**

**M.S. BIOLOGY
NEW MEXICO INSTITUTE OF MINING AND TECHNOLOGY, 2012**

THESIS

Submitted in Partial Fulfillment of the
Requirements for the Degree of

**Master of Science
Biomedical Sciences**

The University of New Mexico
Albuquerque, New Mexico

December, 2015

DEDICATION

To Ezio. The best experiment in the “life-sciences” I’ve ever tried.

ACKNOWLEDGEMENTS

First and foremost, I would like to thank my mentor Dr. Laurie Hudson. I'm sure she wondered what she got herself into, each and every time my carefully made plan veered off course, or I ended up in her office to talk about some life-altering event, but she steered me through it all with the gentle but firm hand of an amazing and caring mentor. For that, I am truly thankful. I would like to thank my committee members, Dr. Helen Hathaway, Dr. Eric Prossnitz, and Dr. Angela Wandinger-Ness, for their patience and guidance. A big thank you to the Hathaway lab members, for letting me use their equipment and space, especially Sara Alcon and Jamie Hu for teaching me about mouse dissections and Laura Laidler for her many hours spent helping me dose and dissect mice.

Thank you to the Hudson lab members both past and present. Especially Brenee King and Krystal Quan whose enthusiasm and cheerful demeanors let me know I was exactly where I needed to be. Karen Cooper for being yet another "lab mom" and keeping us all in line. Sabrina Samudio-Ruiz for being the person to go to if I wanted someone to get really excited about what I was excited about. Michaela Granados for her humor and ability to inject laughter into any situation. Young Mi Cho for all the coffee and food we shared. Erica Dashner, whose drive is overwhelming. Dayna Dominguez, with whom I formed an immediate friendship, and without whom I would have torn my hair out over mouse studies. And finally, my cubicle-mate Ray Kenney, with whom I've shared, celebrated, and commiserated every last step of the writing process.

Thank you to the COP support staff, especially Jodi Perry and Mari Ann Farrell for quickly answering my many emails. Thank you to my BSGP cohort and the BSGP program for their continued support and encouragement. None of this work would have been possible without my funding grant NIH 1R21CA170375-01S.

I thank my family and friends for their many years of support. Thank you to my Mom and Dad for their continuous love and insistence on hard work and perseverance. Many thanks to my dear friend, Siona Curtis-Briley, for keeping me sane when I felt less than stable. Thank you to my in-laws, Tammy and Greg, for being intensely interested in my experiments, and for being some of the most generous people I know.

Finally, I am infinitely grateful to my husband, Jordan Peretti. Every day he challenges me to become a better version of myself but still loves me when I falter. Some time ago, in not quite these exact words, I said, "I want to quit my job and go be a broke, stressed out graduate student." He replied, "Go for it. You'll be amazing." He had the most to lose from this venture, but was, and still is, my biggest supporter.

**THE EFFECTS OF KETOROLAC AND ITS ENANTIOMERS ON BREAST
CANCER PROLIFERATION AND METASTASIS**

by

Amanda S. Peretti

B.S. Biology, New Mexico Institute of Mining and Technology, 2008

M.S. Biology, New Mexico Institute of Mining and Technology, 2012

M.S. Biomedical Sciences, University of New Mexico, 2015

ABSTRACT

Breast cancer is the second leading cause of cancer related deaths in women. Advanced breast cancer can metastasize to the lungs, liver, bones and brain becoming fatal conditions for many patients. There is a dire need for metastasis preventing medications, however the process required for a medication to become FDA approved for clinical use is long and arduous. Studies have found promising benefits for breast cancer patients given Toradol™, or racemic ketorolac, as an NSAID during resection surgery. However, long-term use of racemic ketorolac is not recommended. Currently FDA-approved for use in the racemic form, ketorolac has the potential to become a valuable off-label drug for cancer patients, and if given as a single enantiomer, may not cause toxic effects.

Recent work on ovarian cancer cell lines has shown (R)-ketorolac to have an effect on invasion and migration abilities via interaction with small Rho-GTPases. We hypothesized that (R)-ketorolac would likewise have the ability to inhibit breast cancer invasion and migration by binding to Cdc42, Rac1 and RhoA.

The activity of racemic ketorolac and its enantiomers, (S)-ketorolac and (R)-ketorolac was studied in both *in vivo* and *in vitro* settings. In breast cancer cell lines it was shown that ketorolac does not affect the viability of cells, but does inhibit colony formation and migration. In MMTV-PyMT mouse models, ketorolac treatment does not appear to have toxic effects on the organism, and may prevent early mammary gland tumor growth and, in older mice, metastasis. These studies suggest that the (R)- enantiomer of ketorolac may be useful in preventing tumor growth and metastasis without imparting significant toxicities.

TABLE OF CONTENTS

DEDICATION	iii
ACKNOWLEDGEMENTS.....	iv
ABSTRACT	vi
ABBREVIATIONS.....	xiv
1. INTRODUCTION	1
1.1 Breast Cancer Prevalence	1
1.2 Breast Cancer Treatment Targets and Drugs	3
1.3 Drug Repurposing	6
1.4 Ketorolac	7
1.5 Potential Mechanisms of Action of Ketorolac in Breast Cancer Patients.....	9
1.6 GTPases in Breast Cancer.....	11
1.7 Rho GTPases and Their Regulation.....	13
1.8 The PyMT Mouse Model of Breast Cancer	20
1.9 Objective Study	21
2. THE EFFECTS OF KETOROLAC AND ITS ENANTIOMERS ON BREAST CANCER CELLS <i>IN VITRO</i>	24
2.1 Introduction	24
2.2 Materials and Methods	26
2.2.1 Materials	26
2.2.2 Cell Culture	26

2.2.3 MCF-7 Monolayer and MCA Viability with Racemic Ketorolac.....	27
2.2.4 MCF-7 and MDA-MB-231 Monolayer Viability with Ketorolac Enantiomers.....	27
2.2.5 MCF-7 Cell Cycle with Racemic Ketorolac.....	28
2.2.6 Colony Forming Assays – MDA-MB-231.....	29
2.2.7 Invasion Assays – MDA-MB-231	29
2.2.8 Migration Assays – MCF-7 and MDA-MB-231	30
2.2.9 Zymography – MMP Expression	30
2.3 Results	32
2.3.1 MCF-7 Monolayer and MCA Viability with Racemic Ketorolac.....	32
2.3.2 MCF-7 and MDA-MB-231 Monolayer Viability with Ketorolac Enantiomers at Varying PrestoBlue Incubation Times	36
2.3.3. Cell Cycle in MCF-7, and MDA-MB-231 Cells Treated with Ketorolac	39
2.3.4 Colony Forming Assays – MDA-MB-231.....	42
2.3.5 Invasion Assays – MDA-MB-231	44
2.3.5 Migration Assays – MCF-7 and MDA-MB-231	46
2.3.6 MMP Expression.....	48
2.4 Discussion.....	50
3. THE EFFECTS OF KETOROLAC ON MAMMARY GLAND CANCER CELL PROLIFERATION AND A STUDY OF ITS POTENTIAL TOXICITY IN PYMT MICE	54

3.1 Introduction	54
3.2 Materials and Methods	56
3.2.1 Pill Preparation.....	56
3.2.2 Mice	57
3.2.3 Experimental Design and Dosing Schedule	57
3.2.4 Dissection	58
3.2.5 Mammary Tissue Whole Mounts.....	59
3.2.7 Lung Preservation	60
3.2.8 Tissue Preservation	60
3.2.9 (S)-Ketorolac Mouse Study	60
3.3 Results - 21 day studies	61
3.3.1 Weekly and Final Weights.....	61
3.3.2 Kidney Weights	63
3.3.3 Short Term Study Weekly Palpable Tumor Load	65
3.3.4 Whole mounts of mammary glands.....	67
3.3.5 Histograms of Whole Mounts	70
3.3.6 Lung H&E Staining.....	72
3.4 Discussion.....	74
4. THE EFFECTS OF KETOROLAC ON PROLIFERATION AND METASTASIS OF MAMMARY GLAND TUMOR CELLS IN PYMT MICE.....	76

4.1 Introduction	76
4.2 Materials and Methods	77
4.2.1 Experimental Design and Dosing Schedule	77
4.2.2 Dissection	78
4.2.3 H&E Mammary Tumor Staining	79
4.2.4 RNA Isolation and qRT-PCR.....	79
4.3 Results - 81 Day Studies.....	80
4.3.1 Weekly and Final Weights.....	80
4.3.2 Kidney Weights	83
4.3.4 Weekly Tumor Growth	85
4.3.5 Tumor Mass	87
4.3.6 H&E Mammary Tumor Staining	89
4.3.7 Lung H&E Staining.....	91
4.3.8 qRT-PCR – 12 Weeks.....	94
4.4 Discussion.....	97
5. SIGNIFICANCE AND FUTURE DIRECTIONS	102
6. APPENDIX.....	106
7. REFERENCES	107

LIST OF FIGURES

Figure 1.1 The Rho-GTPase Regulation	14
Figure 1.2 Downstream Effectors and Cancer Implications	16
Figure 1.3 Hypothesized Mechanism of Action of (R)-Ketorolac	23
Figure 2.1 MCF-7 Viability with Racemic Ketorolac on MCAs and Monolayers at Multiple Time Points.....	34
Figure 2.2 MCF-7 Viability on MCAs and Monolayers with Racemic Ketorolac - Ketorolac has no effect on the viability of MCF-7 monolayer or MCA cells.	35
Figure 2.3 MCF-7 Monolayer Viability with Ketorolac Enantiomers.....	37
Figure 2.4 MDA-MB-231 Monolayer Viability with Ketorolac Enantiomers..	38
Figure 2.5 Ketorolac Does Not Change Cell Cycle of MCF-7 Cells at Concentrations Up To 300 μM	40
Figure 2.6 Ketorolac and Its Enantiomers Do Not Affect Cell Cycle in MCF-7 and MDA-MB-231 Cells at 100 μM Concentrations	41
Figure 2.7 Ketorolac Inhibits MDA-MB-231 Colony Formation.....	43
Figure 2.8 MDA-MB-231 Cells Did Not Exhibit Expected Invasive Properties	45
Figure 2.9 Ketorolac Inhibits MCF-7 and MCF-10A Migration in a Dose Dependent Manner	47
Figure 2.10 MMP Expression Does Not Change with Ketorolac Treatment	49
Figure 3.1 MMTV-PyMT Mouse Mammary Tumor Development Timeline ...	55
Figure 3.2 In vivo Experimental Outline	56

Figure 3.3 Short Term Study Mouse Mass	62
Figure 3.4 Short Term Study Kidney Weights	64
Figure 3.5 Short Term Study Weekly Palpable Tumor Load	66
Figure 3.6 Mammary Gland Whole Mount Example	68
Figure 3.7 Treated vs. Untreated Mammary Gland Whole Mounts	69
Figure 3.8 Mammary Gland Whole Mount Histograms	71
Figure 3.9 H&E Stained Lung Tissue	73
Figure 4.1 Long Term Study Weekly Weight Gain and Final Weight	82
Figure 4.2 Long Term Study Kidney Weights	84
Figure 4.3 Long Term Study Weekly Palpable Tumor Load	86
Figure 4.4 Long Term Study Tumor Weights	88
Figure 4.5 H&E Staining of Mouse Mammary Tumors Show No Change	90
Figure 4.6 12 week old H&E Stained Lung Tissue	92
Figure 4.7 14 Week Old H&E Stained Lung Tissue	93
Figure 4.8 qPCR in Tumor Tissue – 12 Weeks	95
Figure 4.9 qPCR in Lung Tissue – 12 Weeks	96
Figure 6.1 MMTV-PyMT Mouse Lung Metastasis Time Course	106

ABBREVIATIONS

ANOVA – analysis of variance

APS – ammonium persulfate

ATCC – American Type Culture Collection

ATO – arsenic trioxide

BSA – bovine serum albumin

cDNA – Complementary Deoxyribonucleic Acid

COX – cyclooxygenase

DLC-1 – deleted in liver cancer 1

DMEM – Dulbecco's modified eagle's medium

DMSO – Dimethyl Sulfoxide

EGF – epidermal growth factor

EMT – epithelial mesenchymal transition

ER – estrogen receptor

FBS – fetal bovine serum

FDA – Food and Drug Administration

GAP – GTPase-activating proteins

GDI – guanine nucleotide dissociation inhibitors

GDP – guanosine diphosphate

GEF – guanine nucleotide exchange factors

GTP – guanosine triphosphate

H&E – hematoxylin and eosin

HER2 – human epidermal growth factor receptor 2

IC50 – Inhibitory Concentration, 50%

MCA – multi-cellular aggregates

MMP – matrix metalloproteinase

MMTV – mouse mammary tumor virus

MTS – 3-(4,5-dimethylthiazol-2-yl)-5-(3-carboxymethoxyphenyl)-2-(4-sulfophenyl)-2H-tetrazolium

NSAID – non-steroidal anti-inflammatory drug

NT – non-treated

PBS – phosphate buffered saline

PCR – polymerase chain reaction

PFA – paraformaldehyde

PI – propidium iodide

PMS – phenazine methosulfate

PyMT – polyoma middle T-antigen

qRT-PCR – quantitative Real-Time PCR

RNA – Ribonucleic Acid

RPMI – Roswell Park Memorial Institute

TEMED – tetramethylethylenediamine

Tiam1 – T-cell lymphoma invasion and metastasis-inducing protein 1

1. INTRODUCTION

1.1 Breast Cancer Prevalence

Breast cancer is the second most commonly diagnosed cancer in women (1). Although it is most often diagnosed in postmenopausal women, breast cancer affects individuals of both sexes and all ages. In 2015, an estimated 234,190 new cases will be documented and 40,730 individuals will die from breast cancer (1). The latest statistics from the American Cancer Society show a decline in the total number of breast cancer related deaths over recent years, but breast cancer is still the second leading cause of cancer related deaths in women after lung cancer (1).

Risk for developing breast cancer is increased by a variety of factors including genetic mutations, lifestyle habits and non-modifiable medical conditions and treatments (1). A conscious effort can be made to decrease risk but ultimately avoiding breast cancer is not an exact science. Modern medicine has enabled us to eradicate breast cancer in a fraction of women but there is still need for more effective treatments. Chemotherapy options with less severe side effects for the patient are necessary, as well as the availability of safe chronic medications for preventing metastasis or relapse.

Breast cancer is a heterogeneous disease that varies between individuals. Various factors affect the severity as well as the treatability of the disease. For example receptor status is a characteristic used to select targeted drugs. Cells that overexpress estrogen receptors (ER) bind estrogen hormones which promote cell growth. ER-positive/PR-positive (ER+/PR+) cancer is treatable with

hormone therapy, such as Tamoxifen as discussed below (reviewed (2)).

Tamoxifen treated ER+ patients experience reductions in the risk of recurrence and mortality (reviewed (3)). However, ER-negative (ER-) cancer does not benefit by this mode of treatment, as its proliferation is due to other factors (4).

Patients whose cells are negative for ER, PR and HER2 are classified as having triple negative breast cancer (TNBC). TNBC is more difficult to treat, as the cells lack traditional specific receptor targets (5). Patients exhibiting TNBC have more aggressive tumors and a greater chance of recurrence and worse prognosis in the first four years after diagnosis, than patients whose cells are ER+, PR+ or HER2-positive (HER2+) (5,6).

Treatments for breast cancer patients generally begin with tumor and lymph node biopsies to determine the extent of disease and characteristics of the tumor (7). Most patients then undergo adjuvant therapy followed by surgical procedures to remove tumors and affected lymph nodes. Surgery may be preceded by chemotherapy to reduce the amount of tissue removed (7). Afterwards, patients receive radiation therapy, chemotherapy or hormone therapy to ablate remaining cancer cells (8). The types of drugs used for treatment vary depending on the receptor status of cells, stage of cancer progression, and the degree of metastasis (8,9).

Current goals in breast cancer research are to decrease the prevalence of breast cancer by improving early detection, increasing the effectiveness of treatments and decreasing relapse.

1.2 Breast Cancer Treatment Targets and Drugs

Breast cancer drugs currently on the market generally work in one of two ways: by interfering with cytoskeleton function, which is essential to cell growth and division or by blocking the availability of growth hormones (e.g. estrogen) to the cell. Breast cancer drugs can take advantage of these known targets to specifically interrupt a cancer cell's growth and proliferation.

Overexpression of the HER2/*neu* (human epidermal growth factor receptor 2) gene is found in about 30% of breast tumors (10). Excess HER2 is associated with malignancy and decreased survival rates in breast cancer patients (reviewed (11,12)). HER2 is involved in regulating cell growth and differentiation signaling pathways, and overexpression of HER2 protein leads to uncontrolled cell growth (11,13). The HER2 gene encodes a cell surface glycoprotein which has tyrosine kinase activity (14,15). Tyrosine kinases phosphorylate proteins, which activate phosphatidyl inositol 3-phosphokinase/protein kinase B (PI3K/Akt) signaling pathways (reviewed (16)). The PI3K/Akt signaling pathway controls normal cellular activities that are inappropriately balanced in tumors such as cellular proliferation and migration (16,17). Increased tyrosine kinase activity is implicated in a number of different cancers, including breast cancer (16,17). In breast cancer, HER2 gene amplification is associated with more aggressive tumors, greater recurrence rates and increased mortality (18–21).

Patients with HER2/*neu*-positive cells generally receive treatment with a monoclonal antibody called Trastuzumab (Herceptin) (3,5,13,22). Trastuzumab

(Herceptin) binds to the human epidermal growth factor receptor 2 (HER2/neu/erbB-2) and inhibits receptor dimerization and activation of the PI3K/Akt pathway (13,23–25). This drug has become a recognized standard treatment for HER2 positive (HER2+) breast cancer patients, and is usually used in combination with, or after chemotherapy (13,24,26). Much like ER+ breast cancer, HER2+ cancer can be more specifically targeted using Trastuzumab (5,11).

Another class of anti-cancer drugs useful in treating breast cancer work by blocking estrogen interaction with the cell, either by competing for estrogen receptors or preventing conversion of androgen to estrogen, as with Letrozole (commercially known as Femara) (27). Tamoxifen, a commonly used estrogen receptor antagonist, can be used long term in postmenopausal patients as a tumoristatic drug (2). This drug only works in estrogen receptor positive (ER+) breast cancers, so it is not effective for all cases of breast cancer(2). In ER+ breast cancer cells, estrogen binds to the estrogen receptor, activating a cascade of events that enable the cell to grow. When Tamoxifen is administered, it is metabolized by the liver into active metabolites that have a great affinity for the estrogen receptor (28). The active metabolites compete with estrogen for receptor binding, preventing estrogen mediated gene transcription and cancer cell growth (28).

Endocrine therapies, like Tamoxifen, are often used to treat individuals with early stage or metastatic breast cancer, as these drugs affect cells all over the body (7). Because these drugs affect all cells, they can create adverse side

effects. For example, Tamoxifen has been shown to induce liver cancer in rats and increase the incidence of other cancers in humans (29,30). Treatment with Tamoxifen for breast cancer induces estrogen-like effects on the uterus and is linked to an increased risk for uterine cancer due to the drug's agonistic effect on G-protein coupled estrogen receptors (GPER) (31–33).

The lack of targetable receptors in TNBC cells creates a unique challenge for cancer drug development. Current work on targeted therapies for TNBC employ PARP (poly ADP-ribose polymerase) inhibitors (7). PARP is an enzyme that repairs damaged DNA. Inhibiting PARP activity prevents cancer cells from repairing damaged DNA causing cells to undergo apoptosis and die instead of proliferating.

Paclitaxel, a Food and Drug Administration (FDA) approved drug commercially known as Taxol, is used to treat ovarian, breast, lung, head and neck cancers (34). Taxol belongs to a group of agents called taxanes, which include doclitaxel and paclitaxel. These agents do not target specific receptors, but instead stabilize microtubule filaments in the guanosine diphosphate (GDP) state preventing microtubules from disassembling, and inhibiting complete mitosis which results in apoptosis of the cell (35).

The problem with all of these treatments is that they are not absolutely cancer cell-specific. Many anti-cancer drugs affect healthy cells as well as the cancer cell targets, which leads to undesirable side effects for the patient. Additionally, due to the various manifestations of breast cancer, a treatment that works for one patient may work only partially or not at all in another patient.

Cancer drug resistance is a common problem (reviewed (36–38)). When a cancer patient experiences relapse, the same drugs that lead to remission in previous treatments may no longer be as effective in subsequent tumors. The cancerous patient cells have developed resistance against drugs that kill cancer in one specific way, e.g. microtubule growth inhibition. The survival rate of relapsed patients is low, and finding anti-cancer treatments that have different mechanisms of action than their previous treatment is important. Overcoming resistance by discovering new targets and discovering new cancer treatments is important in cancer drug discovery.

In recent years, there has been a developing trend towards individualized cancer treatment plans. After initial breast cancer diagnosis, tests are conducted to determine the stage of cancer as well as its specific characteristics (7). Biopsy samples can be used to determine whether the cancer has specific receptors to serve as drug targets. This approach is still only as powerful as the knowledge of modified pathways involved in cancer, and drugs available for targeting said modifications. New targets are in development. Increasing the number of drugs available will allow for more efficient treatments and greater survival rates of cancer patients.

1.3 Drug Repurposing

A large area of cancer research is dedicated to the development of new drugs to modify and change cellular pathways in cancer cells. Nonetheless, even the most effective treatment against cancer cells must be verified in multiple cell lines, tested in *in vivo* models, and undergo animal and human testing for safety.

Finally, it must meet strict requirements set by the FDA for use in humans. The process required to verify that new compounds are safe and effective is long and complicated. Synthesis, biological testing, and pharmacological screening of new compounds can take 5-8 years, after which, compounds must still undergo a three stage process in order to be deemed safe, possibly adding on another eight years before being available for clinical use (39). “Fast forwarding” through any step of this process can cut years off of the time needed for new chemotherapeutics to be put into routine use. Repurposing previously FDA approved drugs for use in cancer treatment is one way to expedite this process.

FDA approved drugs have already been evaluated for human use. The main concern with unconventional use of a drug is using it in concentrations that will not cause long lasting harm to the patient, as some treatment regimens may require dosages far above the pre-determined safe concentration. According to MediLexicon, there are 148 FDA approved drugs available for cancer therapy (27). Many of these drugs are designed for very specific cancers and several, such as the non-steroidal anti-inflammatory drugs (NSAIDs), are used for treating pain associated with cancer.

1.4 Ketorolac

Of particular interest is ketorolac tromethamine, marketed as Toradol™ or Acular™. Ketorolac is an FDA-approved NSAID used for treating pain and inflammation (40,41). In a clinical setting, this drug is administered as a racemic mixture of (R)- and (S)- enantiomers via an initial intravenous (IV) or intramuscular (IM) route, then continued orally for no more than five days (42).

Ketorolac is contraindicated for long-term use due to its association with increased gastrointestinal ulcers, bleeding, and perforation as well as liver and renal failure (42). On the other hand, short-term administration of ketorolac has demonstrated significant beneficial effects for patients over alternative post- or peri-operatively administered pain medications. Recent data have shown that when ketorolac is administered perioperatively, breast cancer patients are less likely to experience an early relapse and there is an increase in survival after surgery (43). Evidence has also shown that perioperative ketorolac administration is correlated with improved survival in lung, and ovarian cancer patients (44,45).

In a 2010 study, Forget et al. conducted studies comparing perioperative analgesics and anesthetics given to Belgian women who received mastectomies from a single surgeon. In these studies, women who had received ketorolac had superior disease free survival rates in the first few years after surgery, with the greatest differences observed during the 9-18 months after surgery (46). These studies were further analyzed by Retsky et al. who hypothesized that ketorolac reduces systemic inflammation and angiogenesis, interfering with the metastatic ability of circulating tumor cells (43,47). Without a suitable host environment, these circulating cells die off. Of note, Retsky et al. proposed that ketorolac could be of benefit to TNBC patients regardless of the current lack of targeted therapy for TNBC cells (43,47).

1.5 Potential Mechanisms of Action of Ketorolac in Breast Cancer Patients

Although given clinically as a racemic mixture, ketorolac's two enantiomers have differing functions. The S- enantiomer of ketorolac is a known cyclooxygenase (COX) inhibitor and useful for managing pain and inflammation (48,49). The R-enantiomer, originally thought to be inert, inhibits actin cytoskeleton regulators such as Rac1 and Cdc42 GTPases and relieves pain independent of COX inhibition (40,50,51).

(S)-ketorolac inhibits COX enzymes and, consequently, is primarily responsible for the ulcerogenic activity associated with racemic ketorolac (52,53). The COX enzyme family consists of two enzymes, COX-1 and COX-2. COX-1 is found throughout the body and is responsible for synthesizing prostaglandins from arachidonic acid (53). Prostaglandins have an active role in vasoconstriction, vasodilation and immunosuppression, a protective role in maintaining the stomach and gastrointestinal lining, and ensure proper renal function in compromised kidneys (53–58). Prostaglandins also promote malignant tumor development and growth (53,54,58–60). COX-2 is found mainly in areas of inflammation, as well as the brain and spinal cord (54). COX-2 contributes to the synthesis of prostaglandins in inflamed tissues and malignant tumors and has been found to promote growth factor and matrix metalloproteinase (MMP) expression (53,61). MMPs enable tumor cells to invade basement membranes, penetrate blood vessels and metastasize (62).

Inflammation accompanying breast cancer surgery is believed to exacerbate the escape of tumor stem cells and contribute to recurrent disease

(47,63). (S)-ketorolac may decrease tumor metastasis by acting as a COX inhibitor, thus decreasing inflammation. Cancer patients are known to have circulating tumor cells (CTCs) (64,65). In an inflammatory environment, the vasculature becomes “leaky” enabling CTCs to extravasate and move into distant tissues (47,63). Administering an NSAID such as ketorolac, perioperatively, may decrease tumor metastasis by acting as a COX inhibitor, thus decreasing the inflammatory response and preventing the escape of CTCs from the vasculature. In addition, ketorolac may prevent angiogenesis, which is another contributing factor to metastatic growth of CTCs (47,63). However, evidence shows that (R)-ketorolac may also be playing an important role in preventing metastasis (45,50,51).

(R)-ketorolac interferes with the activation of Rho GTPase signaling proteins Rac1 and Cdc42 (40,45,50). Small Rho GTPases such as RhoA, RhoC, Rac1, and Cdc42, regulate cell growth, invasion, motility, and metastasis and are often found overexpressed in many cancers including breast cancer (66–70). Rho GTPases are particularly found in highly metastatic breast tumors and overexpression is associated with greater cancer severity (67,68,70). Aberrant Rho-GTPase signaling rather than mutation is responsible for cancer cell growth and progression.

The (R)- enantiomer of ketorolac exhibits analgesic properties with little to none of the ulcerogenic properties seen with (S)-ketorolac (48,49). Unlike (S)-ketorolac, (R)-ketorolac does not have an effect on COX activity, which consequently allows the enzyme to maintain its protective role in the stomach

and gastrointestinal linings (48,52). In one study investigating the ability of compounds to inhibit COX, (S)-ketorolac outperformed (R,S)-ketorolac, followed by a number of other COX inhibitors and (R)-ketorolac at the very end of the list, with the least amount of COX inhibition observed (71). However, (R)-ketorolac is not pharmacologically inactive, as previously thought. In epithelial cancer cells, (R)-ketorolac is able to inhibit Rac1 and Cdc42 activity in a comparable manner to established Rac1 and Cdc42 inhibitors (45,50,51). Docking studies have suggested that (R)-ketorolac's configuration enables the carboxylate moieties of the molecule to chelate magnesium and disables the DOCK GEF's ability to bind to Rac1 and Cdc42 (51). (R)-ketorolac has been shown to selectively bind Rac1 and Cdc42 (51). These Rho-GTPases are necessary for the formation of lamellipodia and filopodia formation which enable a cell to migrate through its environment, invade basement membranes, and metastasize to distant locations (72,73).

1.6 GTPases in Breast Cancer

(R)-ketorolac interferes with the activation of signaling proteins Rac1 and Cdc42 within the Rho GTPase family (40,45,50). Rho GTPases are enzymes that act as regulatory switches by binding to guanosine triphosphate (GTP), hydrolyzing it to guanosine diphosphate (GDP), effectively switching a signaling mechanism from an active "on" form to an inactive "off" form and back again (74,75).

GTPases play an important role in breast cancer. Small Rho GTPases have roles in cell growth, invasion, motility, and metastasis of breast cancer cells

(reviewed (66)). Most often, overexpression rather than mutations of Rho GTPases are found in cancerous tissue (reviewed (66)). Only one Rho GTPase genetic mutation, a mutation in RhoH, has been implicated in human cancer (76,77). RhoA, RhoC, Rac1, and Cdc42, are overly abundant in multiple cancers, including breast cancer (67–70). Rac1b, a splice variant of Rac1, is overexpressed in colon and breast cancer and is found primarily in the GTP-bound active form because it is self-activating and thus GEF independent (69,78). Overexpression of a constitutively active GTPase can lead to uncontrolled cell growth and metastasis. Although Rac1b expression is increased in colorectal tumors when compared to normal colonic mucosa, and studies have found greater levels of Rac1 in malignant breast tissue, when compared to benign breast tissue, Rac1b expression levels are not different between malignant and benign breast tumor tissue (69,78,79). Another mutant, Rac1 (P29S) is a fast cycling mutant, meaning that it is more often found in a GTP bound, or active state, due to increased GDP disassociation (80). The Rac1 (P29S) mutation is found in breast cancer as well as head and neck cancers, and melanoma (80,81). Integral to the signaling cascade that activates cell growth and motility, Rho GTPases are often overexpressed in highly metastatic breast tumors and have been found to correlate positively with breast cancer severity (67,68,70).

1.7 Rho GTPases and Their Regulation

Changes in GTPase regulators, GEFs, GAPs and GDIs, cause Rho GTPases to be aberrantly regulated through mutation or GTPases splicing (Rac1b), altering the ability of cells to properly regulate the cytoskeleton leading to uncontrolled cell growth and migration. Rho GTPases are regulated by three different classes of proteins called guanine nucleotide exchange factors (GEFs), GTPase-activating proteins (GAPs) and guanine nucleotide dissociation inhibitors (GDIs) (82). GEFs, GAPs and GDIs function as Rho-GTPase regulators, cycling GTPase through active and inactive forms. GEFs facilitate the exchange of GDP for GTP; GAPs coordinate the dephosphorylation of nucleotides, converting GTP to GDP, and GDIs inhibit GEFs and GAPs from acting on Rho-proteins preventing the exchange of GTP and GDP (75).

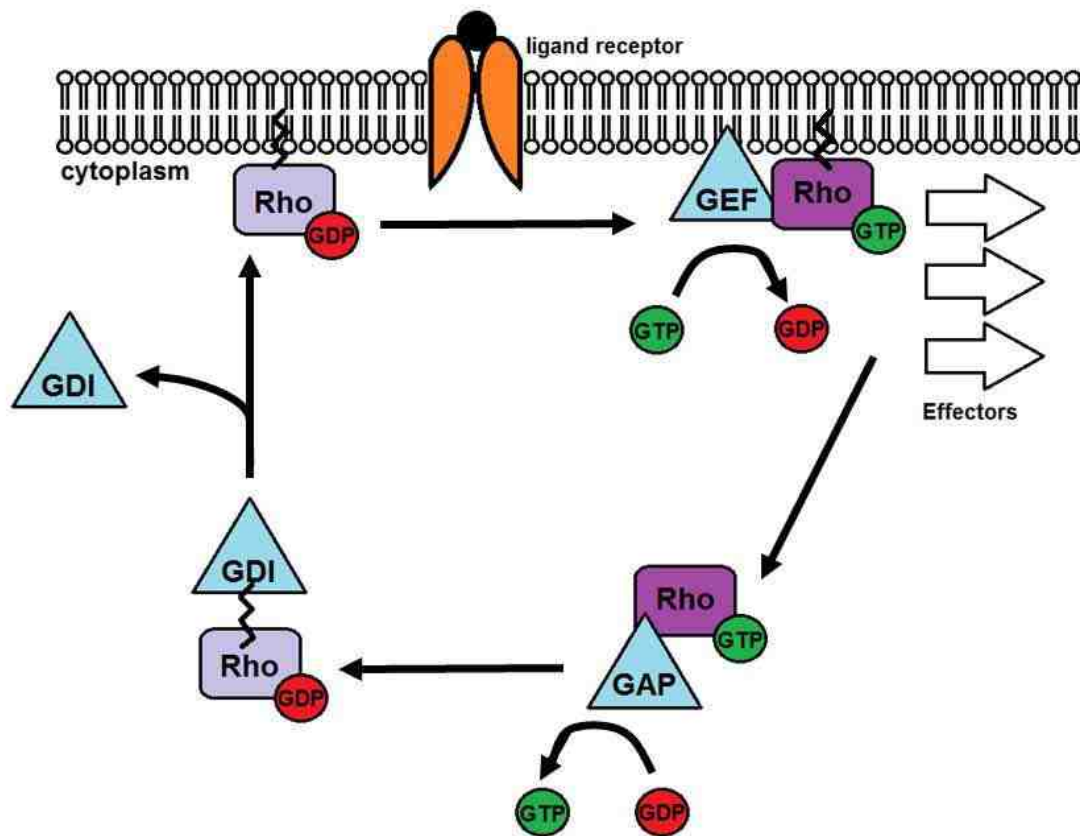


Figure 1.1 The Rho-GTPase Regulation

(adapted from (74,82))

In their inactive form, GTPases are mainly located in the cytoplasm with their C-terminal tail bound by GDIs, which is necessary for plasma membrane localization (74,82). Dissociation from GDIs allows GTPases to relocate to the plasma membrane (74,82). External stimuli to membrane receptors induces the activation of membrane bound GTPases by GEFs which then causes GTPases to bind to effector proteins (74,82). This binding of effector proteins leads to downstream signaling which can be subsequently turned off by the dephosphorylation and inactivation of GTPases by GAPs (74,82).

For example, the cell surface tyrosine-kinase receptor, HER2, interacts with ligands and dimerizes (11). This signaling also increases GTPase cycling and increases the active status of GTPases. HER2 dimerization recruits a GEF, to the cell surface which exchanges GDP for GTP, activating Rac1 (11,83). Rac1 binds to an effector protein, such as p21-activated serine/threonine kinase 1 (PAK1). PAK family members phosphorylate multiple downstream proteins involved in breast cancer progression (reviewed (84)). One target of PAK1 is mitogen-activated protein kinase (MAPK) which itself is involved in multiple pro-cancer functions such as proliferation, differentiation, motility, apoptosis, and survival (reviewed (84)).

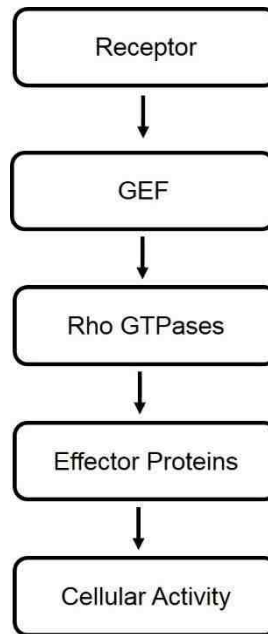


Figure 1.2 Downstream Effectors and Cancer Implications

An activated receptor (HER2, ER) activates GEFs (Tiam1, p190RhoGEF), phosphorylating and activating Rho-GTPases (Rac1, Cdc42, RhoA). Rho-GTPases activate effector proteins (PAK, ROCK) that then activate multiple cellular proteins (MAPK, VEGF) involved in cancer (growth, motility, angiogenesis, survival, differentiation).

Rho GTPases play important roles in actin and cytoskeleton regulation. In a cancer cell, regulation of cytoskeletal structure, adhesion, spreading, and polarity are vital to enabling the cell to migrate and metastasize (74,75,82,85). There are six distinct groups of Rho GTPases: the Rho, Rac, Cdc42-like, Rnd, RhoBTB, and Miro proteins (82). Of these, the best characterized, and the focus of our studies, are Cdc42, RhoA, and Rac1.

Cdc42 is responsible for cell polarity and regulates actin filament assembly, forming filopodia at the cell periphery (86–88). While Cdc42 is not directly responsible for cell growth or protrusion, it helps to direct cellular asymmetry (74). This asymmetry creates a leading edge for the rest of the cell to follow during activities such as migration (74). Directed activity towards the leading edge of the cell enables the cell to move in one unified direction. Increased protein levels of Cdc42 have been observed in breast cancer (67,68). However, an increase in Cdc42 proteins does not correlate with an increase in metastatic potential (89).

RhoA plays a role in contractile actin-myosin bundle (stress fiber) formation (88,90). RhoA's contractile activity on the actin-myosin filaments enable the trailing edge of the cell to be pulled along as the front of the cell protrudes forward during cell movement (91). RhoA is also involved in signaling pathways such as Rho-associated coiled-coil-containing protein kinase (ROCK) activation pathway and the PI3-K/AKT pathway, which are essential for the actin polymerization during cell locomotion, and cell survival and expression of cell proliferation genes respectively (92). Increased amounts of RhoA protein are

found in advanced breast tumors while little RhoA is detected in surrounding tissues (67,68). Experiments injecting anti-RhoA silencing RNA (siRNA) into xenografted MDA-MB-231 breast tumors directly target RhoA containing tumor cells, and have shown great promise in inhibiting growth and angiogenesis (93).

Rac1 regulates actin polymerization at the cell periphery which creates lamellipodia and cell membrane ruffling (72,88). Rac activity at the leading edge of the cell allows it to form membrane protrusions which drive cell movement during invasion and migration (74). In breast cancer, there is a direct correlation between increased Rac1 protein and metastatic potential (89). Furthermore, Rac1 is overexpressed in malignant breast tissue when compared to benign breast tissue, and patients with more aggressive and recurring breast cancer have increased membrane localization of Rac1 (67–69).

One Rho GTPase regulator implicated in breast cancer is deleted in liver cancer 1 (DLC-1). The deregulation of DLC-1 is involved in the formation and progression of breast tumors (94). DLC-1 is a Rho GAP specific for RhoA and Cdc42, and has an important role in actin filament formation and focal adhesions (95). The DLC-1 gene acts as a tumor suppressor gene in breast cancer and genomic deletion of DLC-1 is associated with a variety of cancers including lung, breast, prostate, kidney, colon, uterus, ovary, liver and stomach (reviewed (94,96)). In addition to suppressing tumor growth, DLC-1 has been shown to be a metastasis suppressor in breast cancer cells (97). When DLC-1 is artificially overexpressed *in vitro*, a decrease in cell growth and colony formation can be observed, while the introduction of DLC-1 cDNA *in vivo* abolishes the

tumorigenicity of cancer cells in nude mice, supporting its role as a tumor suppressor (94,98).

Another Rho GTPase regulator is T-cell lymphoma invasion and metastasis-inducing protein 1 (Tiam1) (99). Tiam1 is a fast-cycling GEF exchange factor for Rac, which is responsible for lamellipodia formation necessary for cell movement during migration and invasion (74,100). Tiam1 controls the functioning of cell-cell adhesions including tight junctions and E-cadherin based adherens junctions (101,102). Any disruption in these cell-cell adhesions allows tumor cells the opportunity to invade the circulatory system and metastasize. Like most biological systems, maintaining proper function regarding Tiam1 is a fine balancing act. Loss of Tiam1 causes cells to undergo epithelial mesenchymal transition (EMT), which results in the loss polarity and cell-cell adhesion properties leading to invasive tendencies (101,102). However, increased Tiam1 also correlates to an increase in the invasiveness and advanced degree of progression particularly in breast cancer (103,104).

While Rho-GTPases play important roles in tumorigenesis, it is imperative to consider upstream signaling proteins. For example, one experiment investigating Tiam1 function in mammary tumorigenesis crossed Tiam1 knockout (Tiam1^{-/-}) mice with breast cancer prone HER2/neu or Myc mice (105). Mammary tumor formation was not affected in the Tiam1^{-/-};Myc mice, but it was impaired in the Tiam1^{-/-};neu crosses, suggesting a vital role for Tiam1/Rac interaction in HER2/*neu* tumors (105).

1.8 The PyMT Mouse Model of Breast Cancer

Simulating the intricacies of a living system *in vitro* is complicated, expensive and unfeasible. Manipulated animal models are important tools in scientific research and aid in understanding how cellular pathways, drug treatments, etc. might function in a complex system.

The mouse mammary tumor virus-polyoma middle T-antigen (MMTV-PyMT) mouse model is a genetically engineered metastatic breast cancer model, functioning similar to human metastatic breast cancer both histologically and molecularly (106). Cancer in this mouse model is characterized by “short latency, high penetrance, and a high incidence of lung metastasis occurring independently of pregnancy and with a reproducible kinetics of progression” (107). Like human breast cancer, these mice gradually lose steroid hormone receptors such as the estrogen and progesterone receptors, and they overexpress HER2 and cyclin D1 which is associated with higher rates of breast cancer (13,108–110). Additionally, advanced cases of mammary gland tumors develop metastatic lesions in the lung and lymph nodes.

“In the MMTV-PyMT mouse model, the mouse mammary tumor virus (MMTV) promoter drives the expression of Polyoma Middle T-Antigen (PyMT) in the mammary epithelium and other organs” (111). PyMT, a scaffold protein, binds and activates members of the tyrosine kinase family activating cellular signaling pathways including the Ras/Raf/MEK and PI3K/Akt pathways which play vital roles in cell growth (112,113). Activation of these signaling proteins

leads to mammary epithelium transformation and the appearance of multifocal mammary adenocarcinomas (111).

In mouse mammary glands, terminal end buds form when the mouse goes through puberty and ovarian hormones are released (107). These terminal end buds invade the mammary gland fat pads forming branches (107). During pregnancy and lactation epithelial differentiation occurs and afterwards apoptosis and redifferentiation allow the epithelial cells to return to normal (107). The processes that allow the mammary gland to change for lactation and back again are the same processes that are exploited by cancerous cells to grow and invade tissue (107). Expression of PyMT causes transformation of the mammary epithelium independent of pregnancy related hormones. These changes result in the growth of adenocarcinomas in the mammary glands followed by metastasis to the lung and lymph nodes (106,111). The changes that occur in MMTV-PyMT mice during mammary gland tumor formation, including hyperplasia, adenoma, and early/late carcinoma are the same processes that occur in humans which makes this mouse ideal models for human breast cancer (114).

1.9 Objective Study

The purpose of this study was to characterize a role for (R)-ketorolac as a breast cancer growth and metastasis inhibitor. Breast cancer is a deadly disease that can be difficult to treat due to its heterogenic nature and ability to develop resistance to available treatments. Racemic ketorolac has shown promise of being effective at preventing early relapse in breast cancer patients, but is contraindicated for long term use (43).

Using high throughput screening and cheminformatics approaches, the (R)- enantiomer of ketorolac was identified as a selective inhibitor for Rac1 and Cdc42 activation (51). Docking predictions of (R)-ketorolac on Rac1 and Cdc42 suggest that the rotational configuration of (R)-ketorolac exposes carboxylate moieties which allows for the chelation of magnesium, leading potentially to nucleotide dissociation (disintegration of Rho-GTPase binding) (51).

Recent work has shown that (R)-ketorolac directly inhibits Rac1 and Cdc42, but not RhoA, through an allosteric mechanism preventing invasion and metastasis in ovarian cancer (45,50). We hypothesize that (R)-ketorolac selectively inhibits Rac1 and Cdc42 activity in breast cancer, leading to a significant decrease in mammary tumor invasion and metastasis. Our focus on (R)-ketorolac will lead to the repurposing of an FDA approved drug as a new non-cytotoxic therapeutic for breast cancer.

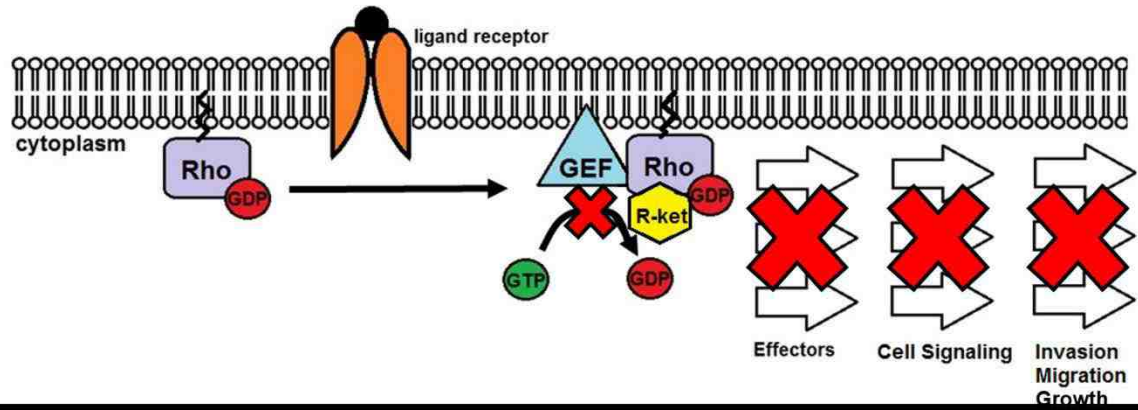


Figure 1.3 Hypothesized Mechanism of Action of (R)-Ketorolac

We hypothesize that (R)-ketorolac selectively binds to Rho-GTPases, Rac1 and Cdc42, preventing the binding of GTP and thus activation of downstream effector proteins involved in cell signaling pathways important in breast cancer cell invasion and migration.

2. THE EFFECTS OF KETOROLAC AND ITS ENANTIOMERS ON BREAST CANCER CELLS *IN VITRO*

2.1 Introduction

Small molecule screening of the Prestwick Chemical Library® coupled with cheminformatics analysis has identified the (R)- enantiomer of ketorolac as having a binding affinity for members of the Rho-GTPase family (40). Racemic ketorolac is an NSAID routinely given to patients in a clinical setting to manage pain and inflammation (48). Patients receiving racemic ketorolac when undergoing tumor reduction surgery demonstrate an improved outcome in both ovarian and breast cancer cases (45,47,115). Until recently, assumptions were made that only the (S)- enantiomer of ketorolac had activity, while the (R)- enantiomer was inert (48,71). However, recently (R)-ketorolac has been shown to be a selective inhibitor of Rac1 and Cdc42, affecting downstream signaling pathways involved in cellular invasion and migration in ovarian cancer cells (50).

GTPases are predicted to regulate proliferation and invasion. In a cell, growth and movement rely on the coordination of polymerization and depolymerization of actin and microtubule dimers that make up the cytoskeleton. This coordination is regulated by cell signaling pathways requiring the activation and deactivation of multiple signaling proteins, including Rho-GTPases. As discussed previously, Rho-GTPases Cdc42, RhoA, and Rac1 work together to direct actin polymerization near the leading edge of a cell for protrusion and forward movement, and depolymerize actin near the trailing edge of the cell for membrane retraction (74,72,88,91). These same actions, regulated by the same

Rho-GTPases are also important when directing the cytoskeleton in cell division during growth (75). Previous research has demonstrated the vital role played by Rho-GTPases in cell proliferation and invasion. When any one of these regulatory proteins is knocked out or disabled, there is a significant decrease in the ability of cells to proliferate and invade (reviewed (75)). Using (R)-ketorolac to bind to and inhibit Rho-GTPase proteins is predicted to interfere with coordination of the cytoskeleton, interfering with tumor cell proliferation and invasion, but not cell viability.

(R)-ketorolac's ability to inhibit Rho-GTPases in ovarian cancer cells, and the positive effects racemic ketorolac has on preventing relapse in ovarian and breast cancer patients, has prompted us to study the mechanism of action of (R)-ketorolac in breast cancer cells. In this study we were interested in distinguishing the differences between (R)- and (S)- ketorolac on proliferation and invasion. Viability assays were conducted on breast cancer cell monolayers and MCAs using both an invasive breast cancer cell line, MDA-MB-231, and a non-invasive breast cancer cell line, MCF-7. Ketorolac's interaction with normal cell cycle was assessed using flow cytometry. Colony forming assays were conducted to examine the effects of ketorolac on cell growth. Migration assays were performed to determine if ketorolac inhibited the migratory ability of breast cancer cells. Finally, MMP9, an enzyme involved in the breakdown of the extracellular matrix, was measured in ketorolac treated cells.

2.2 Materials and Methods

2.2.1 Materials

Ketorolac-tris salt was purchased from Sigma-Aldrich and made into 10 mM stock aliquots in deionized (DI) water. (R)- and (S)- ketorolac enantiomers were purchased from Toronto Research Chemicals and reconstituted according to the package instructions. Etoposide was purchased from Trevigen. Taxol was purchased from Enzo Lifesciences.

2.2.2 Cell Culture

MCF-7 cells (non-invasive human breast adenocarcinoma) and MDA-MB-231 (invasive human breast adenocarcinoma) cells were a generous gift from Dr. Kristina Trujillo (Department of Cell Biology and Physiology, UNM, Albuquerque, NM). MCF-7 and MDA-MB-231 cells were grown in Dulbecco's Modified Eagle Medium (DMEM) (Sigma-Aldrich, St. Louis, MO) supplemented with 10% FBS (Atlanta Biologicals, Norcross, GA), 1% penicillin/streptomycin (Gibco, Grand Island, NY) and 1% Insulin-Transferrin Selenium-A (Gibco, Grand Island, NY). Cells were split 1:3 when they had reached 70-80% confluency. OVCA 433 cells (epithelial ovarian cancer cells) were provided by Dr. Robert Bast Jr., M.D. Anderson Cancer Center, Houston TX and grown in DMEM supplemented with 10% FBS, 0.5% penicillin/streptomycin, and 1% L-glutamine (Gibco, Grand Island, NY), and 1% sodium pyruvate (Sigma-Aldrich, St. Louis, MO). Cells were split 1:4 when they had reached 70-80% confluency. All cell lines were incubated at 37°C and 5% CO₂.

2.2.3 MCF-7 Monolayer and MCA Viability with Racemic Ketorolac

MCF-7 cells were seeded at 15,000 cells/mL (100 μ L/well) into flat bottom 96-well plates, for monolayers, and into Lipidore U-bottom 96-well plates, for multi-cellular aggregates (MCAs), and incubated overnight at 37⁰C and 5% CO₂. A 10 mM ketorolac stock in DI water was diluted with cell culture medium to a 300 μ M ketorolac stock. Eight stock treatments were further created by diluting the 300 μ M ketorolac stock solution with cell culture medium. 50 μ L of each stock treatment was added to respective wells, which already contained 100 μ L of media for the final indicated concentrations.

An 80 μ M etoposide stock solution in cell culture media was used as a positive control, adding 50 μ L into each well containing cells and 100 μ L of cell culture media for final well concentrations of 40 μ M etoposide. Cells were treated in quadruplicate, in both MCA and monolayer plates. The plates were tapped gently to mix and incubated for 48 hours. After the incubation period, 15 μ L of 10X PrestoBlue (Invitrogen, Carlsbad, CA) was added to each well, the plate was tapped gently to mix and incubated at 37⁰C. Well fluorescence readings were taken on a SpectraMax M2 plate reader at 2, 4, 6, and 24 hours. The experiment was repeated a total of three times using the 24 hour PrestoBlue time point.

2.2.4 MCF-7 and MDA-MB-231 Monolayer Viability with Ketorolac

Enantiomers

MCF-7 and MDA-MB-231 cells were plated into 96-well plates at 15,000 cells/mL (100 μ L/well) and allowed to adhere overnight in 37⁰C and 5% CO₂ conditions. 300 μ M stock solutions of each racemic ketorolac, (R)-ketorolac, and

(S)-ketorolac were made in supplemented DMEM media, and 240 μM stock solution of etoposide was made in supplemented DMEM media as a control. In quadruplicate, 50 μL of drug-free supplemented DMEM media was added to all wells designated as non-treated wells and empty wells, with no cells. 50 μL of each of the corresponding stock solutions were added to their respective wells for final well concentrations of 100 μM of each ketorolac treatment and 80 μM of etoposide treatment. The plate was tapped gently to mix and incubated for two days. After the incubation period, 15 μL of 10X PrestoBlue was added to each well and the plate was returned to the incubator. Well absorbency readings were taken at 2, 4, 6, and 24 hours. A one-way ANOVA statistical analysis with a Dunnett's multiple comparison test was used to compare all treatment groups. This experiment was repeated three times.

2.2.5 MCF-7 Cell Cycle with Racemic Ketorolac

MCF-7 cells were seeded at 2.5×10^5 cells/mL with 1 mL/well into 24-well plates and allowed to adhere overnight. Ketorolac stock solutions were made in supplemented DMEM media at 10 μM , 30 μM , 100 μM , and 300 μM from a 10 mM ketorolac stock and 0.5 μM taxol was used as a positive control.

Old DMEM was removed and new DMEM containing ketorolac was added to the wells in triplicate at 1 mL/well. Cells were incubated for 48 hours then washed once with 1X PBS. A few drops of trypsin were used in each well to detach adherent cells then neutralized with DMEM. Samples were moved into 15 mL conical tubes, pelleted, and supernatant was removed. Each sample was re-suspended in 5 mL of PBS and centrifuged at 2500 rpm for 5 minutes as a

washing step. Supernatant was again removed, samples were re-suspended in 1 mL of freshly made propidium iodide (PI) staining solution and incubated for 30 minutes. PI dye was made by mixing 20 mL of 0.1% Triton X-100 in 1X PBS, 40 μ L DNase-free RNase-A (100 mg/mL in PBS) (2 mg total) and 800 μ L of 500 μ g/mL PI stock. Samples were analyzed on a Becton Dickinson FACScan flow cytometer (Immunocytometry Systems) at 20,000 events. Three independent experiments were conducted and a two-way ANOVA with a Bonferroni post-test was used to calculate significance.

2.2.6 Colony Forming Assays – MDA-MB-231

MDA-MB-231 cells (500 cells/mL) were plated in a 24-well plate at 1 mL/well and incubated in 37⁰C and 5% CO₂ conditions to adhere overnight. Cells were treated in triplicate with either 100 μ M racemic ketorolac or the same volume of cell culture media as a control. The cells were allowed to grow for 16 days after treatment. Cells were replenished with fresh culture media and drug on day 6. Intermittently throughout the study, three areas of each well were imaged with the 4X objective and the number of colonies observed in the three images for each well was recorded. Image J software was used to calculate the total area of colony growth for each well. Total area and total colony number per well were calculated and results from the three wells per treatment were averaged. Results were normalized to the placebo control.

2.2.7 Invasion Assays – MDA-MB-231

Invasion assays were conducted using a Cultrex® 3-D Spheroid Cell Invasion Assay kit (Trevigenn Gaithersburg, MD) and MDA-MB-231 cells. Cells

were plated and treated according to the manufacturer's protocol. These cells did not receive any treatment, as this was a test to see if the cells had invasive properties. MCAs were imaged over the course of 7 days.

2.2.8 Migration Assays – MCF-7 and MDA-MB-231

MCF-7 cells (5×10^4 cells/mL) and MCF10A cells (5×10^4 cells/mL) were grown in 8 micron pore Boyden chamber inserts (Becton Dickinson Labware). Cells were serum deprived for 24 hours before treating with 10 μ M, 30 μ M, 100 μ M, 300 μ M ketorolac or 50 μ M NSC23766 (Tocris Bioscience) as a control, 20 nM EGF was added to half of the wells. Cells were allowed to migrate for 48 hours and non-migratory cells were removed. Migratory cells were fixed in ice-cold 100% methanol and stained with 0.02% crystal violet in 10% ethanol. Migratory cells were imaged and counted on an Olympus 1X70 inverted microscope. The total number of migratory cells present in three separate images per membrane were manually counted and averaged. Each migration assay was repeated a minimum of three times and significance was determined using a 1-way ANOVA test. This work was performed in the Hudson lab by S. Ray Kenney.

2.2.9 Zymography – MMP Expression

Sample Preparation

MCF-7, MDA-MB-231, and OVCA 433 cells were seeded into 6-well plates at 5×10^5 cells/mL at 1 mL/well and allowed to grow to 80% confluence in 37°C and 5% CO₂ conditions. Cells were serum deprived by washing in PBS and replacing media with a low serum media containing 1% Bovine Serum Albumin (BSA) for at least 24 hours before adding ketorolac treatments. Cells were

pretreated with 0 μ M, 10 μ M or 100 μ M ketorolac. The plates were incubated for two hours and then half of the wells received 10 nM EGF treatments. The plate was incubated for 24 hours then conditioned media and cell lysates were collected on ice. Media from each sample was transferred to epitubes and centrifuged at 1,000 g for 10 minutes to pellet cell debris. Aliquots of the centrifuged media were transferred into new epitubes and kept at -80°C until needed for further analysis. Sample wells were washed twice with cold PBS and then 70 μ L of 0.1% Triton-X100 in PBS was added to each well and the plate was rocked at 4°C for 30 minutes to lyse cells. Lysate was scraped from the wells and moved to epitubes for 10 seconds of probe sonication using a Branson Sonifier Cell Disruptor 200, then centrifuged for 10 minutes at 10,000 g at 4°C . Supernatant was collected and stored at -80°C until needed for BSA protein assays. BSA protein assays were conducted to determine lysate protein concentration and thus relative media protein concentration as described in the Pierce Protein Assay Kit protocol.

Gel Preparation and Electrophoresis

Samples were run on a 10% SDS-polyacrylamide (Biorad) gel containing 1.5% (w/v) gelatin (Sigma G-2625 gelatin 175 bloom). Conditioned medium (10 μ L), collected earlier from treated cells was combined with 4X non-reducing sample buffer (4.6 mL dH_2O , 0.5 mL 1 M Tris pH 7.4, 1.5 mL glycerol, 0.8 mL 20% SDS, 25 mg bromophenol blue) in a 1:3 sample to sample buffer ratio. Each sample was loaded on the gel along with a stained molecular weight (MW) marker. Gels were run on a Western blot apparatus at 95V until the bands

migrated through the stacking gel, then at 125V until the bands were near the bottom of the gel. Once the run was finished, gels were incubated for 30 minutes at room temperature in renaturing buffer (2.5% Triton X-100 (v/v) in dH₂O), changed to developing buffer (50 mM Tris, pH 7.6, 0.2 M NaCl, 5 mM CaCl₂, 0.2% (w/v) Brij-35, dH₂O pH 7.6) for 30 minutes and then left in fresh developing buffer for 24 hours at 37°C. Gels were then stained in 0.1% PhastGel Blue R (Sigma) in acetic acid for 30 minutes and destained in 10% acetic acid in dH₂O overnight. Proteinase activity was indicated by the presence of zones of staining inhibition. Gels were imaged on a FluorChem R (ProteinSimple, San Jose, CA) and densitometry was analyzed using ProteinSimple AlphaView 3.4 software. Each experiment was repeated a minimum of three times.

2.3 Results

2.3.1 MCF-7 Monolayer and MCA Viability with Racemic Ketorolac

Cell viability assays were performed on MCF-7 breast cancer cell lines to determine if racemic ketorolac affected viability. In both MCF-7 monolayers and the more organotypic multicellular aggregates (MCAs), ketorolac had no effect on cell viability after 48 hours of treatment. Etoposide, a DNA-topoisomerase II inhibitor known for inhibiting cell division by causing DNA strand breaks, was used as a positive control (116,117). Varying incubation times with PrestoBlue revealed the optimal time point at which to take plate readings. Incubation with PrestoBlue for 24 hours was used on all subsequent assays. A one-way ANOVA statistical analysis was used to compare all treatment groups. The etoposide treatment was the only group found to be significantly different from the control

with a p value < 0.05. Visual inspection of the cells showed little to no changes in morphology in cell density or MCA structure when comparing the non-treated and 100 μ M ketorolac-treated cells.

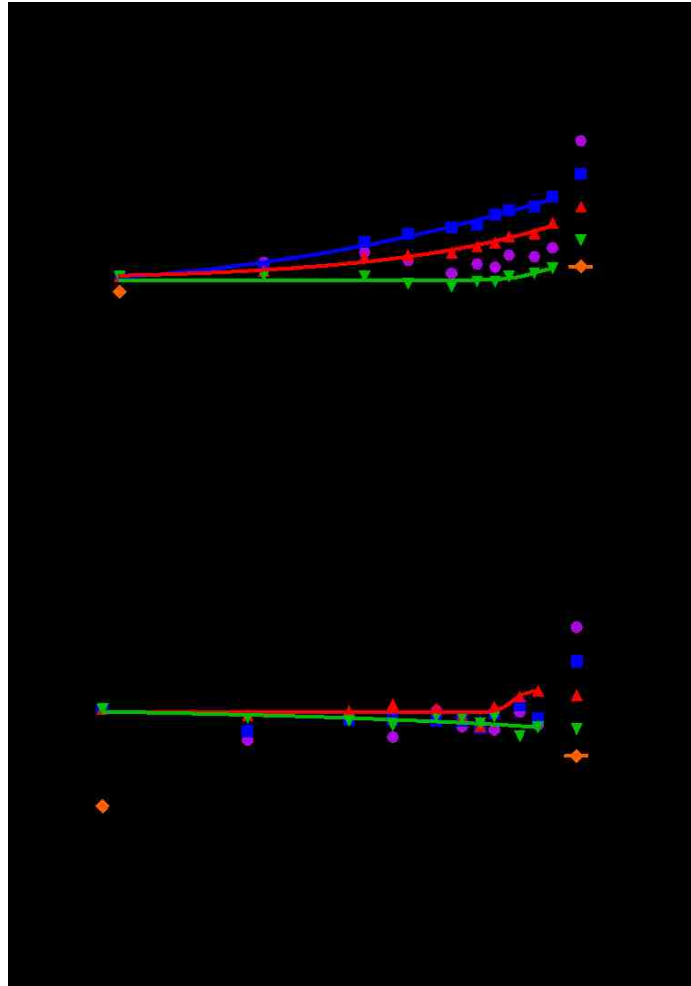


Figure 2.1 MCF-7 Viability with Racemic Ketorolac on MCAs and Monolayers at Multiple Time Points

Viability assays were conducted on MCF-7 monolayers (A) and MCAs (B). Cells were treated for 48 hours and incubated with PrestoBlue at multiple time points to determine the optimal PrestoBlue incubation time. Etoposide was used as a positive control and was significantly different from the ketorolac treated cells ($p < 0.05$). There was no a change in cell viability with ketorolac treatment concentrations up to $100 \mu\text{M}$. Twenty-four hours was chosen as the optimal PrestoBlue incubation time due to the small variability in relative fluorescence when compared to other time points.

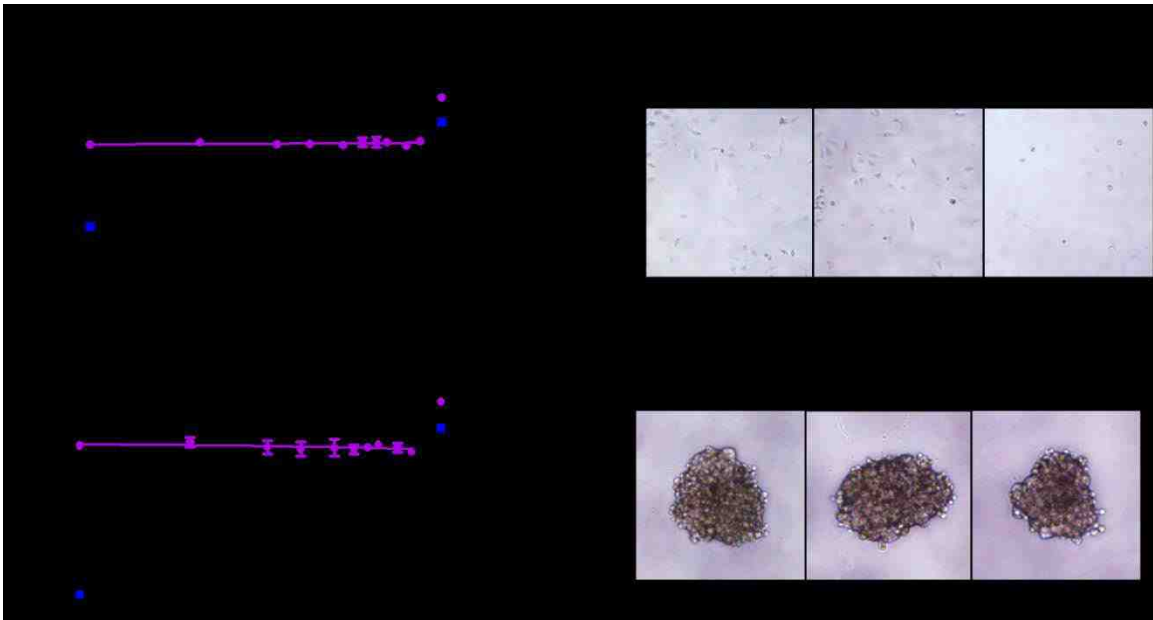


Figure 2.2 MCF-7 Viability on MCAs and Monolayers with Racemic Ketorolac - Ketorolac has no effect on the viability of MCF-7 monolayer or MCA cells.

MCF-7 monolayers (A) and MCAs (B) were treated with ketorolac for 48 hours. Representative images show no difference in cell morphology. Etoposide (80 μ M) was added to MCF-7 monolayers and MCAs for 48 hours as a positive control. Cell viability was assessed using PrestoBlue and a colorimetric plate reader as described in the methods. A one-way ANOVA was used to calculate significance.

2.3.2 MCF-7 and MDA-MB-231 Monolayer Viability with Ketorolac Enantiomers at Varying PrestoBlue Incubation Times

MCF-7 and MDA-MB-231 monolayer cells were treated with either 100 μ M racemic ketorolac, (S)-ketorolac, (R)-ketorolac, or 80 μ M etoposide. In MCF-7 monolayers, at the 2, 4, and 6 hour PrestoBlue time points, (S)-ketorolac had a statistically significant increase in fluorescence from the untreated control with a $p < 0.05$. At 24 hours incubation with PrestoBlue, (S)-ketorolac treatment was no longer statistically different from the untreated control. Racemic and (R)-ketorolac treatments in MCF-7 monolayers were not different from the untreated control at any of the PrestoBlue incubation time points.

None of the ketorolac treatment groups were statistically different from the control group in MDA-MB-231 monolayers at any of the incubation time points. In both experiments, etoposide was statistically decreased from the untreated control at all PrestoBlue time points, with p -value of $p < 0.05$. A one-way ANOVA statistical analysis with a Dunnett's multiple comparison test was used to compare all treatment groups. It is worth noting that the etoposide treatment group's relative fluorescence (an indication of cell viability) was about half that of the normalized control group in the MCF-7 cells but much closer to about 75% of the control group in the MDA-MB-231 cells. As MDA-MB-231s are a more aggressive cell line than MCF-7s, this may indicate a greater resistance to topoisomerase II inhibitors.

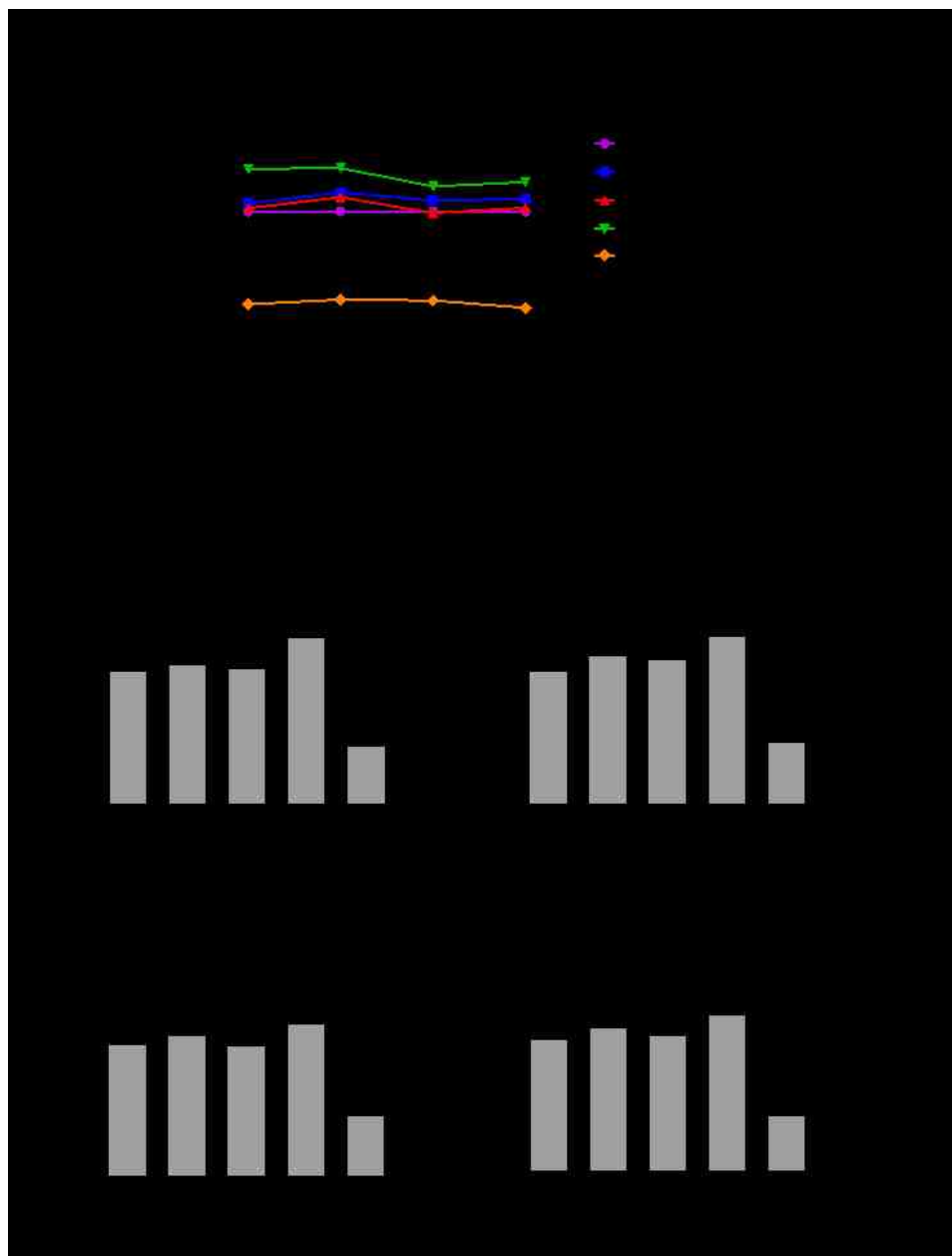


Figure 2.3 MCF-7 Monolayer Viability with Ketorolac Enantiomers

Racemic ketorolac and its enantiomers are non-cytotoxic to MCF-7 monolayers at 100 μ M concentrations. Cell viability with (S)-ketorolac treatment was significantly greater than other treatments at 2, 4, and 6 hours incubation with PrestoBlue but at 24 hours fell within the same range as the other treatments. Etoposide significantly decreased cell viability at all time points.

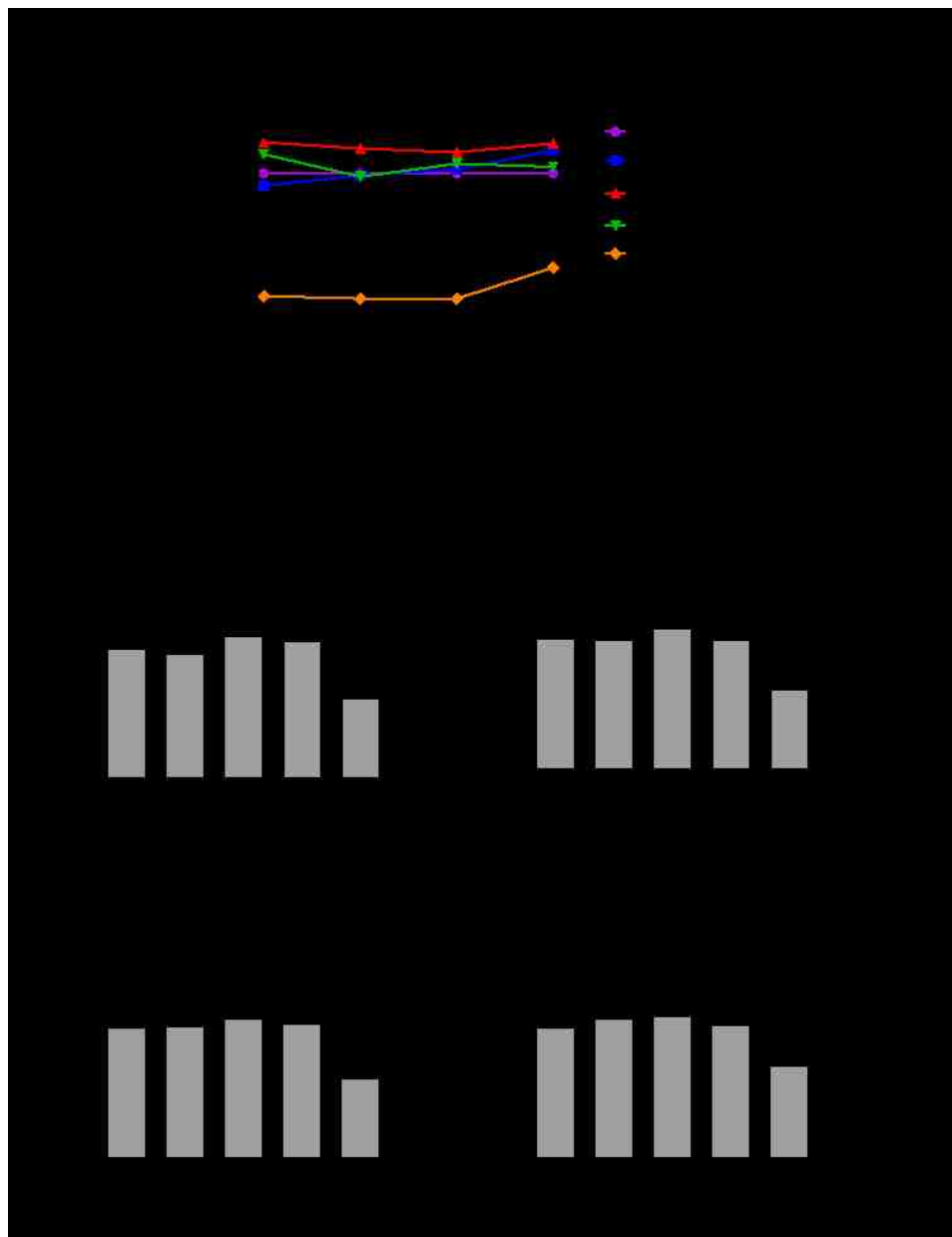


Figure 2.4 MDA-MB-231 Monolayer Viability with Ketorolac Enantiomers

Racemic ketorolac and its enantiomers are non-cytotoxic to MDA-MB-231 monolayers at 100 μM concentrations. Etoposide significantly decreased cell viability at all time points.

2.3.3. Cell Cycle in MCF-7, and MDA-MB-231 Cells Treated with Ketorolac

Cell cycle analysis was performed using flow cytometry to determine if racemic ketorolac causes cell cycle arrest and if it was dose dependent. When cells were treated with 10, 30, 100 and 300 μM ketorolac, there was no change in the cell cycle phase populations when compared to the non-treated (NT) control group. About 20% of cells were in G_0 , 10% in S, and 70% in G_2/M phase in MCF-7 cell lines. In MDA-MB-231 cells, about 30% of cells were in G_0 , 60% in S, and 10% in G_2/M phase. Paclitaxel, a mitotic inhibitor, was used at 0.5 μM as a positive control and showed statistically significant changes in cell cycle when compared to control treatments. In MCF-7 cell lines, the paclitaxel treated cells had a greater percentage of cells in the G_0 phase, and fewer cells in the G_2/M phase, while there was no difference between any of the treatment groups for the S phase of cell cycle. In MDA-MB-231 cells paclitaxel treated cells had a greater percentage of cells in the G_0 phase, and less cells in the S phase, while there was no difference between any of the treatment groups for the G_2/M phase of cell cycle. Significance was determined using a two-way ANOVA analysis with a Bonferroni post-test. Significant differences had p-values of $p < 0.001$.

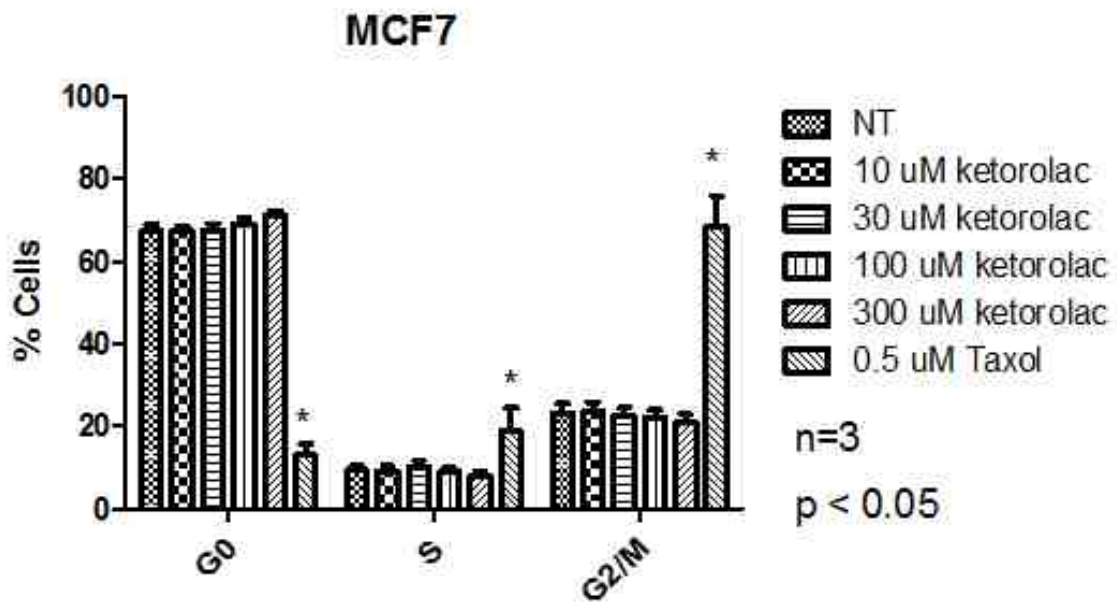


Figure 2.5 Ketorolac Does Not Change Cell Cycle of MCF-7 Cells at Concentrations Up To 300 μ M

MCF-7 cells were treated with ketorolac and cell cycle was analyzed using flow cytometry. Ketorolac does not arrest the cell cycle in MCF-7 cells at concentrations up to 300 μ M. Ketorolac treated cells have the same percent of cells in each phase of the cell cycle as the NT control. Taxol was used as a positive control and had a significant percent of cells arrested in the G₀ phase of the cell cycle when compared to the NT control.

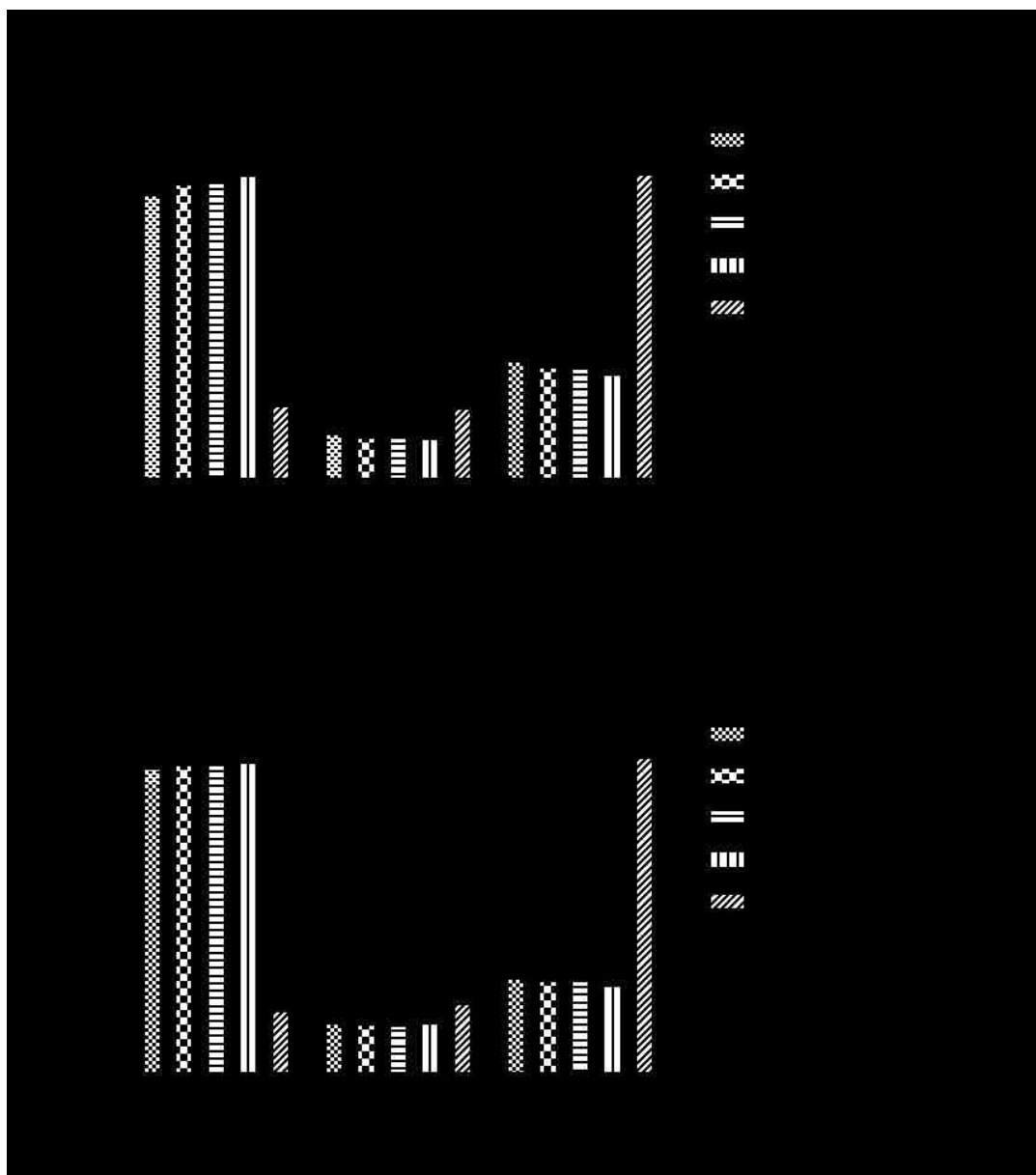


Figure 2.6 Ketorolac and Its Enantiomers Do Not Affect Cell Cycle in MCF-7 and MDA-MB-231 Cells at 100 μ M Concentrations

MCF-7 (A) and MDA-MB-231 (B) cells were treated with 100 μ M of ketorolac or ketorolac enantiomers and cell cycle was analyzed using flow cytometry. In MCF-7 and MDA-MB-231 cells, racemic ketorolac and its enantiomers did not cause cell cycle arrest. The Taxol control had a significant percent of cells arrested in the G₀ phase of the cell cycle when compared to the NT control.

2.3.4 Colony Forming Assays – MDA-MB-231

MDA-MB-231 cells were treated with 100 μ M ketorolac and imaged for colony formation over 16 days. The total number of colonies formed reached a peak at day 6 in both placebo and ketorolac treated cells, with the placebo treated cells forming more individual colonies than the ketorolac treated cells. As the experiment progressed, individual colonies merged into larger, single colonies, resulting in fewer total numbers of colonies counted. By day 16, many of the cells had died and there was only cell debris floating in the media. The total area of colony formation increased over the course of the study and then decreased at day 16 due to cell death from age. Overall, the placebo cells had more growth than the ketorolac treated cells. Ketorolac treatment inhibited MDA-MB-231 cell colony formation and growth. These assays were repeated a minimum of three times and analyzed using a two-way ANOVA. Although trends were observed, changes in colony formation over time were not significant between treatment groups.

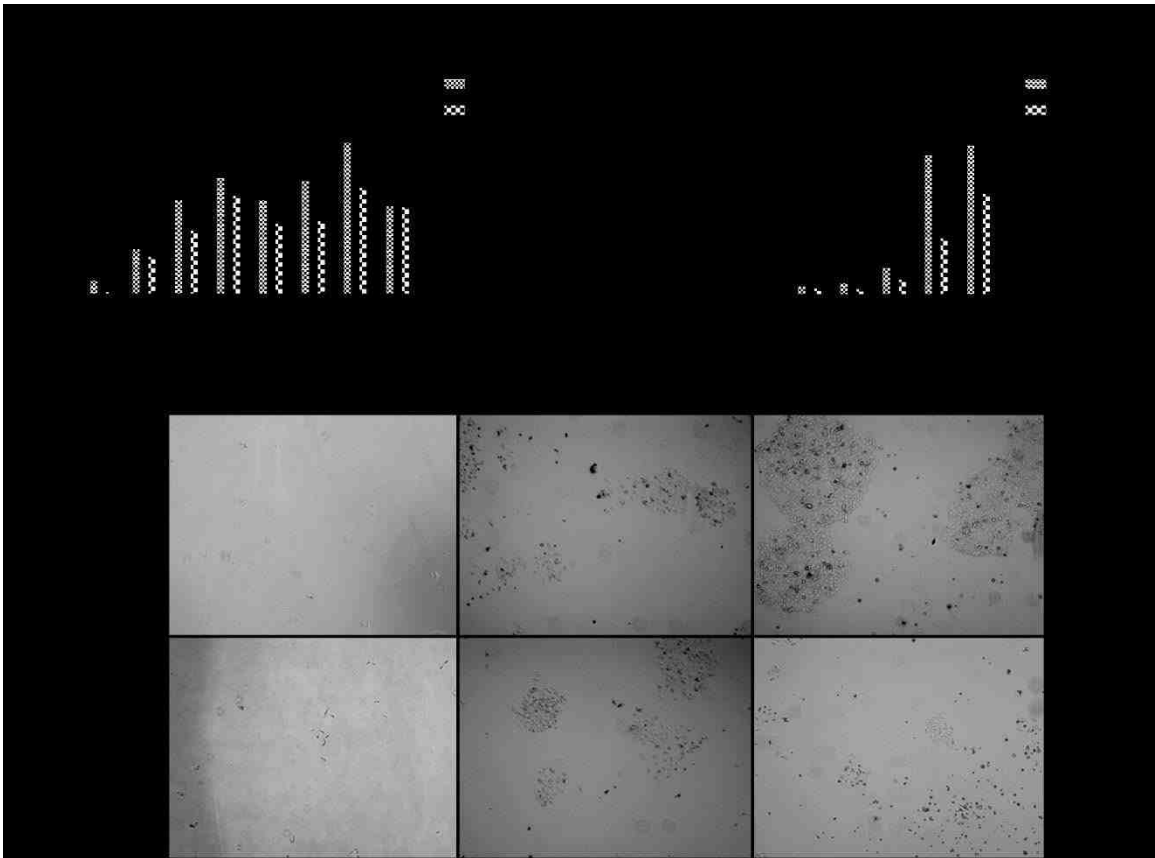


Figure 2.7 Ketorolac Inhibits MDA-MB-231 Colony Formation

MDA-MB-231 cells were plated sparsely, treated with 100 μ M racemic ketorolac, and imaged for 16 days. The number of individual colonies formed, increased and then slowly decreased over time as multiple colonies merged onto a single larger colony. Placebo treated cells grew greater numbers of colonies than ketorolac treated cells (A). The total area of colonies increased over time but ketorolac treatment inhibited total area growth of colonies. (B). Representative images are shown (C).

2.3.5 Invasion Assays – MDA-MB-231

MDA-MB-231 cells were plated according to protocol instructions using the Cultrex® 3-D Spheroid Cell Invasion Assay kit (118). In the kit's example, MDA-MB-231 MCAs that did not receive matrix remained a similar size to the starting MCA. MDA-MB-231 MCAs that received the invasion matrix grew in area over the course of the study (Fig 2.8 A & B) (118). When the MDA-MB-231 cells in our lab were analyzed followed using the kit protocol, MCAs resembled those in the kit example that had not received invasion matrix (Fig 2.8 C). The MCAs did not change significantly in area over the course of the study (Fig 2.8 D).

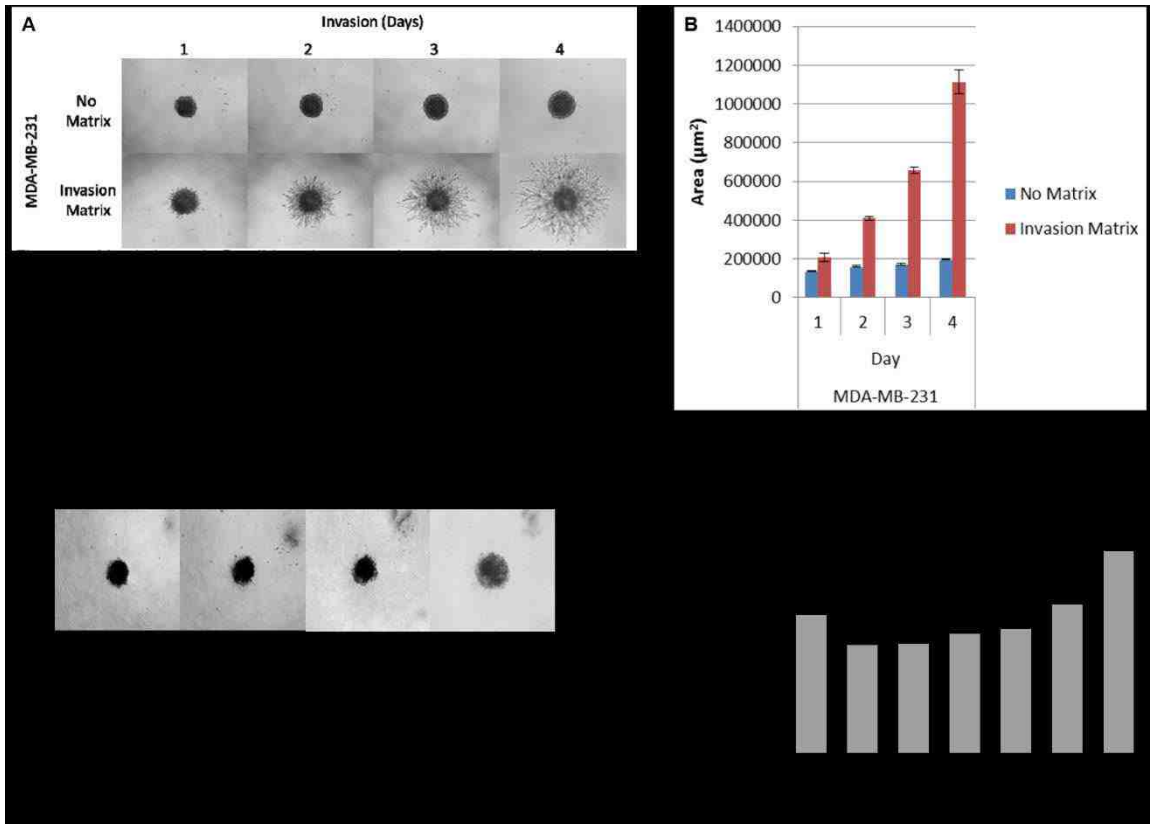


Figure 2.8 MDA-MB-231 Cells Did Not Exhibit Expected Invasive Properties

The invasion assay showed images of MDA-MB-231 cells under invasive and non-invasive conditions. With matrix, cells invaded and without matrix they did not invade (A) (118). The protocol's example graph of MCA diameter shows increased area over the course of the study (B) (118). The MDA-MB-231 cells in our lab were not invasive. The cells resembled the cells in the protocol that were not given matrix (C). The MCAs remained small and did not significantly increase in area over the course of the study (D).

2.3.5 Migration Assays – MCF-7 and MDA-MB-231

MCF-7 and MCF-10A cells were treated with ketorolac at increasing concentrations. There was a dose dependent decrease in the number of cells that were able to migrate through the Boyden chamber pores. The experiment was repeated a minimum of three times and results were found to be statistically significant using a 1-way ANOVA test. This work was conducted by S. Ray Kenney.



Figure 2.9 Ketorolac Inhibits MCF-7 and MCF-10A Migration in a Dose Dependent Manner

Migration was inhibited by ketorolac treatment. Increasing concentrations of ketorolac resulted in fewer migratory cells in both MCF-7 (A) and MCF-10A (B) cell lines. Migrations assays were done by Dr. S. Ray Kenney.

2.3.6 MMP Expression

Matrix metalloproteinase 9 (MMP9) expression was measured in the media of MCF-7 and MDA-MB-231 cells treated with ketorolac and supplemented with epidermal growth factor (EGF). While MMP9 activity was present in all the samples, there was no significant difference between treatment groups in either the MCF-7 cells or the MDA-MB-231 cells. Changes in MMP9 activity in MCF-7 cells were not expected because it is a non-invasive cell line, but there was no change in the MDA-MB-231 invasive cell line either. These results suggest that ketorolac treatment is not affecting the baseline MMP9 activity. Additionally, the MDA-MB-231 cells are not expressing the invasive qualities expected from this cell line. The experiment was repeated three times and results were analyzed using a student's t-test.

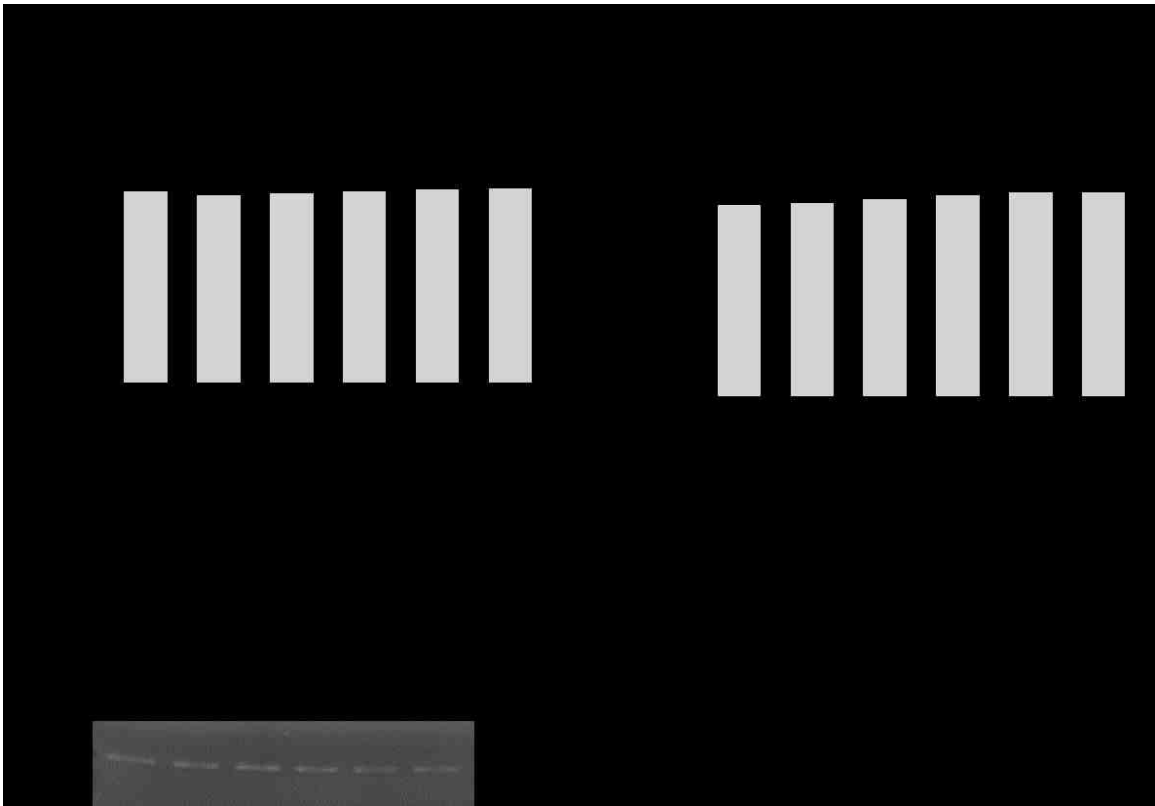


Figure 2.10 MMP Expression Does Not Change with Ketorolac Treatment

MCF-7 (A) and MDA-MB-231 (B) cells were treated with racemic ketorolac and EGF. Representative gel from MCF-7 cell samples show clear MMP9 bands (C). Protein and conditioned media was collected to examine the amount of MMP9 enzyme present using zymograms. There was no significant change in the relative amount of MMP9 detected when treated samples were compared to non-treated samples. MDA-MB-231 and MCF-7 cells had slightly more MMP9 present when treated with EGF in addition to the ketorolac and the amount of MMP9 increased with increasing ketorolac concentration, but the change was not significant. Band density was normalized to the non-treated control. Statistics were conducted using a one way t-test.

2.4 Discussion

These *in vitro* studies were conducted with two goals in mind. The first was to confirm that the ketorolac concentrations used in the studies were non-toxic and the second was to test whether ketorolac decreases breast cancer cell proliferation. There is evidence that (R)-ketorolac inhibits Rho GTPase activity (51). Members of the Rho-GTPase family are important regulators of cellular functions involved in actin reorganization, cell migration, invasion, proliferation and growth (74). In epidemiological studies of breast cancer patients who were given ketorolac as part of their perioperative care, researchers identified a correlation between ketorolac administration and patient survival (43,115). Other studies have exhibited a positive correlation in the ability of (R)-ketorolac to inhibit ovarian cancer cell migration and invasion both *in vitro* and in clinical studies (45,50). These studies have led us to hypothesize that (R)-ketorolac acts in preventing breast cancer metastasis in much the same way as has been identified in ovarian cancer, by inhibiting the activity of Rho-GTPases, Rac1 and Cdc42.

With the viability studies it was found that racemic ketorolac and its enantiomers do not affect the viability of MCF-7 or MDA-MB-231 cells in either monolayers or MCAs up to 300 μ M concentrations. MCAs are more organotypic but, due to concerns that the drug and the viability assay reagent, PrestoBlue, did not penetrate the MCAs fully, monolayer viability assays were also conducted. Additionally, in some exploratory viability assays, after treating with ketorolac, MCAs were centrifuged in flat bottom plates to break apart and spread

out cells for full PrestoBlue penetration. This method did not make a difference in the cell viability results. Cell viability was the same in non-treated cells as in cells treated with ketorolac, suggesting that the drug is non-toxic. When cell viability is affected by a drug, there is less cell growth and fewer cells on the plate. At greater drug concentrations, cells that are present begin to form apoptotic blebs and have fewer protrusions. Finally, cells begin to pull off of the plate, forming spheroids and floating around the dish, and pieces of un-intact cellular membrane are present in the media. In our cell viability assays there were no visual changes in monolayer or MCA morphology, when cells were treated with ketorolac. Considering these findings, ketorolac does not decrease breast cancer metastasis by causing apoptosis, or cell death, in cancer cells.

Colony forming assays were able to show that while ketorolac is non-toxic, it is able to inhibit cell growth and colony formation, without killing the cells. Breast cancer cells treated with ketorolac were able to grow and form colonies, but at a much slower rate than the placebo treated controls, leading us to hypothesize that the drug is impeding the cell's ability to grow and divide.

MCF-7 and MDA-MB-231 cells were treated with ketorolac and analyzed using flow cytometry to determine if ketorolac causes cell cycle arrest. One mechanism of some anti-cancer drugs, like paclitaxel, is interference with normal microtubule activity (reviewed (38)). When cells cannot properly regulate microtubule polymerization and depolymerization, the cell can get "stuck" in one phase of cell cycle, unable to complete mitosis. The roles Rac1 and Cdc42 have in cytoskeletal reorganization support the theory that arrest of these two Rho-

GTPases may cause cell cycle arrest. When MCF-7 and MDA-MB-231 cells were treated with ketorolac, there was no cell cycle arrest observed. These results indicate that ketorolac does not affect the cytoskeletal polymerization or depolymerization abilities of breast cancer cells.

Based on correlations between ketorolac administration and decreased breast cancer metastasis, we hypothesized that treating breast cancer cells *in vitro* with ketorolac would decrease their migration and invasion abilities (43,46). Zymograms using both MCF-7 and MDA-MB-231 cells were used to examine the effects ketorolac has on MMP9 expression. MMPs are enzymes used by the cell to break down basement membranes, penetrate through blood vessels and metastasize to distant locations (62). If ketorolac was affecting cell invasion and migration via MMP production, we should expect to see a decrease in MMP protein with increasing concentrations of ketorolac. MDA-MB-231 cells are known to be an invasive cell type, while MCF-7 cells are non-invasive, thus a more drastic change in MMP9 production in MDA-MB-231 cells than in MCF-7 cells was expected when treating with ketorolac. While zones of inhibition were observable and measurable in the zymogram gels, there was no significant difference in the band density between treatment groups suggesting that the ketorolac treatment is not affecting the invasiveness of the cells. Also, the MDA-MB-231 cells in our lab do not have invasive qualities expected of them.

Work done in our lab by S. Ray Kenney showed that when MCF-7 and MCF-10A cells were treated with ketorolac, they lost their ability to migrate in a

concentration dependent manner. These same migration assays were conducted in MDA-MB-231 cells and no change in migratory ability was observed.

Invasion assays using untreated MDA-MB-231 cells were conducted to determine if our invasive breast cancer cell line was able to be invasive, however invasion into the matrix gel was not apparent. Combining these results with the lack of migration and considering there was no change in MMP9 expression when cells were treated with ketorolac, it was concluded that the MDA-MB-231 cells in our laboratory are not the phenotypically normal MDA-MB-231 cells we expected to have. The MDA-MB-231 breast cancer cells in our laboratory do not exhibit the migratory and invasive characteristics expected of this cell line. These changes may have been caused by multiple factors such as undergoing too many passages or poor culturing techniques. New MDA-MB-231 cells should be obtained and the *in vitro* assays described here should be repeated.

In future work it would be useful to conduct Western blots to examine the effects of (R)-ketorolac on downstream effectors of Rac1 and Cdc42 in breast cancer cells. This information may reveal the Rho-GTPase activation pathway that is affected by (R)-ketorolac and provide more insight to the exact mechanism of action of the drug.

3. THE EFFECTS OF KETOROLAC ON MAMMARY GLAND CANCER CELL PROLIFERATION AND A STUDY OF ITS POTENTIAL TOXICITY IN PYMT MICE

3.1 Introduction

Breast cancer is the second most commonly diagnosed cancer in women after skin cancer (1). Its heterogeneity and multiple forms of induction, including genetic inheritance, and random mutation, make it a convoluted disease. Overexpression of cell surface receptors like *HER2/neu* can give rise to tumorigenesis by causing uncontrolled activation of proteins involved in cell growth and migration, angiogenesis and anti-apoptotic pathways. Testing anti-cancer drugs in cell culture can tell us how various proteins and signaling pathways may be altered, but it cannot serve as a predictive measure for the complexities of a living system. Reliable animal models allow for the manipulation of signaling pathways involved in tumorigenesis and application of drug treatments before human testing.

MMTV-PyMT mice were chosen as the model system because of their similarities to human breast cancer as well as tumor formation characterized by a short latency and high lung metastasis incidence occurring independently of pregnancy (107). MMTV-PyMT mice develop primary mammary gland tumors around 4-8 weeks of age, externally visible tumors around 10 weeks of age, and

exhibit widespread lung metastasis around 12-14 weeks of age (108).

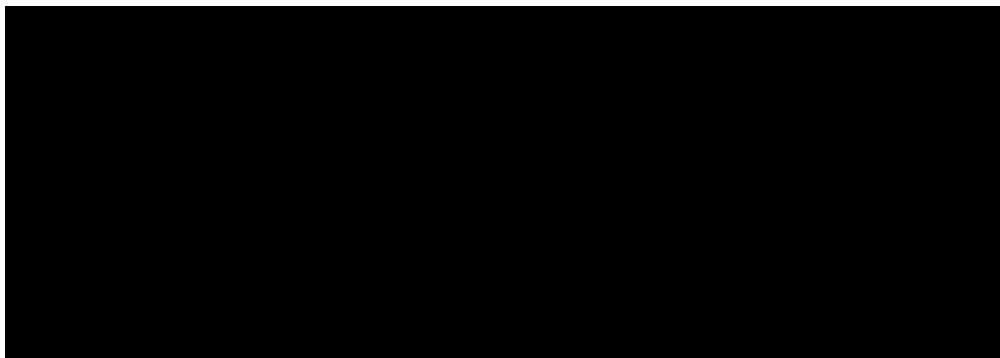


Figure 3.1 MMTV-PyMT Mouse Mammary Tumor Development Timeline

MMTV-PyMT mice develop palpable tumors around 8 weeks of age. Around 10 weeks the tumors become large enough to observe externally and between 12 and 14 weeks of age, the mammary tumors begin metastasizing to the lungs.

As in humans, tumor formation in MMTV-PyMT mice can be categorized into multiple stages according to severity: hyperplasia, adenoma/mammary intra-epithelial neoplasia, and early and late carcinoma (106). These similarities to human breast cancer allow us to examine the effects of anti-cancer drugs at various stages in cancer progression.

In this study we were interested in the potential toxic effects and early therapeutic effects of ketorolac and its enantiomers on an organism. This study was also used to examine initial differences between enantiomer and racemic treatment groups and to provide information for future longer experiments. The mice in this study were examined for any signs of toxic side effects of the drugs and mammary gland samples were collected at the point when hyperplasia was just beginning to become apparent. We hypothesized that racemic ketorolac and

its enantiomers, at this stage, would not present any toxic effects to the organism and that we would observe few effects on early stage mammary gland tumors.

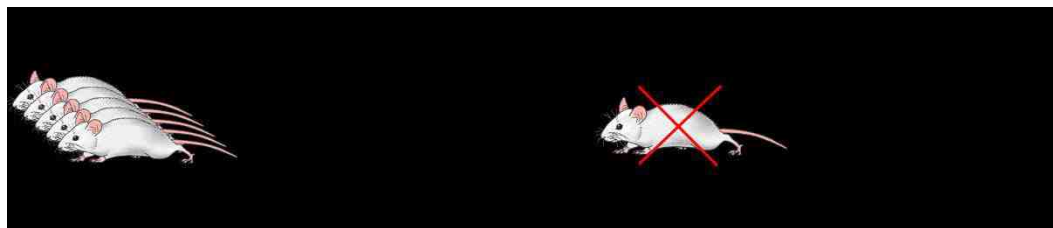


Figure 3.2 *In vivo* Experimental Outline

MMTV-PyMT mice were trained at 5 weeks old to consume a pill containing either ketorolac treatment or placebo treatment. In the short study mice consumed pills containing placebo, racemic ketorolac, (R)-ketorolac, or (S)-ketorolac every 12 hours for 21 days. In the longer studies mice consumed pills containing placebo or (R)-ketorolac every 12 hours, 5 days a week for either 47 (12 week old mice) or 64 (14 week old mice) days. At the end of the experiment, mice were sacrificed, their organs harvested and examined for signs of drug toxicity and tumor burden. (mouse image adapted from http://www.dianliwenmi.com/postimg_4436338_10.html)

3.2 Materials and Methods

3.2.1 Pill Preparation

Estimating an average mouse weight of 22 g, mice were dosed with 1 mg/kg ketorolac twice a day. Pills were made to contain 22 μ g/pill ketorolac. To make 100 racemic ketorolac pills with, 2.2 mg ketorolac tris salt (Sigma #K1136) was dissolved in 200 μ L dH₂O and 2 μ L of 2% bromophenol blue was added to serve as a mixing aid. Then the solution was dropped onto 12 grams of bacon flavored transgenic dough (BioServ #S3472) and mixed with a spatula until no

blue streaks remained. The dough was pressed into a 100 mg pill molds and left to dry for two days (119). Stock solutions of (R)-Ketorolac (Lot # 2-KMT-132-2), and (S)-Ketorolac (Lot # 2-KMT-129-2) (Toronto Research Chemicals Inc.) were made by adding 1 mL of 100% methanol directly to the 5 mg of powdered drug in each vial. To make 100 pills, 440 μ L of the stock solution was combined with bromophenol blue, added to dough, mixed and put into pill molds, as described before.

3.2.2 Mice

FVB/N-Tg(MMTV-PyVT)634Mul/J mice, hereafter referred to as MMTV-PyMT mice were originally obtained from The Jackson Laboratory. The female mice used are heterozygotes bred by crossing a MMTV-PyMT male to a wild type FVB female resulting in approximately half the offspring being transgenic (MMTV-PyMT positive). Animals were housed at the animal research facility at the University of New Mexico Health Sciences Center. They were maintained under a controlled temperature of 22–23°C with a 12hr light, 12hr dark cycle and fed normal chow *ad libitum*. All procedures were approved by the University of New Mexico Institutional Animal Care and Use Committee and carried out in accordance with the NIH Guide for the Care and Use of Laboratory Animals. Animal studies were conducted under an approved protocol 14-101235-HSC.

3.2.3 Experimental Design and Dosing Schedule

Three cohorts of mice were used for this study. At five or six weeks of age, MMTV-PyMT female transgenic mice were housed into treatment groups of 2-3 mice per cage and trained to eat pills by being offered placebo pills twice a day

for three days. An oral route of dosing was chosen to most accurately reflect the kind of drug administration a patient might experience. Standard clinical ketorolac dosing includes one initial IV or IM dose and then, if continued, oral dosing (42). The pill method of dosing was chosen over oral gavage to decrease the amount of stress to which the animals were subjected (119).

After the training period, mice were dosed with 1 mg/kg of correlating drug or placebo every 12 hours for the duration of the study (119). At varying intervals, mice were sedated with isoflurane, weighed and palpated for tumor growth. No tumor became externally visible.

This study included 38 mice. At least one mouse was dropped from the final data sets due to refusal to consume the pill. Mice were housed into one of four treatment groups: placebo, racemic ketorolac, (R)-ketorolac, or (S)-ketorolac and dosed every 12 hours for 20 days. On day 20 of dosing (8 weeks old), mice were sacrificed and organs and tissue were harvested and preserved.

3.2.4 Dissection

Mice were euthanized, two at a time, by injecting 200 μ L of Sleepaway into the peritoneal cavity. After death was confirmed, they were weighed and then doused with 70% EtOH. Cardiac punctures were performed using heparin coated needles and stored in heparin tubes. Blood was stored in epi tubes on ice until it could be separated by centrifuging at 2500 rpm for 10 minutes. Serum was stored at -80°C . Clamping forceps were used to clamp off the right lung which was then cut out and snap frozen in liquid nitrogen. A probe was used to lift the trachea and cut a small slit into which a small blunted needle was inserted and

4% paraformaldehyde (PFA) was injected to gently inflate the left lung. The trachea was clamped off with locking forceps and the lung was separated from the body and kept in 4% PFA at 4⁰C. The stomach was removed, slit open and cleaned out with PBS, and kept in 4% PFA. One kidney from each mouse was removed, weighed, bisected sagittally and fixed in 4% PFA. Sizeable mammary tumors were removed and snap frozen in liquid nitrogen. Skin bands around the 4th mammary glands were removed and pinned to a tray which was then flooded with 4% PFA. The next day the mammary glands were removed from the skin and placed in embedding cassettes in PBS for processing. Axillary and inguinal lymph nodes and a piece of liver were removed and put into epitubes with 4% PFA. Unless otherwise noted, all tissue preserved in 4% PFA was later moved into 50% EtOH or paraffin embedded for permanent storage.

3.2.5 Mammary Tissue Whole Mounts

Mammary glands were isolated from mice in the 21 day study. Mammary glands stored in 4% PFA underwent two changes of acetone over 8-24 hours and then were changed to water for 1 hour. Carmine alum stain (made by combining 1 g carmine, 2.5 g aluminum potassium sulfate and 450 mL dH₂O, boiling for 20 minutes and adjusting the volume to 500 mL with dH₂O and filtering) was used to stain the mammary glands overnight. The mammary glands were sequentially changed into water, 70%, 85%, 95%, 100% and 100% EtOH for one hour each, then left in HemoDE (Electron Microscopy Sciences, Hatfield, PA) overnight. Mammary glands were kept in individual vials in methyl salicylate (Wintergreen) (Sigma-Aldrich, St.Louis, MO). Whole mounts were imaged with

MoticCam 2300 running Motic software on an Olympus SZH dissection microscope. Pixel intensity of tumor and non-tumor areas was analyzed using ImageJ software.

3.2.7 Lung Preservation

Left lungs, previously inflated with 4% PFA, were rinsed twice in PBS and embedded in paraffin. Cassettes containing tissue were immersed in 50%, 70%, 70%, 80%, 95%, 100%, and 100% EtOH, HemoDE twice, and paraffin twice for one hour each. Tissue was embedded in paraffin blocks and, 3-10 μm sections, 100 μm apart were placed on slides, and stained with hematoxylin and eosin (H&E).

3.2.8 Tissue Preservation

Tumor, kidney, liver, and lymph node tissue preserved in 4% PFA overnight was moved into 50% EtOH for permanent storage or was rinsed three times in PBS for at least 30 minutes each time and embedded in paraffin. Cassettes containing tissue were immersed in 50%, 70%, 70%, 80%, 95%, 100%, and 100% EtOH, HemoDE twice, and paraffin twice for one hour each. Tissue was embedded in paraffin blocks and kept at room temperature.

3.2.9 (S)-Ketorolac Mouse Study

Three mice were used in this study to examine the conversion of (S)-ketorolac to (R)-ketorolac. At the beginning of 6 weeks of age, these mice were trained for three days to eat a placebo pill as described before (119). They were then fed a pill containing 1 mg/kg of (S)-ketorolac every 12 hours, 5 days a week, for 7 days. Mice were sacrificed using CO₂ gas, and cardiac punctures were

performed. Blood samples were placed into plain epi tubes. Samples were centrifuged at 2500 rpm for 10 minutes, separated into serum and red blood cells and stored at -80°C , until HPLC could be performed.

3.3 Results - 21 day studies

3.3.1 Weekly and Final Weights

To investigate the effects of ketorolac on tumor growth and to analyze the potential toxic effects of the drug mice were treated with 1 mg/kg of ketorolac or its enantiomers for 21 days. Over the course of the study, mice were weighed as an indicator of positive health and growth. One mouse in the racemic ketorolac treatment group was found to have malocclusions and was ultimately dropped from the study. When the data was normalized the placebo treated mice gained significantly more weight than the R-ketorolac and S-ketorolac treated mice, but not the racemic ketorolac treated mice. These differences may be attributed to differences between litters, as the mice were not randomly chosen from different litters for each treatment group. In later experiments, mice from each litter were more evenly distributed amongst treatment groups. One cohort of mice were dropped from the weight gain data but included in the final mass data because their mass was recorded on different days than the other cohorts. Statistical analysis was conducted using a two-way ANOVA with a Bonferroni post-test. There were no significant differences in the final mouse mass between treatment groups. Final mouse weights were recorded at the time of sacrifice at 8 weeks of age. All of the mice had a final mass of around 20 grams. No significant differences were observed between treatment groups.

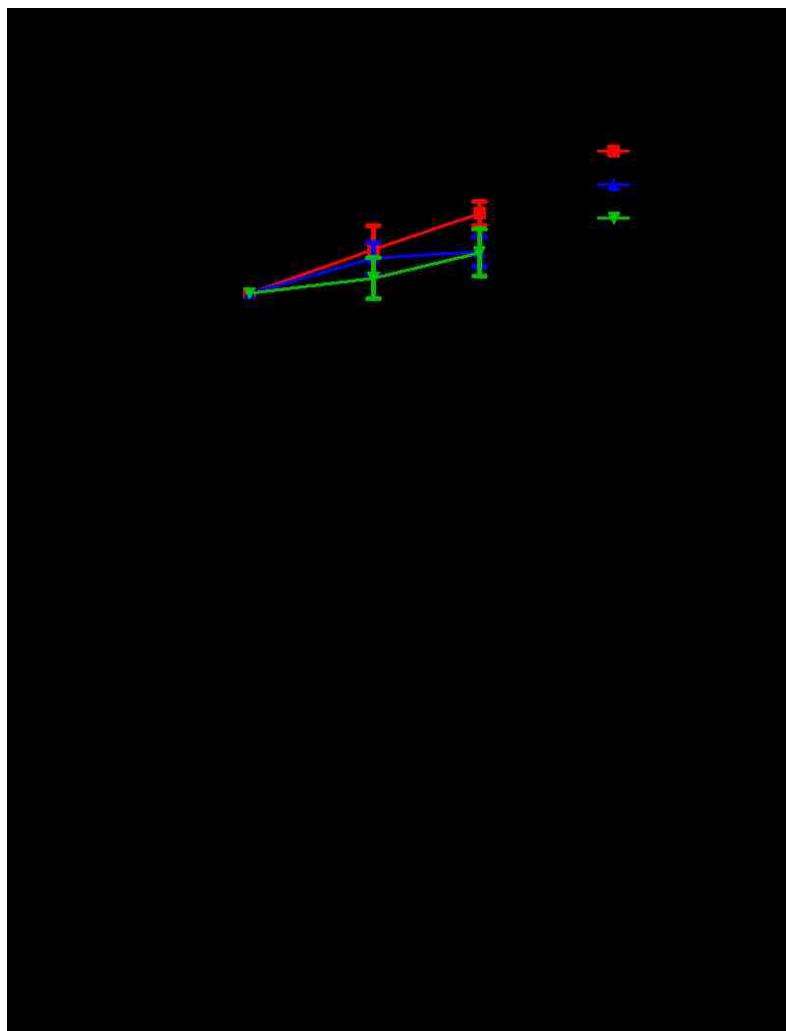


Figure 3.3 Short Term Study Mouse Mass

Mouse weights were recorded routinely over the course of the study and final mouse weights were recorded at the end of the study. The study was concluded after 21 days of treatment when the mice were about eight weeks old. In the normalized mouse weight gain, the R-ketorolac and S-ketorolac treated groups gained significantly less weight than the placebo treated group. Statistical analysis was conducted using a two-way ANOVA with a Bonferroni post-test. There were no significant differences in final un-normalized body mass between treatment groups (B).

3.3.2 Kidney Weights

Renal toxicity is a primary concern associated with long term ketorolac treatment(42). Because of this concern, one kidney from each mouse was removed and weighed. All of the mouse kidneys had a mass of 0.093-0.16 grams. The average kidney weight was 0.122 g for the placebo group, 0.13 for the racemic group, 0.132 for the (S)-ketorolac group and 0.126 for the (R)-ketorolac group. There was no significant difference in mouse kidney weights between treatment groups.

The kidney weight over total weight ratio was calculated for each treatment group and no significant differences were seen between treatment groups. All of the mice had a kidney weight to total weight ratio of about 0.006.

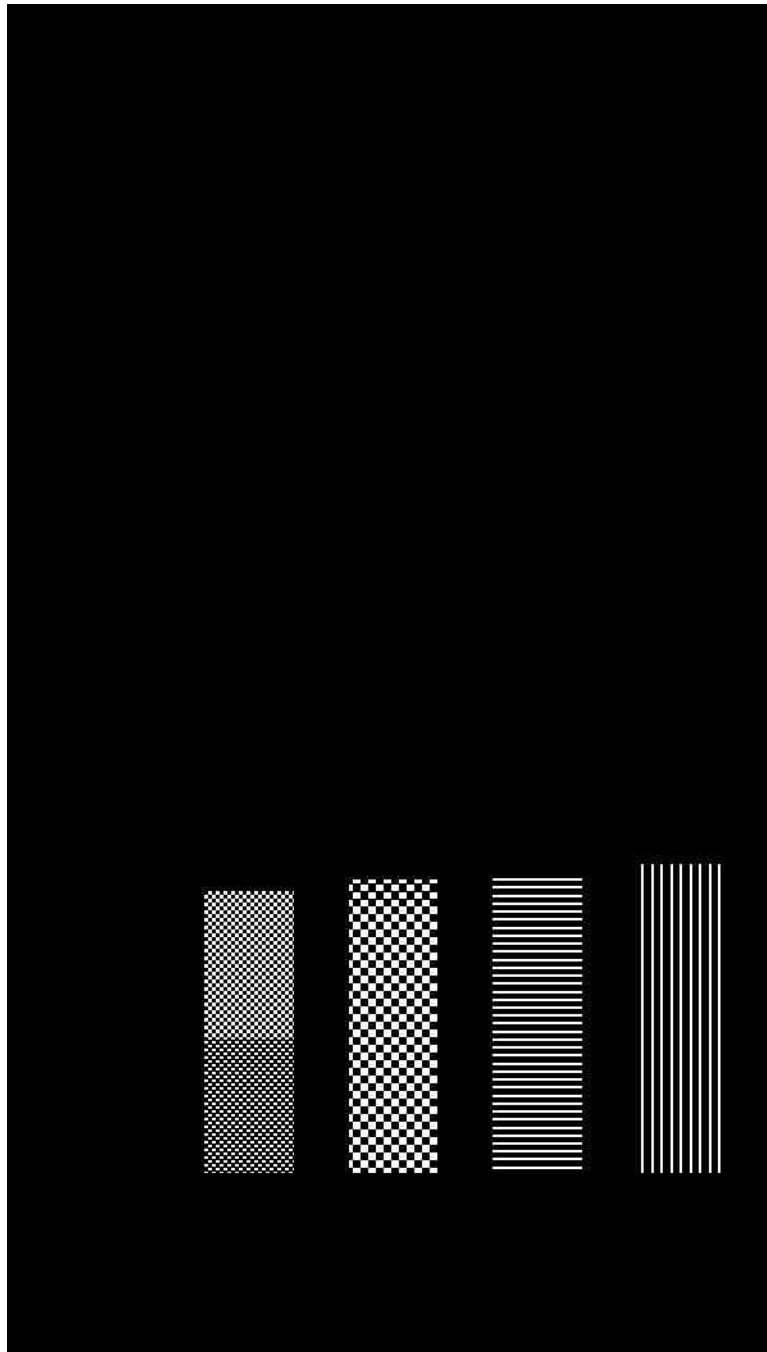


Figure 3.4 Short Term Study Kidney Weights

At the time of dissection, kidney weight was recorded as an assessment of kidney toxicity of ketorolac. There was no significant change between treatment groups when compared to placebo controls either in total kidney weight (A) or in the kidney weight versus total weight ratio.

3.3.3 Short Term Study Weekly Palpable Tumor Load

Tumor growth was monitored by routine palpations over the course of the study. The overall number of palpable tumors increased with age and over the course of treatment in mice. No immediately discernable differences were observed between treatment groups. It is important to note that the number of tumors that could be felt by palpation from week to week is subjective and not an exact indicator of tumor growth.

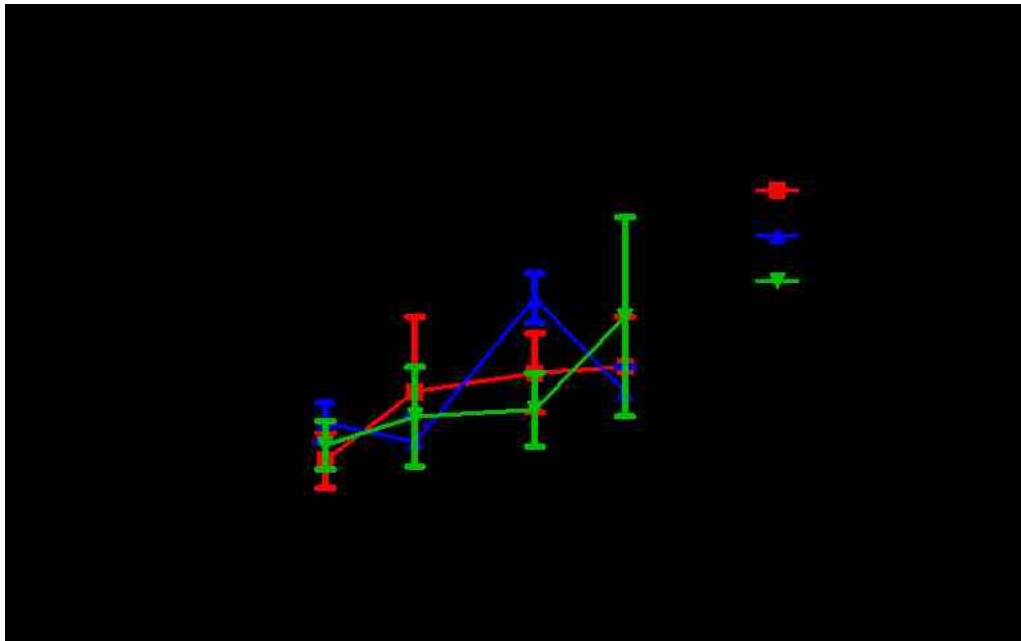


Figure 3.5 Short Term Study Weekly Palpable Tumor Load

Over the course of the study, mouse mammary glands were palpated for presence of tumor growth. The amount of tumors detected increased over time but the difference between groups was not significant.

3.3.4 Whole mounts of mammary glands

The mammary tumors did not grow large enough to separate from the mammary gland for weighing so instead, the fourth mammary glands were removed and imaged as whole mounts. Whole mounts of carmine stained mammary glands were imaged on a dissection microscope. The figure below is representative of a typical mammary gland. Most mammary glands in the 8-week old PyMT mouse had an area of denser tumor tissue in the proximal area of the gland which gradually decreased in amount and density moving distally through the gland. If not obscured by tumor tissue, the lymph node can be observed as a distinctly darker oval area slightly more proximal from the center of the gland. The mammary ducts spread out from the proximal end of the mammary gland, normally ending in slightly rounded terminal end buds. Mammary gland structures are surrounded by a combination of fatty tissue, and connective tissue which stains a slightly darker color than the fatty tissue but not as dark as tumor tissue.

Whole mount mammary gland images are representative of a range of mouse mammary gland morphologies observed. In the mammary gland from the placebo treated mouse the darker areas of tissue are tumorigenic and are spread throughout the gland. In the mammary gland from a (R)-ketorolac treated mouse some tumors are visible, but they are fewer in number and size than in the placebo treated mammary gland.

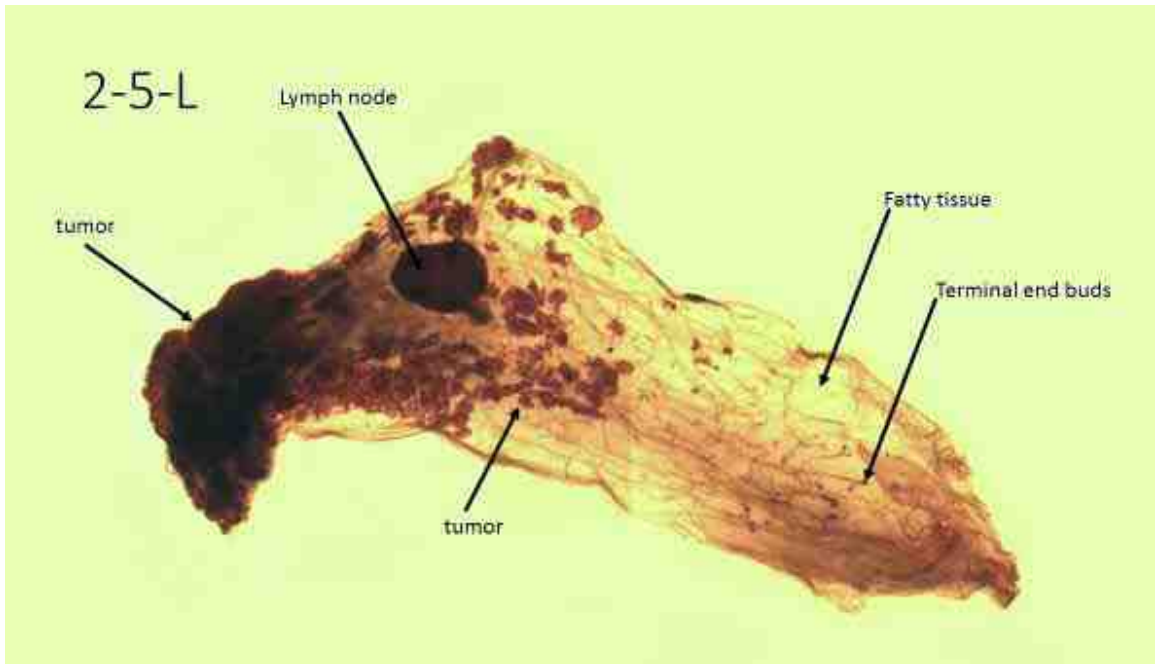


Figure 3.6 Mammary Gland Whole Mount Example

In the carmine stained whole mount mammary gland from an 8 week old MMTV-PyMT mouse, tumor tissue can be observed as well as the lymph node, fatty tissue and terminal end buds of the ductal network. This is a typical representative image.

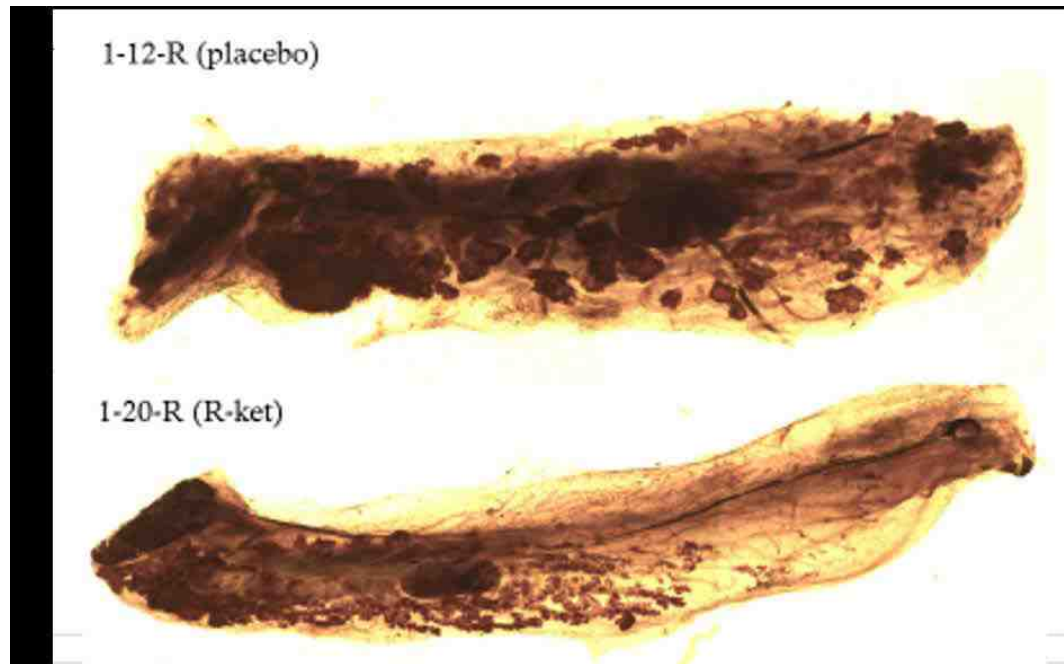


Figure 3.7 Treated vs. Untreated Mammary Gland Whole Mounts

Mammary glands from (R)-ketorolac treated mice had less tumor growth and more areas with fatty tissue and clearly delineated terminal end buds than mammary glands from placebo treated mice.

3.3.5 Histograms of Whole Mounts

Using ImageJ, pixel intensity information was collected from each mammary gland whole mount and compiled into histograms. ImageJ assigned numbers 0 through 255 to indicate the intensity of pixel color ranging from white to black, then counted how many pixels fit into each category of pixel intensity. The left and right mammary glands from each mouse were analyzed and averaged into one set of pixel data for each mouse. Pixel counts for each treatment group were compiled into linear histograms

In the whole mount image, the lighter pixels (pixels in the lower range) are non-tumorigenic tissue, while the darker pixels (pixels in the higher range) are tumorigenic tissue. Additionally, the drawing tool was used to exclude the lymph node and include only tissue up to the terminal end buds before analyzing the image. The resulting histograms showed peaks in pixel counts in the darker spectrum of pixels, representing a delineation between normal tissue and tumorigenic tissue.

Pixels that were dark enough to be considered tumor areas generally fell into the 175-225 range. Comparison of histograms for each treatment group show significant differences between the treatment groups and the placebo groups of mice. Mice in the placebo group had significantly higher amounts of tumorigenic lesions in their mammary glands than either the racemic ketorolac, (S)-ketorolac, or (R)-ketorolac treatment groups. Each group had an n of 9 and a p value less than 0.0001. Significance was determined using the student's unpaired t-test.

Mammary Gland Tumor Histogram

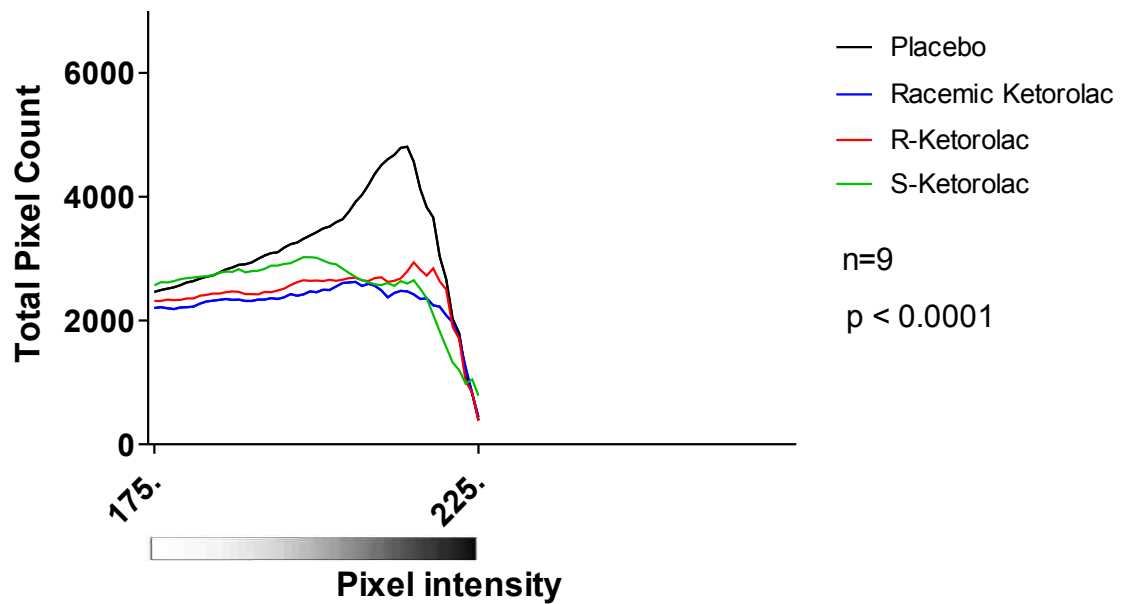


Figure 3.8 Mammary Gland Whole Mount Histograms

Darker pixels indicated more tumorigenic tissue while lighter pixels indicated areas with more fatty tissue. Placebo treated mice had significantly greater density of tumor tissue in their mammary glands than the racemic or enantiomeric ketorolac treated groups. There was no significant difference in tumor density between the ketorolac treated groups. Significance was determined using the student's unpaired t-test.

3.3.6 Lung H&E Staining

In this study it was hypothesized that ketorolac treatment would decrease the occurrence of mammary gland tumors metastasizing to the lung. Lung tissue was collected and analyzed for the presence of metastasis. H&E stained lung tissue in mice at eight weeks of age showed no tumor metastasis. There were no differences in lung tissue appearance between placebo and ketorolac treated mice. The lung tissue observed appeared to be visually normal healthy mouse lung tissue.

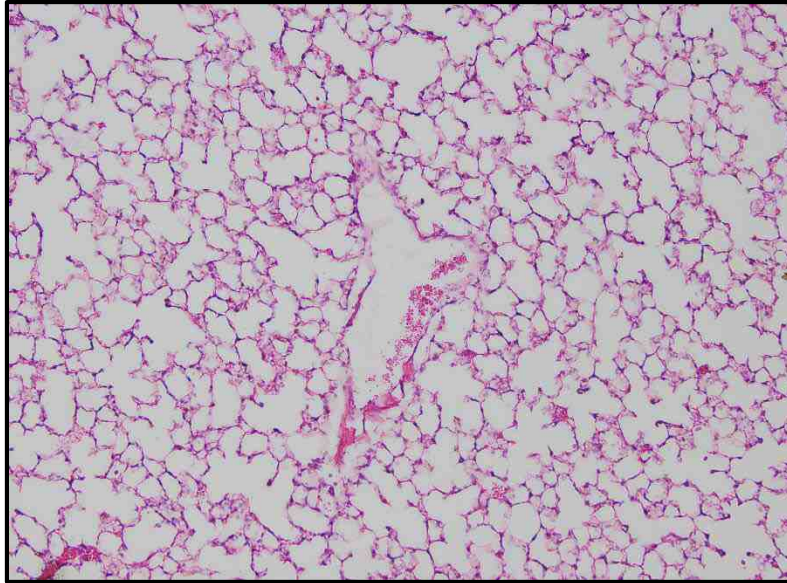


Figure 3.9 H&E Stained Lung Tissue

Mouse lungs were inflated with 4% PFA and paraffin embedded. Lung tissue was sliced in 3-10 μm sections and H&E stained. At eight weeks of age, no difference in lung tissue could be discerned between placebo and ketorolac treated mice, and no metastasis was detected. The image shown is a representative sample.

3.4 Discussion

This 21 day study was conducted to provide information about the early effects of ketorolac treatment, to determine toxicity, and to examine differences, or lack thereof, between treatment groups helping to set standard protocols for a longer study.

Mouse mass was routinely recorded as an indicator of drug toxicity and overall mouse health. When the data was normalized, by normalizing each mouse's weight to its starting weight, the placebo treated mice weighed significantly more than the R-ketorolac and S-ketorolac treated mice, but not the racemic treated mice. This difference may have been caused by the individual attributes of each litter of mice that were used, as the mice from each litter were not evenly distributed amongst all the treatment groups. In future experiments, mice from the same litter were even distributed between treatment groups. Final un-normalized mouse weights were not significantly different, indicating that ketorolac has little toxic effects on the mouse's ability to gain weight normally.

A second indicator of drug toxicity, kidney mass and kidney mass to total body mass ratios, showed no significant differences between treatments or when compared to placebo treated mice. These results suggest that ketorolac is not highly toxic when used for 21 days.

Whole mount images of the short term study mammary glands were imaged and assessed for tumor density. The mice were 8 weeks old at the time of sacrifice. This is the age at which the mammary glands begin growing tumors. Due to this timing, we were able to see a delay or decrease in tumor growth as a

result of ketorolac treatment that is not as easily observed as the disease progresses. The extent and distribution of tumor growth and burden in the placebo treated mice was typical for their age. Visually, there was less tumor burden in ketorolac treated mice than in placebo treated mice. Histograms describing tumor growth in the mammary gland whole mount images indeed showed a significant decrease in tumor burden in the ketorolac treated mice, when compared to placebo treated mice. The significant decrease in tumors was present in racemic, (S)-, and (R)-ketorolac treated groups. Keeping in mind the ability of mice to interconvert (S)-ketorolac to (R)-ketorolac, these results are logically sound.

Lung tissue was assessed for metastatic lesions, but as the mice were still very young and metastasis is not generally observed in MMTV-PyMT mice until at least 12 weeks of age, no metastasis was present (33,106). The short term study mouse lungs were visually normal and healthy.

In this shorter treatment duration, therapeutic concentrations of ketorolac did not cause toxic effects in MMTV-PyMT breast cancer mouse models. The mice remained healthy looking and did not suffer any measurable toxic effects from the treatment. Ketorolac treatment significantly decreased the amount of mammary gland hyperplasia. The results observed with racemic ketorolac and its enantiomers did not vary significantly. As a result, in further experiments, (R)-ketorolac treatment only, was conducted.

4. THE EFFECTS OF KETOROLAC ON PROLIFERATION AND METASTASIS OF MAMMARY GLAND TUMOR CELLS IN PYMT MICE

4.1 Introduction

Metastasis is the main cause of death in breast cancer patients (120). Human breast cancer most often metastasizes to the lung, liver, bones and brain (121). Two mouse breeds commonly used to model human breast cancer and metastasis are MMTV-HER2/neu/ErbB2 (hereafter MMTV-HER2) and MMTV-PyMT mice. MMTV-HER2 mice overexpress HER2, leading to the development of multifocal adenocarcinomas and lung metastasis lesions 15 weeks after pregnancy (122). In humans, HER2 gene overexpression is found in 15-30% of all breast cancers and contributes to mammary tumor formation (10). HER2 is an EGF family-type receptor tyrosine kinase, which regulates cell growth, differentiation and cell survival by activating proteins involved in signaling pathways such as MAPK, and PI3K/Akt pathways (reviewed (11)). HER2 overexpression specifically induces tumor formation and progression through the GEF protein, Tiam1 (105).

The MMTV-HER2 mouse tumor formation has a longer latency than in MMTV-PyMT mice, and only occurs after pregnancy (107). Like MMTV-HER2 mice, MMTV-PyMT mice overexpress HER2 resulting in the constitutive activation of cell growth, differentiation and cell survival signaling pathways. Also, tumor formation in MMTV-PyMT mice occurs independently of pregnancy with a shorter latency (107). The propensity for lung metastasis in MMTV-PyMT mice,

and their similarities to human breast cancer, makes them a good model for studying potential anti-metastatic compounds such as (R)-ketorolac.

This study focused on (R)-ketorolac treatments compared to placebo treatments, and the ability of (R)-ketorolac to prevent lung metastasis. Tumor growth in relation to treatment was documented and lung tissue samples were collected to measure metastasis. We hypothesized that (R)-ketorolac would inhibit the metastatic ability of mammary gland tumor cells resulting in fewer metastatic lesions in the lungs of (R)-ketorolac mice when compared to placebo treated mice.

4.2 Materials and Methods

4.2.1 Experimental Design and Dosing Schedule

Pills were prepared as described previously. Five cohorts of mice were used total. Three cohorts were sacrificed at 12 weeks of age and two cohorts were sacrificed at 14 weeks of age. The 12 and 14 week experimental data is combined in the results where appropriate. The experiment proceeded much as described previously with the following changes: Mice were dosed twice a day, 12 hours apart, 5 days a week. On the day of dissection, mice did not receive their morning dose. Once a week mice were sedated with isoflurane, weighed and palpated for tumor growth. Externally visible tumors were measured using calipers and an approximate volume was calculated using the formula: volume = length*width*($\pi/4$).

This study included 24 mice in the 12 week group, and 13 mice in the 14 week group. Two mice were dropped from the 12 week study, and 3 mice were

dropped from the 14 week study. Mice were housed into one of two treatment groups: placebo, or (R)-ketorolac, and dosed until the age of 12 weeks and 5 days or 14 weeks and 1 day. The limiting age of mice for the time of sacrifice in the first, 12 week study, was determined when one individual within the first group of mice grew a tumor that exceeded the maximum 15 mm diameter limit set by University of New Mexico's Institutional Animal Care and Use Committee (IACUC) guidelines. This end date decision put the mice between 48 and 51 days of treatment at the time of sacrifice. On day 48-51 of dosing (12 weeks, 5 days old), mice were sacrificed and organs and tissue were harvested and preserved. Further cohorts of mice were treated until 14 weeks of age as there were not enough metastatic lesions in the lungs of the 12 week old mice to make any conclusions about lung metastasis. Data from the 14 week old mouse cohort was combined with the weight change and palpable tumor load data of the 12 week old mice to increase the n but tumor weight and lung metastasis data was reported separately due to the age, and thus tumor progression difference, at time of sacrifice.

4.2.2 Dissection

Mice were euthanized by injecting ~100 μ L Phenobarbital (Fatal Plus 59mg/mL, 0.1 mL/25 g mouse) into the peritoneal cavity. Mice were weighed and then doused with 70% EtOH, as previously described. Cardiac punctures were performed with plain non-coated needles and blood was put into plain 1.5 mL epi tubes and stored on ice until it could be separated by centrifuging at 2500 rpm for 10 minutes. Serum was stored at -80°C . Tumors from all 10 mammary glands

were removed, photographed, weighed and cut in half. Half the tumor was snap frozen in liquid nitrogen and half was preserved in 4% PFA until it could be paraffin embedded. Lung, stomach, kidney and liver collection and storage were performed as previously described.

4.2.3 H&E Mammary Tumor Staining

Mammary gland tumors were fixed in 4% PFA, then paraffin embedded. Sample sectioning, H&E staining, and analysis was conducted by Donna Kusewitt, DVM, PhD, ACVP.

4.2.4 RNA Isolation and qRT-PCR

Lung and mammary tumor tissue samples from the 81 day studies were weighed into 30 mg samples and put into 1.5 mL epi tubes. Liquid nitrogen was added to the epi tubes to freeze tissue. 300 μ L of RLT buffer, from an RNeasy Mini Kit (Qiagen, Valencia, CA) was added to the sample and an electric hand drill fitted with nuclease-free 1.5 mL pestles (Kimble-Chase, Vineland, New Jersey) was used to break down the tissue. The lysate was homogenized using the QIAshredder (Qiagen, Valencia, CA) and RNA was isolated using the RNeasy Mini Kit according to the manufacturer's protocol. RNA was converted into cDNA using a High Capacity cDNA Reverse Transcription Kit (Applied Biosystems, Inc. Foster City, CA) and a TC-3000X Thermocycler (Techne Inc., Burlington, NJ). cDNA was generated from 1000 ng of RNA of each sample. The resulting cDNA samples were diluted 1:3 with nuclease-free water.

Quantitative Real-Time polymerase chain reaction (qRT-PCR) was conducted using six mouse primers: Rac1, Rac1b, RhoA, Cdc42, PyMT and β -

actin (Qiagen, Valencia, CA; excluding PyMT, catalog numbers QT01070146, QT00127673, QT00197568, QT00091560, QT00095242 respectively). PyMT primers used were, PyMT forward: 5'-CGG CGG AGC GAG GAA CTG AGG AGA G-3' and reverse: 5' TCA GAA GAC TCG GCA GTC TTA-3' (33). Fast SYBR® Green Master Mix (Applied Biosystems, Inc. Foster City, CA) was used to make a 1:5 master mix for each primer. Samples were loaded in triplicate in 384-well plates using 6 µL of master mix and 4 µL of sample per well. A nuclease-free water sample was used as a negative control, and β-actin was included as a positive control. Genes were amplified on a 7900 HT Fast Real-Time PCR System (Applied Biosystems, Inc. Foster City, CA). Relative expression was calculated with the $\Delta\Delta\text{Ct}$ method, using β-actin as the normalizer and analyzing the treated samples in reference to placebo samples.

4.3 Results - 81 Day Studies

4.3.1 Weekly and Final Weights

Mice were weighed on a weekly basis. In the 12 week study, at ages 9, 10, 11 and 12 weeks, the placebo treated mice had a significantly greater overall body mass than the (R)-ketorolac treated mice, but this significance disappeared when the data was normalized. Each mouse's weight was normalized to its starting weight to reflect relative change in mass. In the 14 week studies, there were no significant differences in body mass between treatment groups. Mouse body mass at four weeks old ranged from 15-20 grams across both treatment groups. Final mouse body mass for the mice sacrificed at 12 weeks of age was between 24.2-29.5 grams in the placebo group and 22-26.3 grams in the (R)-

ketorolac group. The placebo group and (R)-ketorolac group had an n=11. Final mouse body mass for the mice sacrificed at 14 weeks of age was between 27.2-32.7 grams in the placebo group and 24.2-34.0 grams in the (R)-ketorolac group. The placebo group for the 14 week treated mice had an n=6 while the R-ketorolac group had an n=7. Three mice were dropped from the study in the 14 week old mouse group. Two mice had malocclusions and were much smaller than other mice in the study, and one mouse was much larger than all other mice in the study. Significance was determined using an unpaired student's t-test.

Final mouse body weights were significantly different at 12 weeks but not at 14 weeks. At 12 weeks, placebo treated mice had a greater average body mass than (R)-ketorolac treated mice. Placebo treated mice had an average mass of 26.5 grams while (R)-ketorolac mice had a final average mass of 25 grams. Significance was determined using an unpaired student's t-test and yielded a $p < 0.05$. At 14 weeks there was no significant difference in mouse body mass, although there were only 5 mice in each treatment group. So, the small n is likely to be the reason for no significant difference.

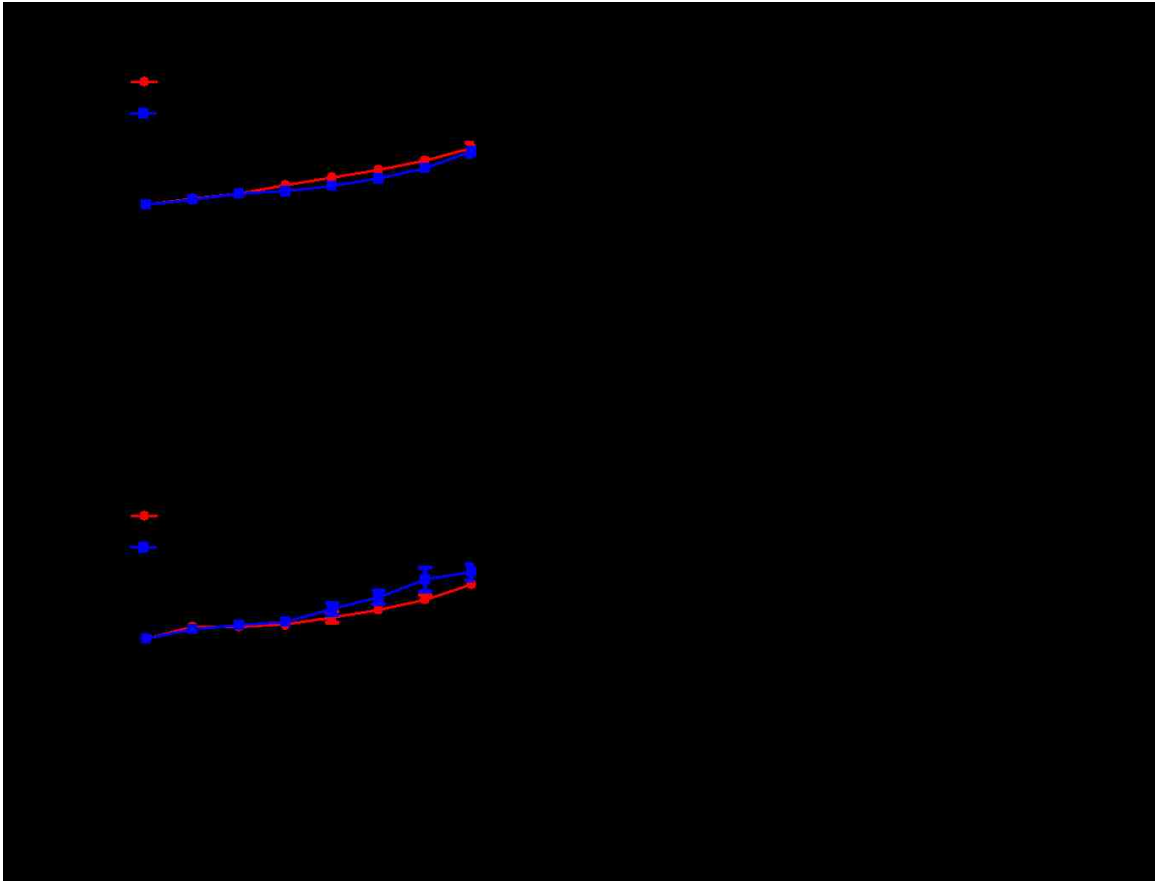


Figure 4.1 Long Term Study Weekly Weight Gain and Final Weight

Mouse mass was measured and recorded weekly. There was no significant difference in weight gain between the two treatment groups over the course of the study. When only the 12 week final mass was considered, there was a significant difference between the placebo and (R)-ketorolac treated groups (B). In the 14 week old mice, there was no significant difference in mass between treatment groups (D). Significance was determined using an unpaired student's t-test (B, D).

4.3.2 Kidney Weights

There was no significant difference in the kidney weights between the placebo and (R)-ketorolac treatment groups in either age group. At 12 weeks the average kidney weight was 0.126 grams in the placebo group and 0.125 grams for the (R)-ketorolac group. At 14 weeks the average kidney weight was 0.135 grams in the placebo group and 0.14 grams for the (R)-ketorolac group. Additionally, there was no significant difference between the two treatment groups when comparing the kidney weight to total weight ratios. One mouse was excluded from the 12 week group when calculating kidney weight:total weight ratio because its end mass was an outlier due to very large tumors. The kidney mass in this particular mouse was comparable with the other mouse kidneys.

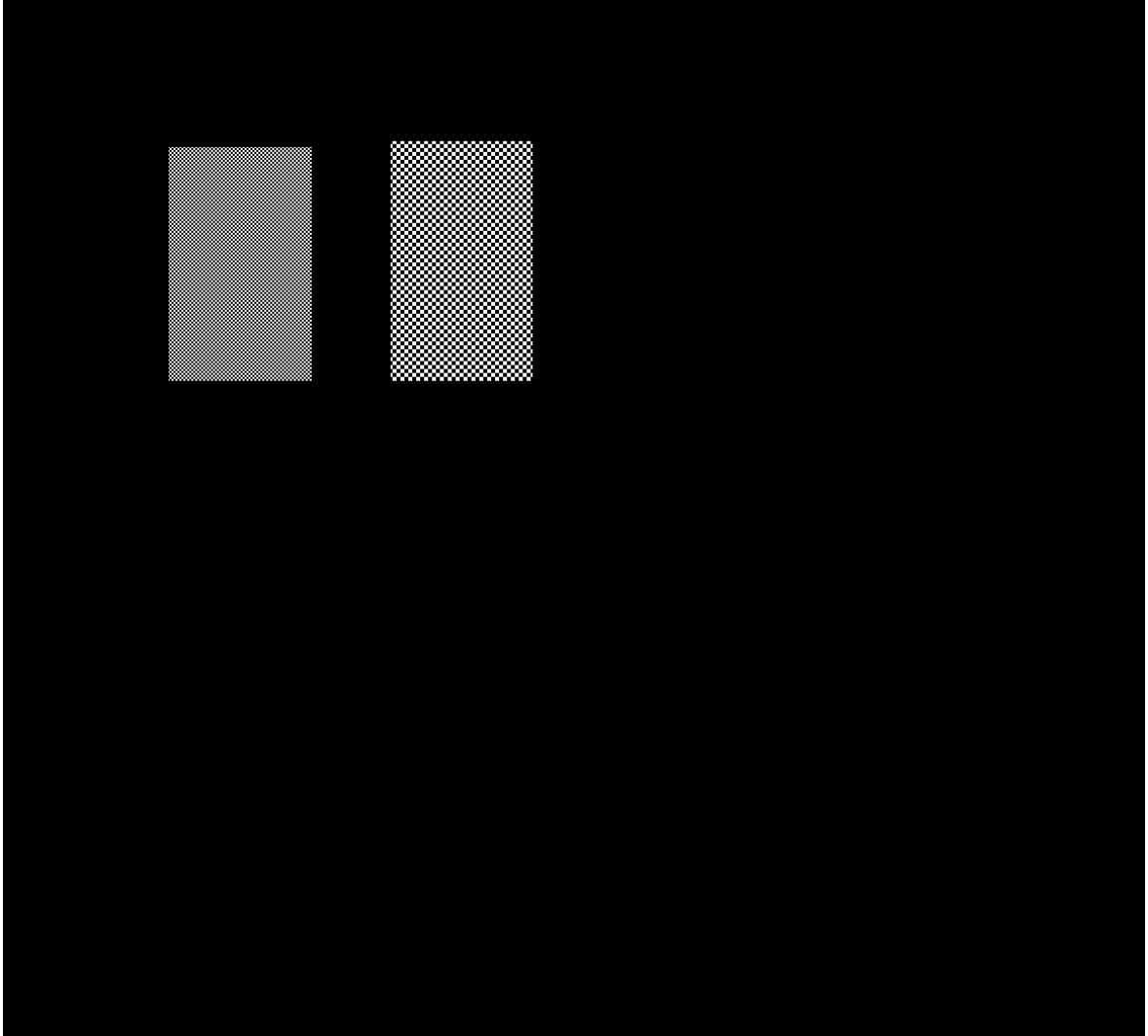


Figure 4.2 Long Term Study Kidney Weights

Kidney weight and total weight ratios were calculated. There was no significant difference in kidney weight:total weight ratios between placebo and (R)-ketorolac treated groups (A). There was no significant difference in kidney weights between treatment groups in either the 12 week or the 14 week mice (B, C).

4.3.4 Weekly Tumor Growth

The number of palpable tumors increased over the course of the experiment and with increasing mouse age. While the placebo group had slightly more palpable tumor growth than the (R)-ketorolac treatment group over much of the study, the difference was not significant. Additionally, palpation is a subjective measurement that varies from session to session and cannot be considered an exact indicator of tumor growth.

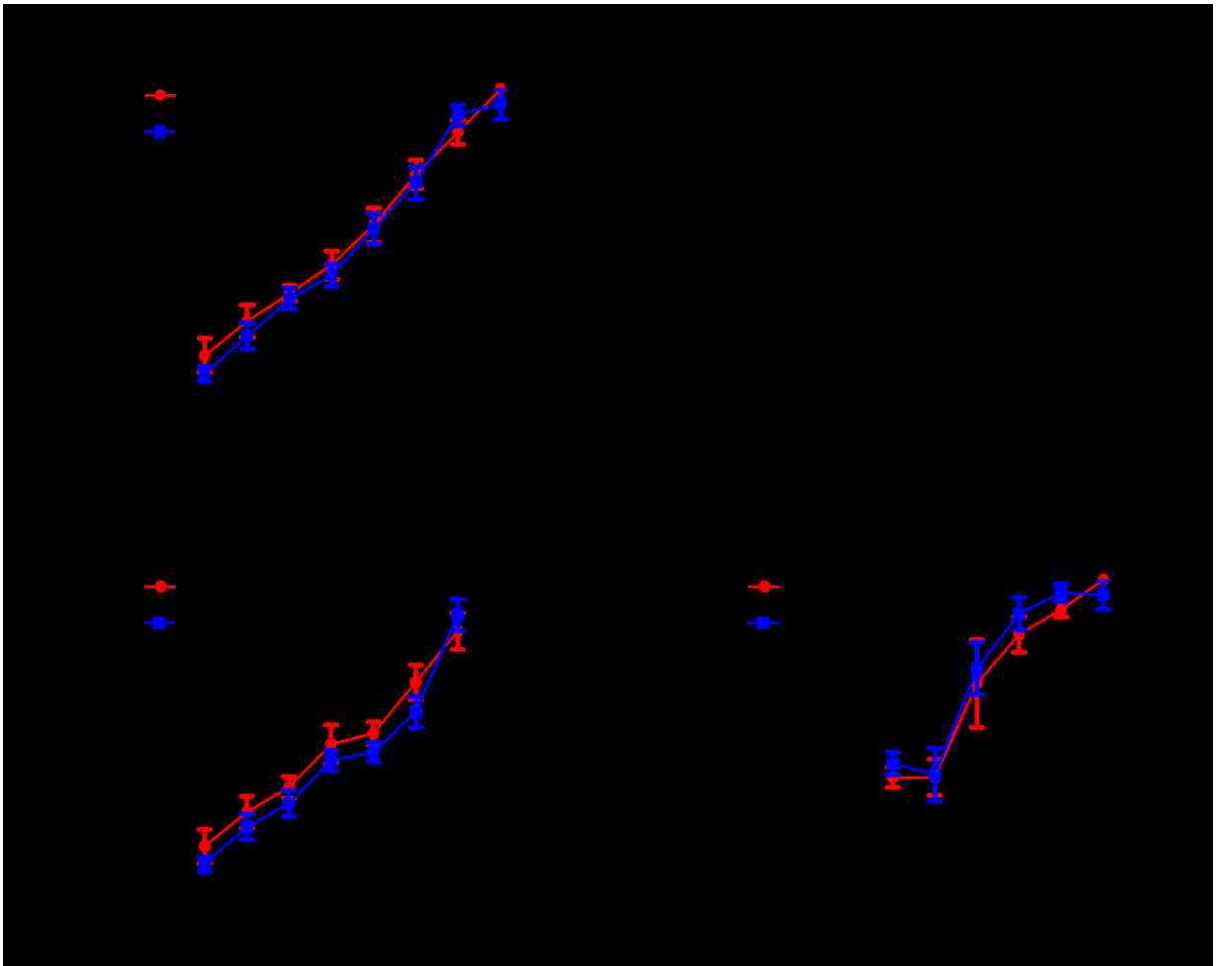


Figure 4.3 Long Term Study Weekly Palpable Tumor Load

Throughout the course of the study, mouse mammary glands were palpated, and tumor growth was recorded weekly. Palpable tumors increased over the course of the study in placebo and (R)-ketorolac treated groups. Shown are the combined 12 and 14 week mouse experiments (A), 12 week only (B) and 14 week only (C). There was no significant difference between treatment groups in the number of tumors felt.

4.3.5 Tumor Mass

Mammary tumors grew large enough to completely encompass each mammary gland and were impossible to separate from the mammary glands. The mass of each mammary gland/tumor was recorded. To compile the tumor mass to total mass ratio, the total tumor mass was summed for each mouse and compared to total mouse weight. A difference in tumor weight, while slightly greater in the placebo treated mice, was not significant between treatment groups. The tumor weight to total weight ratio was slightly greater in the placebo treated mice, but not significant. At 12 weeks, the average tumor weight in the placebo group was 3.4 grams and in the (R)-ketorolac group was 2.7 grams. At 14 weeks, the average tumor weight in the placebo group was 5.2 grams and in the (R)-ketorolac group was 5.5 grams. One mouse was excluded from the (R)-ketorolac group because abnormally large tumors caused it to be an outlier.

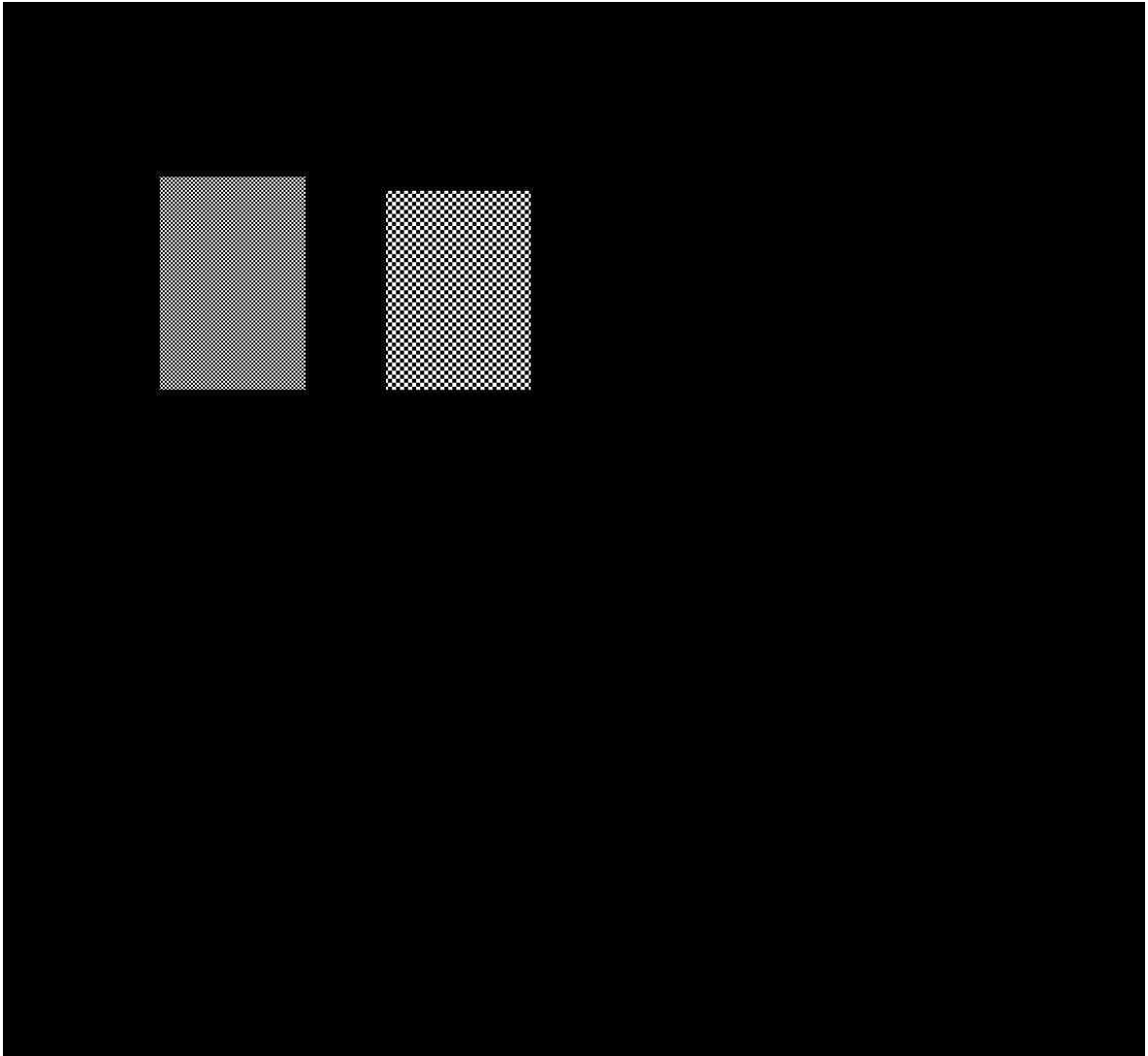


Figure 4.4 Long Term Study Tumor Weights

The tumor mass total:mouse mass ratio was calculated. There were no significant differences between the two treatment groups (A). The total tumor mass from each mouse was recorded and found to not be significantly different between placebo and (R)-ketorolac treated mice. 14 week old mice had greater total tumor mass than 12 week old mice (B, C).

4.3.6 H&E Mammary Tumor Staining

H&E mammary tumor staining was conducted by Donna Kusewitt, DVM, PhD, ACVP, on 12 week old mouse mammary gland tumors. There was no significant difference in the average number of lesions per mouse. There were fewer mice in the (R)-ketorolac treated group than the placebo control group affected by early adenoma (Ad) and early carcinoma (Ca) suggesting that (R)-ketorolac may help to inhibit early cancer cell proliferation, but the results were not significantly different.



Figure 4.5 H&E Staining of Mouse Mammary Tumors Show No Change

Mouse mammary tumors were stained and analyzed for the presence of cell proliferation. There were no statistically significant differences in the average number of lesions present between the (R)-ketorolac treated mice and the placebo control (A). There was a suggestion of a delayed early tumor progression in the (R)-ketorolac treated mice when the percent of mice affected was analyzed, but the differences were not significant (B).

4.3.7 Lung H&E Staining

H&E stained lung tissue sections were scanned for presence of tumor metastasis. Normal lung tissue had a lacy appearance with pink stained blood vessels throughout. Red blood cells left behind also stained pink. Areas of metastasis were defined as 10 or more purple stained nuclei grouped together in a disorganized arrangement.

ImageJ was used to outline the areas of metastasis and measure the total number of pixels within the outlined area per mouse. The total number of metastasis sites per mouse were also counted. There was no significant difference in the amount of lung metastasis between the (R)-ketorolac treatment group and the placebo group in the 12 week old mice. In the 12 week old placebo treated mice 8 out of 11 mice had less than 5 detectable metastatic sites, and in the (R)-ketorolac treated mice 8 out of 9 mice had less than 5 detectable metastatic sites. So, a longer study was conducted to increase the chances of the presence of lung metastasis. In the 14 week old mice there was a slight increase in the metastatic area and a slight increase in the total number of metastatic sites in the placebo treated mice, when compared to the R-ketorolac treated mice, but the increase was not significant. It is important to note, as of this writing, the 14 week studies are not yet complete and thus, the population size is still small. A greater population size may result in significant findings.



Figure 4.6 12 week old H&E Stained Lung Tissue

Mouse lungs were inflated with 4% PFA and paraffin embedded. Lung tissue was sliced in 3-10 μm sections and H&E stained. Typical metastatic lung tissue is represented by image A. Metastasis in lung tissue was identified and quantified by using ImageJ to quantify the total number of metastasis foci (B) and the total number of pixels in each metastatic area (C). There was no significant difference in the amount of metastasis quantified in placebo and (R)-ketorolac treated mice, at 12 weeks of age.

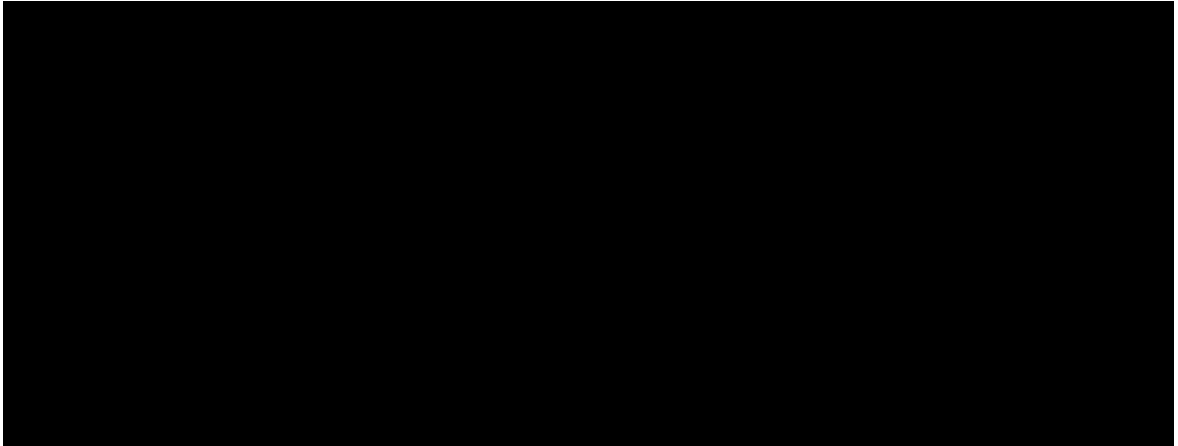


Figure 4.7 14 Week Old H&E Stained Lung Tissue

Metastasis in lung tissue was identified and quantified by using ImageJ. The number of metastasis foci (A), and the total number of pixels in each metastatic area (B) per mouse, were measured. There was a slight increase in the area and number of metastatic sites in the placebo treated mice when compared to the R-ketorolac treated mice, but the differences were not significant.

4.3.8 qRT-PCR – 12 Weeks

qRT-PCR was used to assess gene expression of Rho-GTPases, Rac1, Rac1b, RhoA and Cdc42, and the mouse mammary tumor gene of interest, PyMT. All results were corrected using β -actin controls then normalized to their respective placebo control. A relative expression value of one, indicated no change from the placebo control. In the tumor tissue, there was no change in gene expression when comparing the treatment groups with the placebo control. In the lung tissue of (R)-ketorolac treated mice, there were slight upregulations of Rac1b and Cdc42 gene expression when compared to their respective placebo controls but the differences were not statistically significant. There was a small upregulation of PyMT gene expression in placebo controls when compared to the (R)-ketorolac treated control, which is the change we were expecting to see in the lung tissue of these animal models, but the change was not statistically significant.

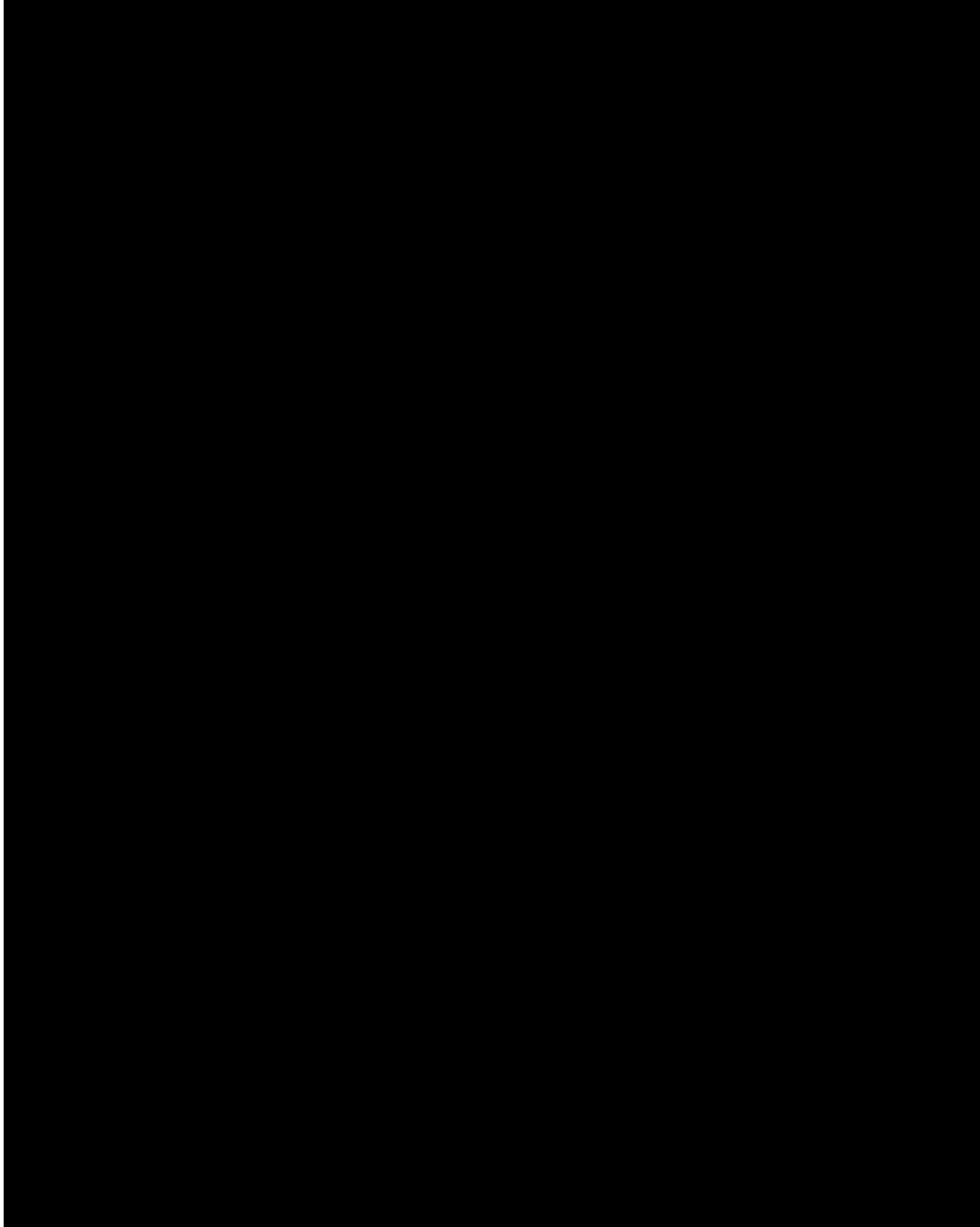


Figure 4.8 qPCR in Tumor Tissue – 12 Weeks

Gene expression levels in the tumors of (R)-ketorolac treated mice were not different from the placebo control treated mice. In both treatment groups the gene expression of Rac1 (A), Rac1b (B), RhoA (C), Cdc42 (D) and PyMT (E) were the same.

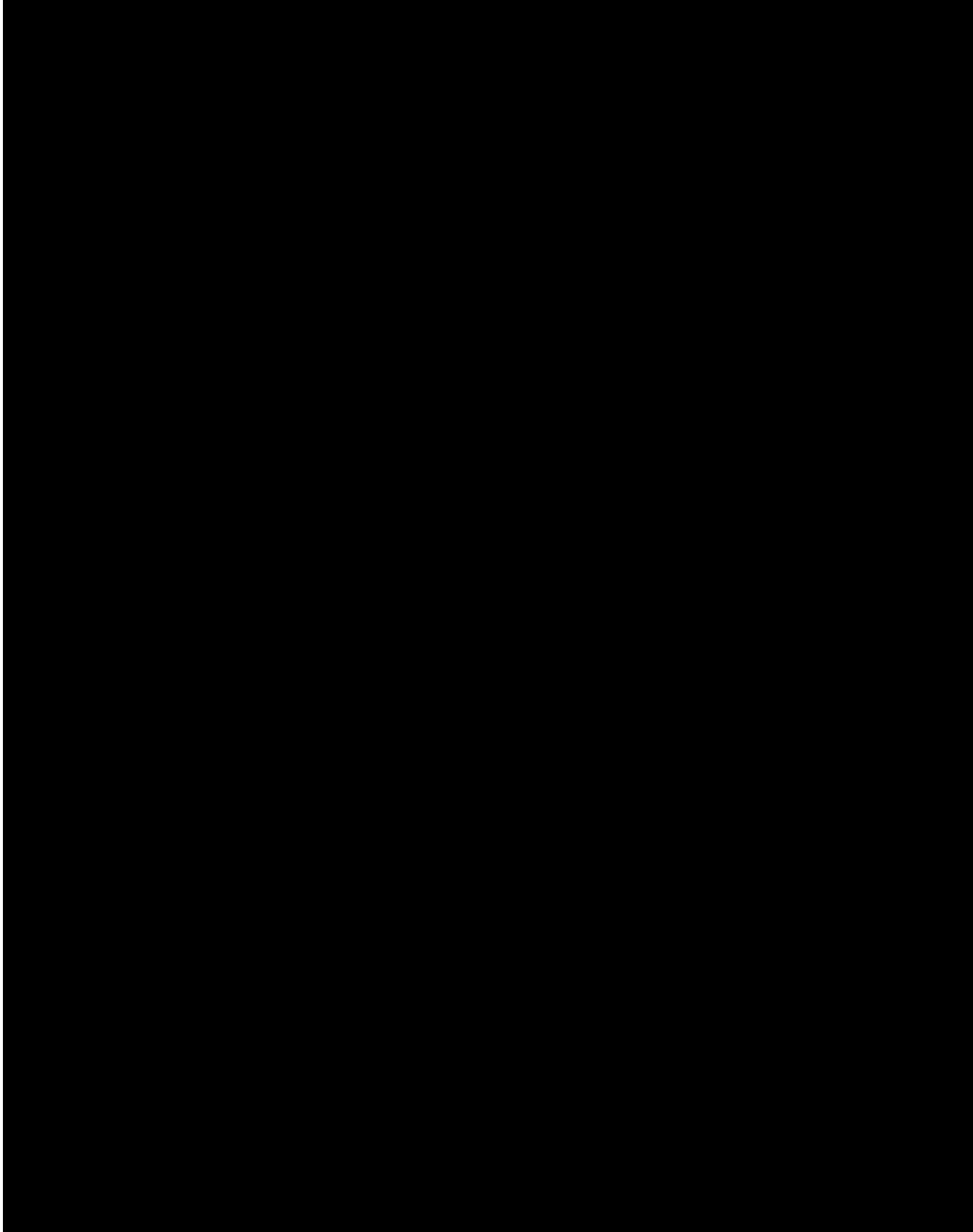


Figure 4.9 qPCR in Lung Tissue – 12 Weeks

Gene expression of Rac1b (B) and Cdc42 (D) was upregulated in the (R)-ketorolac treated mice but the difference was not significant. PyMT gene expression in the lungs of placebo treated mice and (R)-ketorolac treated mice was not significantly different (E). Gene expression of Rac1 (A), and RhoA (C) was not changed.

4.4 Discussion

This 81 day study was conducted to examine long term effects of ketorolac treatment on tumor growth and metastasis as well as long-term toxicity studies. In humans, racemic ketorolac is not recommended for use longer than 5 days duration due to adverse toxic effects (42). These longer studies were terminated earlier than the projected 81 days, due to a limiting factor of tumor growth exceeding 15 mm in length according to IACUC guidelines. The first set of long term experiments were terminated at 12 weeks because one mouse exceeded the tumor growth limits. However, that particular mouse was ultimately dropped from the study. A second, and now ongoing, set of experiments is being conducted to 14 weeks because no lung metastasis was observed in the 12 week old mice and the majority of mice were within ethical animal treatment limits, as set by IACUC. According to other studies conducted, the MMTV-PyMT mice in this study are expected to have significant lung metastasis between 12 and 14 weeks of age (33,106). It has been suggested that this particular line of MMTV-PyMT mice may have genetically drifted, resulting in tumor metastasis at a later age. These mice require a longer time for tumor and metastasis development. (see appendix for metastasis development)

MMTV-PyMT mouse models in this study developed palpable tumors around 8 weeks of age and caliper measurable tumors around 10 weeks of age. In the 12 week studies, there was a small increase in the number of palpable tumors in the placebo treated group when compared to the (R)-ketorolac treated group, but the difference was not significant and may have been attributed to

biased observation as the palpations were not conducted blindly. Overall, the number of palpable tumors increased with age, however the number of tumors felt is very subjective and difficult to accurately quantify from week to week. Additionally, external measurement of tumor volume could only be estimated because not all tumors were perfectly spherical. Some tumors grew oblong and flattened while other tumors, particularly the 2nd and 3rd mammary gland tumors, and later the 4th and 5th mammary gland tumors, began to grow into a single mass as they became larger.

In this study a significant difference final in mouse mass was observed in the 12 week study, but not in the 14 week study. When the rate of weight gain was normalized, there was no significant difference in weight between the two treatment groups. The differences at 12 weeks could be attributed to more than one reason. When overall tumor mass was measured in the longer term study, the placebo mice had a greater overall tumor mass and a greater tumor:body mass ratio, however the differences were not significant. The placebo treated mice may have had a greater mass due to their increased tumor burden. On the other hand, the (R)-ketorolac treated mice may have exhibited decreased growth due to toxic effects of the drug. Considering the lack of other toxicity indicators, i.e. kidney mass differences, the former explanation is more likely to be true. The differences in mouse mass between treatment groups at 14 weeks of age were not significant. This could be an indication that the (R)-ketorolac treated mouse tumors were delayed in growth and not contributing to overall mass until that time

point. It also may be due to the small number of mice in the 14 week study. A larger population may change these final results.

In the long term studies, the mammary tumor growth was so extensive, separation of mammary gland and tumor was deemed impossible and instead whole tumor/mammary gland sections were removed for analysis. Tumor weight totals per mouse were recorded and compared as whole numbers and as a ratio of tumor weight to total mouse weight. There was no significant difference in tumor weight totals in either the 12 week or the 14 week old mice. Although, the 14 week old mice had a greater overall tumor weight than the 12 week old mice, which was expected. There was also no significant difference in the tumor weight:total weight ratios between the two treatment groups. These results indicate that (R)-ketorolac is not affecting the overall tumor growth.

Lung tissue was assessed for metastatic lesions. Between 12 and 14 weeks of age, the MMTV-PyMT mouse model exhibits mammary tumor metastasis to the lungs (33,106). In the 12 week old mouse population, some mice had obvious metastatic lesions, while some had possible small initial sites that were difficult to identify, and still others exhibited no lung metastasis at all. There was no trend observed between the presence of metastatic sites and treatment groups. A longer study treating MMTV-PyMT mice to 14 weeks of age is currently underway to allow adequate time for lung metastasis to develop. Preliminary results indicate that while there is more overall lung metastasis in the 14 week old mice, the amount of metastasis is not as great as expected for this age of PyMT mouse. Studies of lung tissue collected months earlier, from the

same line of MMTV-PyMT mice have shown abundant lung metastasis as early as 13 weeks of age (see appendix). It is suspected there has been a genetic drift in the expected phenotype of this particular line of mice and it may be prudent to end this colony and purchase new breeding pairs, before continuing these experiments.

Considering the lack of lung metastasis trend in the 12 week old mouse models, a difference in Rho-GTPase and PyMT gene expression was not expected between treatment groups. Nonetheless, PCR was conducted on both tumor samples and lung tissue samples from the study, to examine what changes, if any, were able to be observed in small Rho-GTPase and PyMT expression levels. There were no significant changes in gene expression in the tumor samples, most likely because both the (R)-ketorolac and placebo treated mice grew tumors at nearly the same rate and had tumors of similar sizes. In the lung tissue, there were small upregulations of Rac1b and Cdc42 gene expression in the (R)-ketorolac treated mice but the differences were not significant. It was expected that the (R)-ketorolac treated mice would exhibit less lung metastasis and thus less PyMT gene expression in the lungs than the placebo treated mice and while there was a noticeable trend, the difference was not significant. The 14 week animal studies are expected to exhibit more significant changes in gene expression and solidify the trends observed.

While the animal experiments did not yield complete results, we were able to observe interesting trends in ketorolac treated animal models. Therapeutic concentrations of ketorolac did not cause toxic effects in MMTV-PyMT breast

cancer mouse models. There was a trend in decreased PyMT expression in the lungs of mice treated with (R)-ketorolac, suggesting a decrease in tumor metastasis, but more work will have to be done to confirm these results.

5. SIGNIFICANCE AND FUTURE DIRECTIONS

Cancer is often described as having specific hallmarks that distinguish it from other diseases, one of those being inflammation (123). It has been demonstrated that several NSAIDs, such as ketorolac, possess anti-cancer properties that may be useful as part of anti-cancer therapies (40). Racemic ketorolac is routinely used to reduce pain and inflammation in surgical cases. However, the (S)- form of ketorolac is primarily responsible for the drug's anti-inflammatory properties (48). (R)-ketorolac, previously believed to be relatively inert, has recently been shown to have an important role in decreasing tumor metastasis and thus increasing patient survival rates (45). Work performed in our research group has found that in ovarian cancer cells, (R)-ketorolac inhibits small Rho-GTPases, Rac1 and Cdc42 which are vital in enabling the cell to metastasize (50).

This study demonstrated the ability of (R)-ketorolac to inhibit early breast tumor growth without causing significant toxic effects to surrounding cells, or the organism as a whole. The main concern with long term use of ketorolac is the drug's toxic effects on the body, including gastrointestinal ulcerations and bleeding (42). These toxic effects can be attributed to the (S)- enantiomer of ketorolac which inhibits COX1/2, enzymes important in maintaining mucosal linings in the stomach and intestines (52). (R)-ketorolac, when used to treat cells in culture, was not cytotoxic at relatively high concentrations. It did not alter the viability of breast cancer cells, nor did it alter their cell cycle behavior. In mouse models, when (R)-ketorolac was used for durations longer than the clinically

recommended limit of five days, there were no immediate toxic effects. These results indicated that (R)- enantiomer of ketorolac alone may be considered safe for long term use.

The *in vitro* experiments yielded many negative, but not necessarily inconclusive results. From these experiments, we found that (R)-ketorolac is a relatively benign drug, not decreasing cell viability or growth but inhibiting the cell's ability to migrate and form colonies. We have not shown a direct interaction between (R)-ketorolac and Rac1 and Cdc42 in breast cancer cells, so further experiments are imperative to understanding (R)-ketorolac's mechanism of action in breast cancer cells. Immunoblotting to examine the activity of Rac1 and Cdc42 in breast cancer cell lines when treated with (R)-ketorolac is one step that could be taken.

The animal studies conducted had a few limitations that are important to note. The ability to give each mouse an exact dose of ketorolac every 12 hours was not feasible. The mice were given oral doses of ketorolac in the form of bacon flavored pills. Sometimes certain mice did not eat their pills, and as the study was not conducted by oral gavage, we could not force the mice to eat their pills if they refused. Careful notes were taken and mice that refused their pills the majority of the time were dropped from the study. The occasional missed dose was noted, but not considered an absolute reason to drop the mouse from the study. While not optimal, it is very likely that an actual human may occasionally forget to take their medication at the exact indicated time.

One complication that arose with the mouse studies was lack of knowledge of the exact duration of time necessary to run the experiment. While the literature indicates positive lung metastasis in MMTV-PyMT mice at 14 weeks of age, this particular group of MMTV-PyMT mice has been known in the past to have lung metastasis at 12-13 weeks old (33). However, there was a suspected genetic drift, because at 12 weeks old, there was little to no lung metastasis observed in the lung sections. Briefly, lung tissue samples from untreated PyMT mice in this same breeding group at 12, 13, 14, and 16 weeks of age were H&E stained and examined for metastasis. It was decided that 14 weeks would be the best age of sacrifice for examining lung metastasis. Currently, another study is being conducted, carrying out this experiment to 14 weeks, and some of that data has been included in the results. We hope to see a positive effect of (R)-ketorolac treatment on lung metastasis.

Future animal experiments could involve other known breast cancer mouse models such as a HER2 mouse models. It is important to ask the question: Does (R)-ketorolac treatment yield significant benefits in other breast cancer models? It would also be interesting to examine the effects of (R)-ketorolac treatment on xenograft or allograft mouse models. Additionally, conducting longer term experiments, modeling a chronically medicated individual, could yield information about how long a patient may benefit from (R)-ketorolac treatment, and answer the questions: Is there a point where (R)-ketorolac treatment is no longer significantly beneficial? And is (R)-ketorolac treatment able to keep metastasis at bay, long term? Finally, because (R)-ketorolac has been

shown to have positive results in multiple cancer forms, including ovarian, colon and now breast cancer, testing its effectiveness on preventing metastasis of other forms of cancer could be a logical next step.

What we know from these experiments, it is possible that the (R)-ketorolac enantiomers may be safely used for long term treatment in an effort to decrease breast cancer metastasis, although more evidence is needed. As FDA guidelines become stricter, it will be important to look at pre-approved drugs in new ways. Currently, much of the focus of cancer drug discovery is on creating new compounds that have toxic effects on cancer cells. While some of these compounds may be effective at killing cancer cells, they can often be so toxic that they could never be successfully used in vivo without causing serious damage or death. New drugs take approximately 10-15 years to advance from invention to routine clinical use and can cost millions of dollars during the course of development (124). Utilizing FDA approved drugs in off-label use against cancerous cells can improve cancer treatment options and decrease the time it takes for a therapeutic approach to move from the bench to clinical treatment. These experiments and other evidence in the literature suggest a benefit to administering even racemic ketorolac to cancer patients over other pain or anti-inflammatory medications. A decrease in early breast cancer metastasis will lead to more positive patient outcomes, enabling patients to live a longer, better quality of life.

6. APPENDIX

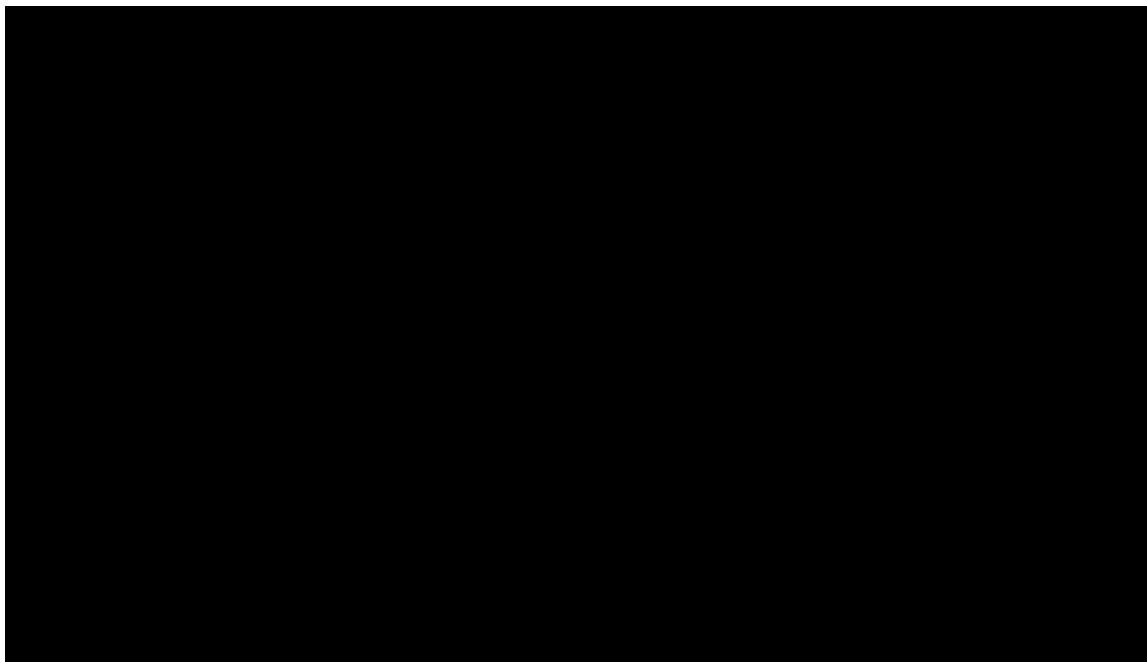


Figure 6.1 MMTV-PyMT Mouse Lung Metastasis Time Course

MMTV-PyMT mice were sacrificed at increasing age time points and lung tissue was H&E stained and analyzed for presence and size of metastasis lesions. These mice were not given any drug treatments. At 12 weeks of age, almost no mice had lung metastasis. At 13 weeks of age the numbers of lung metastasis foci increased and remained around the same quantity at 16 weeks. This information helped us form the decision to repeat the long term (R)-ketorolac study to extend the sacrifice age to 14 weeks rather than 12 weeks. The total lung metastasis area increased around 13 weeks and remained around the same area at 16 weeks. There was a decrease in lung metastasis area at 14 weeks for this set of data, but there were only two data points at 14 weeks. There were no samples available for the 15 week time point.

7. REFERENCES

1. American Cancer Society. Cancer Facts & Figures 2015. 2015;
2. Jordan VC. Fourteenth Gaddum Memorial Lecture. A current view of tamoxifen for the treatment and prevention of breast cancer. *Br J Pharmacol*. 1993;110:507–17.
3. Cianfrocca M, Goldstein LJ. Prognostic and predictive factors in early-stage breast cancer. *Oncologist* [Internet]. 2004;9:606–16. Available from: <http://www.ncbi.nlm.nih.gov/pubmed/23220842>
4. Group EBCTC. Tamoxifen for early breast cancer: an overview of the randomised trials. *Lancet* [Internet]. 1998;351:1451–67. Available from: <http://www.ncbi.nlm.nih.gov/pubmed/9605801>
5. Dent R, Trudeau M, Pritchard KI, Hanna WM, Kahn HK, Sawka C a., et al. Triple-negative breast cancer: Clinical features and patterns of recurrence. *Clin Cancer Res*. 2007;13:4429–34.
6. Haffty BG, Yang Q, Reiss M, Kearney T, Higgins S a., Weidhaas J, et al. Locoregional relapse and distant metastasis in conservatively managed triple negative early-stage breast cancer. *J Clin Oncol*. 2006;24:5652–7.
7. Breast Cancer Treatment (PDQ®): Treatment Option Overview [Internet]. Natl. Cancer Inst. NIH. 2015 [cited 2015 May 25]. Available from: http://www.cancer.gov/types/breast/patient/breast-treatment-pdq#section/_185
8. Types of Breast Cancer: ER Positive, HER2 Positive, and Triple Negative [Internet]. WebMD. 2012 [cited 2015 May 25]. Available from: <http://www.webmd.com/breast-cancer/breast-cancer-types-er-positive-her2-positive>
9. Silberman A. ER-Positive Breast Cancer: Prognosis, Life Expectancy, and More [Internet]. Healthline. 2014 [cited 2015 May 25]. Available from: <http://www.healthline.com/health/breast-cancer/er-positive-prognosis-life-expectancy#Overview1>

10. Slamon DJ, Clark GM, Wong SG, Levin WJ, Ullrich A, McGuire WL. Human breast cancer: correlation of relapse and survival with amplification of the HER-2/neu oncogene. *Science*. 1987;235:177–82.
11. Yarden Y. Biology of HER2 and its importance in breast cancer. *Oncology*. 2001;61 Suppl 2:1–13.
12. Slamon DJ, Godolphin W, Jones LA, Holt JA, Wong SG, Keith DE, et al. Studies of the HER-2/neu proto-oncogene in human breast and ovarian cancer. *Science*. 1989;244:707–12.
13. Mitri Z, Constantine T, O'Regan R. The HER2 Receptor in Breast Cancer: Pathophysiology, Clinical Use, and New Advances in Therapy. *Chemother Res Pract* [Internet]. 2012;2012:743193. Available from: <http://www.pubmedcentral.nih.gov/articlerender.fcgi?artid=3539433&tool=mcentrez&rendertype=abstract>
14. Stern DF, Heffernan P a, Weinberg R a. P185, a Product of the Neu Proto-Oncogene, Is a Receptorlike Protein Associated With Tyrosine Kinase Activity. *Mol Cell Biol*. 1986;6:1729–40.
15. Akiyama T, Sudo C, Ogawara H, Toyoshima K, Yamamoto T. The product of the human c-erbB-2 gene: a 185-kilodalton glycoprotein with tyrosine kinase activity. *Science*. 1986;232:1644–6.
16. Olayioye M a, Neve RM, Lane H a, Hynes NE. The ErbB signaling network: receptor heterodimerization in development and cancer. *EMBO J*. 2000;19:3159–67.
17. Morgensztern D, McLeod HL. PI3K/Akt/mTOR pathway as a target for cancer therapy. *Anticancer Drugs*. 2005;16:797–803.
18. Borg a, Tandon a K, Sigurdsson H, Clark GM, Ferno M, Fuqua S a, et al. HER-2/neu amplification predicts poor survival in node-positive breast cancer. *Cancer Res*. 1990;50:4332–7.
19. Winstanley J, Cooke T, Murray GD, Platt-Higgins a, George WD, Holt S, et al. The long term prognostic significance of c-erbB-2 in primary breast cancer. *Br J Cancer*. 1991;63:447–50.

20. Clark GM, McGuire WL. Follow-up Study of HER-2 / neu Amplification in Primary Breast Cancer. *Cancer Res.* 1991;51:944–8.
21. Tandon a. K, Clark GM, Chamness GC, Ullrich a., McGuire WL. HER-2/neu oncogene protein and prognosis in breast cancer. *J Clin Oncol.* 1989;7:1120–8.
22. Slamon DJ, Leyland-Jones B, Shak S, Fuchs H, Paton V, Bajamonde A, et al. Use of chemotherapy plus a monoclonal antibody against HER2 for metastatic breast cancer that overexpresses HER2. [Internet]. *N. Engl. J. Med.* 2001. Available from: <http://www.nejm.org/doi/full/10.1056/NEJM200103153441101>
23. Cho H-S, Mason K, Ramyar KX, Stanley AM, Gabelli SB, Denney DW, et al. Structure of the extracellular region of HER2 alone and in complex with the Herceptin Fab. *Nature.* 2003;421:756–60.
24. Marrazzo JM, Ramjee G, Richardson BA, Gomez K, Mgodhi N, Nair G, et al. Tenofovir-based preexposure prophylaxis for HIV infection among African women. *N Engl J Med* [Internet]. 2015;372:509–18. Available from: <http://www.ncbi.nlm.nih.gov/pubmed/25651245>
25. Vogel CL, Cobleigh M a, Tripathy D, Gutheil JC, Harris LN, Fehrenbacher L, et al. Efficacy and Safety of Trastuzumab as a Single Agent in First-Line Treatment of HER2-Overexpressing Metastatic Breast Cancer. *J Clin Oncol.* 2003;20:719–26.
26. Romond EH, Perez E a, Bryant J, Suman VJ, Geyer CE, Davidson NE, et al. Trastuzumab plus adjuvant chemotherapy for operable HER2-positive breast cancer. *N Engl J Med.* 2005;353:1673–84.
27. Cancer Drugs & Oncology Drugs [Internet]. MediLexicon. 2013. Available from: <http://www.medilexicon.com/drugs-list/cancer.php>
28. Wang D-Y, Fulthorpe R, Liss SN, Edwards EA. Identification of estrogen-responsive genes by complementary deoxyribonucleic acid microarray and characterization of a novel early estrogen-induced gene: EEIG1. *Mol Endocrinol.* 2004;18:402–11.
29. Williams GM, Iatropoulos MJ, Djordjevic M V, Kaltenberg OP. The

triphenylethylene drug tamoxifen is a strong liver carcinogen in the rat. *Carcinogenesis*. 1993;14:315–7.

30. Rutqvist LE, Johansson H, Signomklao T, Johansson U, Fornander T, Wilking N. Adjuvant tamoxifen therapy for early stage breast cancer and second primary malignancies. Stockholm Breast Cancer Study Group. *J. Natl. Cancer Inst.* 1995.
31. Polin S a., Ascher SM. The effect of tamoxifen on the genital tract. *Cancer Imaging*. 2008;8:135–45.
32. Kedar RP, Bourne TH, Powles TJ, Collins WP, Ashley SE, Cosgrove DO, et al. Effects of tamoxifen on uterus and ovaries of postmenopausal women in a randomised breast cancer prevention trial. *Lancet*. 1994;343:1318–21.
33. Marjon N a, Hu C, Hathaway HJ, Prossnitz ER. G protein-coupled estrogen receptor regulates mammary tumorigenesis and metastasis. *Mol Cancer Res [Internet]*. 2014 [cited 2014 Nov 20];12:1644–54. Available from: <http://www.ncbi.nlm.nih.gov/pubmed/25030371>
34. Rowinsky EK, Eisenhauer EA, Chaudhry V, Ar buck SG, Donehower RC. Clinical toxicities encountered with paclitaxel (Taxol). *Semin Oncol*. 1993;20:1–15.
35. Morrison KC, Hergenrother PJ. Whole cell microtubule analysis by flow cytometry. *Anal Biochem [Internet]*. 2012 [cited 2015 Mar 24];420:26–32. Available from: <http://www.sciencedirect.com/science/article/pii/S0003269711005409>
36. Gottesman MM. Mechanisms of cancer drug resistance. *Annu Rev Med*. 2002;53:615–27.
37. T. T, M. N, a. T, N. F, T. M, H. S, et al. Molecular targeting therapy of cancer: Drug resistance, apoptosis and survival signal. *Cancer Sci [Internet]*. 2003;94:15–21. Available from: <http://ovidsp.ovid.com/ovidweb.cgi?T=JS&PAGE=reference&D=emed6&N EWS=N&AN=2003198227>
38. Holohan C, Van Schaeybroeck S, Longley DB, Johnston PG. Cancer drug

resistance: an evolving paradigm. *Nat Rev Cancer* [Internet]. Nature Publishing Group; 2013;13:714–26. Available from: <http://www.ncbi.nlm.nih.gov/pubmed/24060863>

39. Mestre-Ferrandiz, J., Sussex, J., Towse A. *The R&D Cost of a New Medicine*. London: Office of Health Economics; 2012.
40. Oprea TI, Bauman JE, Bologna CG, Buranda T, Chigaev A, Edwards BS, et al. Drug Repurposing from an Academic Perspective. *Drug Discov Today Ther Strateg* [Internet]. Elsevier Ltd; 2011 [cited 2014 Jun 19];8:61–9. Available from: <http://www.pubmedcentral.nih.gov/articlerender.fcgi?artid=3285382&tool=mcentrez&rendertype=abstract>
41. Gillis JC, Brogden RN. Ketorolac. A reappraisal of its pharmacodynamic and pharmacokinetic properties and therapeutic use in pain management. *Drugs*. 1997;53:139–88.
42. ketorolac (Rx) - Toradol [Internet]. WebMD. 2015 [cited 2015 Jun 30]. Available from: <http://reference.medscape.com/drug/ketorolac-343292>
43. Retsky M, Demicheli R, Hrushesky WJM, Forget P, De Kock M, Gukas I, et al. Reduction of breast cancer relapses with perioperative non-steroidal anti-inflammatory drugs: new findings and a review. *Curr Med Chem* [Internet]. 2013;20:4163–76. Available from: <http://www.pubmedcentral.nih.gov/articlerender.fcgi?artid=3831877&tool=mcentrez&rendertype=abstract>
44. Forget P, Machiels J-P, Coulie PG, Berliere M, Poncelet AJ, Tombal B, et al. Neutrophil:lymphocyte ratio and intraoperative use of ketorolac or diclofenac are prognostic factors in different cohorts of patients undergoing breast, lung, and kidney cancer surgery. *Ann Surg Oncol* [Internet]. 2013;20 Suppl 3:S650–60. Available from: <http://www.ncbi.nlm.nih.gov/pubmed/23884751>
45. Guo Y, Kenney SR, Cook LS, Adams SF, Rutledge T, Romero E, et al. A novel pharmacologic activity of ketorolac for therapeutic benefit in ovarian cancer patients. *Clin Cancer Res* [Internet]. 2015; Available from: <http://clincancerres.aacrjournals.org/cgi/doi/10.1158/1078-0432.CCR-15-0461>

46. Forget P, Vandenhende J, Berliere M, MacHiels JP, Nussbaum B, Legrand C, et al. Do intraoperative analgesics influence breast cancer recurrence after mastectomy? A retrospective analysis. *Anesth Analg*. 2010;110:1630–5.
47. Retsky M, Rogers R, Demicheli R, Hrushesky WJ, Gukas I, Vaidya JS, et al. NSAID analgesic ketorolac used perioperatively may suppress early breast cancer relapse: particular relevance to triple negative subgroup. *Breast Cancer Res Treat* [Internet]. 2012 [cited 2014 Jun 19];134:881–8. Available from: <http://www.ncbi.nlm.nih.gov/pubmed/22622810>
48. Handley DA, Cervoni P, McCray JE, McCullough JR. Preclinical enantioselective pharmacology of (R)- and (S)- ketorolac. *J Clin Pharmacol* [Internet]. 1998 [cited 2014 Jun 19];38:25S – 35S. Available from: <http://www.ncbi.nlm.nih.gov/pubmed/9549656>
49. Jerussi TP, Caubet JF, McCray JE, Handley D a. Clinical endoscopic evaluation of the gastroduodenal tolerance to (R)- ketoprofen, (R)- flurbiprofen, racemic ketoprofen, and paracetamol: a randomized, single-blind, placebo-controlled trial. *J Clin Pharmacol*. 1998;38:19S – 24S.
50. Guo Y, Kenney SR, Muller CY, Adams S, Rutledge T, Romero E, et al. R-ketorolac Targets Cdc42 and Rac1 and Alters Ovarian Cancer Cell Behaviors Critical for Invasion and Metastasis. *Mol Cancer Ther* [Internet]. 2015; Available from: <http://mct.aacrjournals.org/cgi/doi/10.1158/1535-7163.MCT-15-0419>
51. Oprea, Tudor I., Sklar, Larry A., Agola, Jacob O., Guo, Yuna, Silberberg, Melina, Roxby, Joshua et al. Novel activities of select NSAID R-enantiomers against Rac1 and Cdc42 GTPases. *PLoS One*. 2015;
52. Mroszczak E, Combs D, Chaplin M, Tsina I, Tarnowski T, Rocha C, et al. Chiral kinetics and dynamics of ketorolac. *J Clin Pharmacol*. 1996;36:521–39.
53. Dempke W, Rie C, Grothey a, Schmoll HJ. Cyclooxygenase-2: a novel target for cancer chemotherapy? *J Cancer Res Clin Oncol*. 2001;127:411–7.
54. Vane JR, Bakhle YS, Botting RM. Cyclooxygenases 1 and 2. *Annu Rev Pharmacol Toxicol*. 1998;38:97–120.

55. Moskowitz MA, Coughlin SR. Clinical applications of prostaglandins and their inhibitors. *Stroke*. 1981;12:882–6.
56. Hejna M, Raderer M, Zielinski CC. Inhibition of metastases by anticoagulants. *J Natl Cancer Inst*. 1999;91:22–36.
57. Leung KH, Mihich E. Prostaglandin modulation of development of cell-mediated immunity in culture. *Nature*. 1980;288:597–600.
58. Brunda MJ, Herberman RB, Holden HT. Inhibition of murine natural killer cell activity by prostaglandins. *J Immunol*. 1980;124:2682–7.
59. Milas L, Kishi K, Mason K, Jaime L, Tofilon PJ. BRIEF Enhancement of Tumor. *Communication*. 1999;91:1501–4.
60. Taketo MM. Cyclooxygenase-2 Inhibitors in Tumorigenesis (Part I). 1998;90:1529–36.
61. Fosslien E. Molecular pathology of cyclooxygenase-2 in neoplasia. *Ann Clin Lab Sci [Internet]*. Institute for Clinical Science; [cited 2015 Mar 25];30:3–22. Available from: <http://cat.inist.fr/?aModele=afficheN&cpsidt=1292972>
62. Nelson a R, Fingleton B, Rothenberg ML, Matrisian LM. Matrix metalloproteinases: biologic activity and clinical implications. *J Clin Oncol*. 2000;18:1135–49.
63. Pakneshan P, Birsner AE, Adini I, Becker CM, D’Amato RJ. Differential suppression of vascular permeability and corneal angiogenesis by nonsteroidal anti-inflammatory drugs. *Investig Ophthalmol Vis Sci*. 2008;49:3909–13.
64. Krebs MG, Hou J-M, Ward TH, Blackhall FH, Dive C. Circulating tumour cells: their utility in cancer management and predicting outcomes. *Ther Adv Med Oncol*. 2010;2:351–65.
65. Zhe X, Cher ML, Bonfil RD. Circulating tumor cells: finding the needle in the haystack. *Am J Cancer Res [Internet]*. 2011;1:740–51. Available from:

<http://www.pubmedcentral.nih.gov/articlerender.fcgi?artid=3195935&tool=pmcentrez&rendertype=abstract>

66. Tang Y, Olufemi L, Wang M-T, Nie D. Role of Rho GTPases in breast cancer. *Front Biosci* [Internet]. 2008 [cited 2014 Jun 25];13:759–76. Available from: <http://www.bioscience.org/2008/v13/af/2718/list.htm>
67. Fritz G, Just I, Kaina B. Rho GTPases are over-expressed in human tumors. *Int J Cancer*. 1999;81:682–7.
68. Fritz G, Brachetti C, Bahlmann F, Schmidt M, Kaina B. Rho GTPases in human breast tumours: expression and mutation analyses and correlation with clinical parameters. *Br J Cancer*. 2002;87:635–44.
69. Schnelzer a, Prechtel D, Knaus U, Dehne K, Gerhard M, Graeff H, et al. Rac1 in human breast cancer: overexpression, mutation analysis, and characterization of a new isoform, Rac1b. *Oncogene* [Internet]. 2000;19:3013–20. Available from: <http://www.ncbi.nlm.nih.gov/pubmed/10871853>
70. Kleer CG, van Golen KL, Zhang Y, Wu Z-F, Rubin M a, Merajver SD. Characterization of RhoC expression in benign and malignant breast disease: a potential new marker for small breast carcinomas with metastatic ability. *Am J Pathol* [Internet]. American Society for Investigative Pathology; 2002;160:579–84. Available from: [http://dx.doi.org/10.1016/S0002-9440\(10\)64877-8](http://dx.doi.org/10.1016/S0002-9440(10)64877-8)
71. Jett MF, Ramesha CS, Brown CD, Chiu S, Emmett C, Voronin T, et al. Characterization of the analgesic and anti-inflammatory activities of ketorolac and its enantiomers in the rat. *J Pharmacol Exp Ther*. 1999;288:1288–97.
72. Ridley AJ, Paterson HF, Johnston CL, Diekmann D, Hall A. The small GTP-binding protein rac regulates growth factor-induced membrane ruffling. *Cell* [Internet]. 1992 [cited 2015 Mar 24];70:401–10. Available from: <http://www.sciencedirect.com/science/article/pii/0092867492901648>
73. Hall a. Rho GTPases and the Actin Cytoskeleton. *Science* (80-). 1998;279:509–14.

74. Etienne-Manneville S, Hall A. Rho GTPases in cell biology. *Nature*. 2002;420:629–35.
75. Van Aelst L, D'Souza-Schorey C. Rho GTPases and signaling networks. *Genes Dev*. 1997;11:2295–322.
76. Pasqualucci L, Neumeister P, Goossens T, Nanjangud G, Chaganti RS, Küppers R, et al. Hypermutation of multiple proto-oncogenes in B-cell diffuse large-cell lymphomas. *Nature*. 2001;412:341–6.
77. Preudhomme C, Roumier C, Hildebrand MP, Dallery-Prudhomme E, Lantoine D, Lai JL, et al. Nonrandom 4p13 rearrangements of the RhoH/TTF gene, encoding a GTP-binding protein, in non-Hodgkin's lymphoma and multiple myeloma. *Oncogene*. 2000;19:2023–32.
78. Jordan P, Brazão R, Boavida MG, Gespach C, Chastre E. Cloning of a novel human Rac1b splice variant with increased expression in colorectal tumors. *Oncogene* [Internet]. 1999;18:6835–9. Available from: <http://www.ncbi.nlm.nih.gov/pubmed/10597294>
79. Katz E, Sims AH, Sproul D, Caldwell H, Dixon JM, Meehan RR, et al. Targeting of Rac GTPases blocks the spread of intact human breast cancer ABSTRACT : *Oncotarget*. 2012;3:608–13.
80. Kawazu M, Ueno T, Kontani K, Ogita Y, Ando M, Fukumura K, et al. Transforming mutations of RAC guanosine triphosphatases in human cancers. *Proc Natl Acad Sci U S A* [Internet]. 2013;110:3029–34. Available from: <http://www.pubmedcentral.nih.gov/articlerender.fcgi?artid=3581941&tool=pmcentrez&rendertype=abstract>
81. Alan JK, Lundquist EA. Mutationally activated Rho GTPases in cancer. *Small GTPases* [Internet]. 2013;4:159–63. Available from: <http://www.tandfonline.com/doi/abs/10.4161/sgtp.26530>
82. Ellenbroek SIJ, Collard JG. Rho GTPases: Functions and association with cancer. *Clin Exp Metastasis*. 2007;24:657–72.
83. Mertens AE, Roovers RC, Collard JG. Regulation of Tiam1-Rac signalling. *FEBS Lett*. 2003;546:11–6.

84. Gururaj AE, Rayala SK, Kumar R. P21-Activated Kinase Signaling in Breast Cancer. *Breast Cancer Res.* 2005;7:5–12.
85. Jaffe AB, Hall A. Rho GTPases: biochemistry and biology. *Annu Rev Cell Dev Biol.* 2005;21:247–69.
86. Nobes CD, Hall a. Rho, rac, and cdc42 GTPases regulate the assembly of multimolecular focal complexes associated with actin stress fibers, lamellipodia, and filopodia. *Cell.* 1995;81:53–62.
87. Kozma R, Ahmed S, Best a, Lim L. The Ras-related protein Cdc42Hs and bradykinin promote formation of peripheral actin microspikes and filopodia in Swiss 3T3 fibroblasts. *Mol Cell Biol.* 1995;15:1942–52.
88. Hall a. Rho GTPases and the control of cell behaviour. *Biochem Soc Trans.* 2005;33:891–5.
89. Baugher PJ, Krishnamoorthy L, Price JE, Dharmawardhane SF. Rac1 and Rac3 isoform activation is involved in the invasive and metastatic phenotype of human breast cancer cells. *Breast Cancer Res.* 2005;7:R965–74.
90. Ridley AJ, Hall A. The small GTP-binding protein rho regulates the assembly of focal adhesions and actin stress fibers in response to growth factors. *Cell.* 1992;70:389–99.
91. Worthyake R a., Lemoine S, Watson JM, Burridge K. RhoA is required for monocyte tail retraction during transendothelial migration. *J Cell Biol.* 2001;154:147–60.
92. Denoyelle C, Albanese P, Uzan G, Hong L, Vannier JP, Soria J, et al. Molecular mechanism of the anti-cancer activity of cerivastatin, an inhibitor of HMG-CoA reductase, on aggressive human breast cancer cells. *Cell Signal.* 2003;15:327–38.
93. Pillé JY, Denoyelle C, Varet J, Bertrand JR, Soria J, Opolon P, et al. Anti-RhoA and Anti-RhoC siRNAs inhibit the proliferation and invasiveness of MDA-MB-231 breast cancer cells in vitro and in vivo. *Mol Ther.*

2005;11:267–74.

94. Yuan B-Z, Zhou X, Durkin ME, Zimonjic DB, Gumundsdottir K, Eyfjord JE, et al. DLC-1 gene inhibits human breast cancer cell growth and in vivo tumorigenicity. *Oncogene*. 2003;22:445–50.
95. Durkin ME, Avner MR, Huh CG, Yuan BZ, Thorgeirsson SS, Popescu NC. DLC-1, a Rho GTPase-activating protein with tumor suppressor function, is essential for embryonic development. *FEBS Lett*. 2005;579:1191–6.
96. Liao YC, Lo SH. Deleted in liver cancer-1 (DLC-1): A tumor suppressor not just for liver. *Int J Biochem Cell Biol*. 2008;40:843–7.
97. Goodison S, Yuan J, Sloan D, Kim R, Li C, Popescu NC, et al. The RhoGAP Protein DLC-1 Functions as a Metastasis Suppressor in Breast Cancer Cells The RhoGAP Protein DLC-1 Functions as a Metastasis Suppressor in Breast Cancer Cells. 2005;6042–53.
98. Plaumann M, Seitz S, Frege R, Estevez-Schwarz L, Scherneck S. Analysis of DLC-1 expression in human breast cancer. *J Cancer Res Clin Oncol*. 2003;129:349–54.
99. Sander EE, Ten Klooster JP, Van Delft S, Van Der Kammen R a., Collard JG. Rac downregulates Rho activity: Reciprocal balance between both GTPases determines cellular morphology and migratory behavior. *J Cell Biol*. 1999;147:1009–21.
100. Michiels F, Habets GG, Stam JC, van der Kammen R a, Collard JG. A role for Rac in Tiam1-induced membrane ruffling and invasion. *Nature*. 1995. page 338–40.
101. Mertens a. EE, Rygiel TP, Olivo C, Van Der Kammen R, Collard JG. The Rac activator Tiam1 controls tight junction biogenesis in keratinocytes through binding to and activation of the Par polarity complex. *J Cell Biol*. 2005;170:1029–37.
102. Hordijk PL, ten Klooster JP, van der Kammen R a, Michiels F, Oomen LC, Collard JG. Inhibition of invasion of epithelial cells by Tiam1-Rac signaling. *Science*. 1997;278:1464–6.

103. Adam L, Vadlamudi RK, McCrea P, Kumar R. Tiam1 Overexpression Potentiates Heregulin-induced Lymphoid Enhancer Factor-1/ β -Catenin Nuclear Signaling in Breast Cancer Cells by Modulating the Intercellular Stability. *J Biol Chem*. 2001;276:28443–50.
104. Minard ME, Kim LS, Price JE, Gallick GE. The role of the guanine nucleotide exchange factor Tiam1 in cellular migration, invasion, adhesion and tumor progression. *Breast Cancer Res Treat*. 2004;84:21–32.
105. Strumane K, Rygiel T, Van Der Valk M, Collard JG. Tiam1-deficiency impairs mammary tumor formation in MMTV-c-neu but not in MMTV-c-myc mice. *J Cancer Res Clin Oncol*. 2009;135:69–80.
106. Lin EY, Jones JG, Li P, Zhu L, Whitney KD, Muller WJ, et al. Progression to malignancy in the polyoma middle T oncoprotein mouse breast cancer model provides a reliable model for human diseases. *Am J Pathol* [Internet]. 2003 [cited 2015 Feb 4];163:2113–26. Available from: <http://www.sciencedirect.com/science/article/pii/S0002944010635687>
107. Fantozzi A, Christofori G. Mouse models of breast cancer metastasis. *Breast Cancer Res*. 2006;8:212.
108. Maglione JE, Moghanaki D, Young LJT, Manner CK, Ellies LG, Joseph SO, et al. Transgenic Polyoma middle-T mice model premalignant mammary disease. *Cancer Res*. 2001;61:8298–305.
109. Gillett C, Smith P, Gregory W, Richards M, Millis R, Peters G, et al. Cyclin D1 and Prognosis in Human Breast Cancer. 1996;99:92–9.
110. Lapidus RG, Nass SJ, Davidson NE. The loss of estrogen and progesterone receptor gene expression in human breast cancer. *J Mammary Gland Biol Neoplasia*. 1998;3:85–94.
111. Guy CT, Cardiff RD, Muller WJ. Induction of mammary tumors by expression of polyomavirus middle T oncogene: a transgenic mouse model for metastatic disease. *Mol Cell Biol*. 1992;12:954–61.
112. Rodriguez-Viciano P, Collins C, Fried M. Polyoma and SV40 proteins differentially regulate PP2A to activate distinct cellular signaling pathways involved in growth control. *Proc Natl Acad Sci U S A* [Internet]. 2006 [cited

2015 Apr 10];103:19290–5. Available from:
<http://www.pnas.org/cgi/content/long/103/51/19290>

113. Urich M, Senften M, Shaw PE, Ballmer-Hofer K. A role for the small GTPase Rac in polyomavirus middle-T antigen-mediated activation of the serum response element and in cell transformation. *Oncogene* [Internet]. 1997;14:1235–41. Available from:
<http://www.ncbi.nlm.nih.gov/pubmed/9121774>
114. Kim IS, Baek SH. Mouse models for breast cancer metastasis. *Biochem Biophys Res Commun* [Internet]. Elsevier Inc.; 2010 [cited 2014 Jul 2];394:443–7. Available from:
<http://www.ncbi.nlm.nih.gov/pubmed/20230796>
115. Forget P, Bentin C, Machiels JP, Berliere M, Coulie PG, De Kock M. Intraoperative use of ketorolac or diclofenac is associated with improved disease-free survival and overall survival in conservative breast cancer surgery. *Br J Anaesth*. 2014;113:82–7.
116. Hande K. Etoposide: four decades of development of a topoisomerase II inhibitor. *Eur J Cancer* [Internet]. Elsevier Science Ltd.; 1998 [cited 2014 Jun 25];34:1514–21. Available from:
<http://linkinghub.elsevier.com/retrieve/pii/S0959804998002287>
117. Loike JD, Horwitz SB. Effects of podophyllotoxin and VP-16-213 on microtubule assembly in vitro and nucleoside transport in HeLa cells. *Biochemistry* [Internet]. 1976 [cited 2014 Jun 25];15:5435–43. Available from: <http://pubs.acs.org/doi/abs/10.1021/bi00670a003>
118. Trevigen. Table of Contents 96 Well 3D Spheroid BME Cell Invasion Assay [Internet]. Gaithersburg: Trevigen, Inc.; 2012. Available from:
http://www.trevigen.com/docs/1354634644.3500-096-k_e10-18-12v0.pdf?guid=1447177437
119. Walker MK, Boberg JR, Walsh MT, Wolf V, Trujillo A, Duke MS, et al. A less stressful alternative to oral gavage for pharmacological and toxicological studies in mice. *Toxicol Appl Pharmacol* [Internet]. Elsevier Inc.; 2012 [cited 2014 Jun 19];260:65–9. Available from:
<http://www.pubmedcentral.nih.gov/articlerender.fcgi?artid=3306547&tool=pmcentrez&rendertype=abstract>

120. Lu J, Steeg PS, Price JE, Krishnamurthy S, Mani S a., Reuben J, et al. Breast cancer metastasis: Challenges and opportunities. *Cancer Res.* 2009;69:4951–3.
121. Lee YT. Breast carcinoma: pattern of metastasis at autopsy. *J Surg Oncol.* 1983;23:175–80.
122. Muller WJ, Sinn E, Pattengale PK, Wallace R, Leder P. Single-step induction of mammary adenocarcinoma in transgenic mice bearing the activated c-neu oncogene. *Cell.* 1988;54:105–15.
123. Hanahan D, Weinberg RA. Hallmarks of cancer: the next generation. *Cell* [Internet]. 2011 [cited 2014 Jul 9];144:646–74. Available from: <http://www.sciencedirect.com/science/article/pii/S0092867411001279>
124. Gavura S. What does a new drug cost? Part II: The productivity problem [Internet]. *Sci. Med.* 2012 [cited 2013 Apr 9]. Available from: <http://www.sciencebasedmedicine.org/index.php/what-does-a-new-drug-cost-part-ii-the-productivity-problem/>